AAiT
Addis Ababa Institute of Technology
Addis Ababa University

ADDIS ABABA UNIVERSITY
ADDIS ABABA INSTITUTE OF TECHNOLOGY
SCHOOL OF MECHANICAL AND INDUSTRIAL ENGINEERING
(Thermal Stream)

TEMPERATURE, DEFORMATION, STRESS AND STRAIN ANALYSIS IN METAL CUTTING PROCESS USING FINITE ELEMENT METHOD

By: Aderaw Awoke

ADVISOR: Dr-Ing Demis Alemu

A Thesis Submitted to the School of Mechanical and Industrial Engineering in Partial Fulfillment of the Requirements for the Degree of Masters of Science in Mechanical Engineering

June, 2016

Addis Ababa, Ethiopia

ADDIS ABABA INSTITUTE OF TECHNOLOGY

SCHOOL OF GRADUATED STUDIES

POSTGRADUATE PROGRAM IN MECHANICAL ENGINEERING

ADDIS ABABA UNIVERSITY

Temperature, Deformation, Stress and Strain analysis in metal cutting process using finite element method

By: - Aderaw Awoke

APPROVED BY BOARD OF EXAMINERS

Dr-Ing Demis Alemu	______________________	____________________
Advisor	Signature	Date
Araya Abera	______________________	____________________
Internal examiner	Signature	Date
Dr. Tesfaye Dama	______________________	____________________
External examiner	Signature	Date
Getasew Taddese	______________________	____________________
Chair man of the school	Signature	Date

DECLARATION

I hereby declare that the work which is being presented in this thesis entitled “Temperature, deformation, stress and strain analysis in metal cutting process using finite element method ” is original work of my own, has not been presented for a degree of any other University and all the resource of materials used for this thesis has been duly acknowledged.

Aderaw Awoke Date

This is to certify that the above declared made by the candidate is correct to the best of my knowledge.

Dr-Ing Demis Alemu (Advisor) Date

Getasew Taddese (Dean of school) Date

Aderaw Awoke

Addis Ababa
June /2016

Acknowledgement

First of all, thanks God for giving me the courage to hold on my beliefs and never give up. Secondly, there are people directly or indirectly involved in this work for it to come true. Thus, I would like to give the deserved credit to them.

First , I would like to express my deep gratitude for my advisor DR-ING Dimes Alemu for having interest in this thesis area, for providing me with help full comments and suggestions which are vital input for the work.

Mr. Araya, you are a great man. You help me for ANSYS software tutorials which were the vital tool to bring my work in to reality. Even the suggestion and advices on my work, you deserved special thanks.

I would like to thank my family for always being there for me at times of extreme situations. Lastly, I would like to thank my fellow classmates for their kind cooperation works and suggestions.

Abstract

There are many causes for overheating, large stress, strain, deformation and fracture as well as tool wears of metal cutting process. velocity, feed rate, depth of cut, type of material (work piece and tool) and lubricant type takes the lion’s share those parameters:

This thesis deals the effect of metal cutting variables, depth of cut and cutting speed on temperature, cutting forces, strain and von-misses stress and obtaining optimum conditions of cutting speed and depth of cut using finite element method rather than experimental techniques which makes the investigation very time consuming and expensive.

At this point, finite element modeling and simulation becomes main tool. For this purpose, orthogonal milling simulation of AISI 1045 steel as work piece and un coated tungsten as tool are performed and modeled.

The effects of cutting variables on cutting forces and thrust force also investigated by comparing simulation results with experimental results available in the literature. Then, thermo- mechanical and thermal analyses are performed using ANSYS software. Lastly, strain, temperature and stress distributions are investigated[8].

Here metal cutting variables of velocity 1m/s,1,5m/s,2m/s,2.5m/s and 3m/s with depth of cut of 1mm,1.5mm,2mm considered and the resulting temperature,strain,stress and total deformation of each condition is investigated. here at increasing parameters the resulting temperature is above working service temperature and the material melts.

Table of content

Contents

Acknowledgement i
Abstract ii
Table of content iii
List of tables vi
List of figures vii
CHAPTER ONE: INTRODUCTION 1
1.1 Background 1
1.2Types of metal cutting 1
1.2.1 Turning 2
1.2.2 Drilling 2
1.2.3 Milling 2
1.3 finite element methods and variables in metal cutting 3
1.5 Objective of the study 6
1.5.1 Main objective 6
1.5.2 Specific objective 6
1.6 Methodology 6
1.6.1 Primary data collection 6
1.6.2 Analytical solutions for temperature 7
1.6.3 Finite element analysis 7
1.6.4 Analysis of the results obtained 7
1.6.5 Discussion on findings 8
1.6 Significance of the research 8
CHAPTER TWO:LITERATURE REVIEW 9
2.1 Introduction 9
2.2 Failure due to overheating 9
2.2.1 Thermal cracks 9
2.2.2 Induced Tensile residual stresses 10

2.2.3 Cutting Force 10
2.3 Related literatures 11
2.3.1 Velocity 11
2.3.2 Temperature 14
2.3.3 feed rate 15
2.3.5 Tool shape 16
2.3.6 Work piece material type 17
2.4 lubricant selections 19
CHAPTER THREE:NUMERICAL AND ANALYTICAL SOLUTIONS 20
3.1 Numerical solutions 20
3.1.1 Material properties 20
3.1.2 Object boundary conditions 21
3.1.3 Galarkins approach 24
3.2.1Analytical solution for maximum cutting temperature 28
3.2.2 Analytical Model for frictional force 28
3.3 Cutting Force and Thrust Force analysis 29
3.3.1 Proposed methodology for cutting force calculation 30
3.4 Shear Stress and strain distribution 39
3.4.1 Shear stress distribution in metal cutting 39
3.5 Power calculations 42
3.6 Analytical heat flux calculation 42
3.6.1 Heat flux due to plastic deformation 42
3.6.2 Heat flux due to friction at the tool and chip interface 43
3.6.3 Heat flux due to new machined surface 44
CHAPTER FOUR:FINITE ELEMENT ANALYSIS 45
4.1 Introduction 45
4.2 Finite element analysis using Ansys-15.0 45
4.2.1 General procedures of ANSYS software 45
4.3 Analysis of the cutting variables using ANSYS -15.0 46
4.3.1Geometrical model 46
4.3.2 material property definition 47

4.3.3 Mesh generation......47
4.3.4 Defining Boundary conditions and loads......48
CHAPTER FIVE:RESULT AND DISCUSSION 49
5.1 introduction 49
CHAPTER SIX:CONCLUSION, RECOMMENDATION AND FUTURE WORKS...... 57
6.1 Conclusion......57
6.2 Recommendations 58
6.3 Future Work 58
Appendix 59
REFERENCES 83

List of tables

Table3. 1: Percentage material composition of AISI1045 21

Table3. 2: Percentage material composition of un coated tungsten 21

Table3. 4:input parameters for AISI1045 34

Table 3.5:cutting force from experiment and from the proposed methodology 35

Table 3.6: The effect of velocity 35

Table 3.7: The effect of feed on cutting force and thrust force 37

Table3. 8: Thrust force calculated 38

Table 3.9: Summary of calculated heat flux due to plastic deformation 43

Table 3.10: Summary of calculated heat flux due to friction at the tool and chip interface 44

Table 3.11: Summary of calculated heat flux due to new machined surface 44

Table 5.1: Summary of result as impossible and possible conditions. 57

List of figures

Figure 1.1: turning operation..2

Figure 1.2:drilling operation...2

Figure 1. 3: Milling Orthogonal Cutting Model...3

Figure 1. 4:simple 3-D model of orthogonal cutting..3

Figure1.5:FEM discretization and heat exchange to the surrounding due to boundary condition 4

Figure 1. 6: The three metal cutting zones 5

Figure 3.1: Velocity boundary condition 22

Figure 3.2: Heat transfer boundary condition 22

Figure 3.3: Environment boundary condition 23

Figure3.4: The shape function for solid node 55 quadrilateral element......................26

Figure 3.5:assumption in dimensions of cutting process...34

Figure3.7: Thrust force and velocity at different depth of cut having constant feed=0.2mm............39

Figure3.6:cutting force and velocity at different depth of cut having feed=0.2mm........................ ..39

Figure 3.8: The effect of feed on cutting force having constant depth of cut=2mm....40

Figure 3.9: The effect of feed on thrust force having constant depth 41

f cut=2mm...41

Figure 3.10: Given parameters are for the process of stress calculation......................42

Figure 3.11:principle of stress theory...43

Figure 4.1: Finite element model constructed using solid works13.............................50

Figure 4.2: Mesh generation...51

Figure 5.1:applied loads for thermal analysis 52

Figure 5.2:a)temperature b)total deformation c)strain d) stress at v=1m/s and d=1mm54

Figure 5.3:a)temperature b)total deformation c) strain d)von-mises stress at v=1.5m/s and d=1mm..56

Figure 5.4:a)temperature b) total deformation c)strain d(von-mises stress at v=2m/s and d=1mm..58

Nomenclature

ε_1	Heat partitioning parameter between work piece and surrounding
ε_2	Heat partitioning parameter between work piece and tool
$F_c=F_N$	cutting force
h	Convective heat transfer coefficient
I	Moment of inertia
K	Thermal conductivity of the material
K_a	Thermal conductivity of air
k	Thermal diffusivity
Q	Heating power per unit volume
dQ/dt	Heat flux induced
q_{diss}	Heat dissipated by convection and radiation
q_{gen}	Heat generated
T_{reff}	Surrounding temperature
T_{avg}	Average temperature
T_{max}	Maximum temperature
T	Elapsed time
$\mu^{'}$	Equivalent coefficient of friction
ΔEK	The change in translational kinetic energy
ΔEP	The change in potential energy
FEA	Finite element analysis

ø	cutting angle
v	cutting velocity
P	Density of the material
C	Specific heat of a material
t	Uncut thickness of cutting condition
AISI	American institute of steel and iron
β	the angle between the resultant force and the normal force
F_P	power force
f	feedrate
U	specific energy
E	The emissive power
A	the surface area exposed to the surrounding
m	mass
f_f	$the\ frictonal\ force\ per\ unit\ contact\ area$
σ	$Stefan\ Boltzman\ constant (5.67 * 10^{-8})$
μ_{va}	$viscosity\ of\ the\ air$
c_{pa}	$specific\ heat\ capacity\ of\ the\ air$
d	depth of cut
E	young modulus
Ϭ	stress
Ɛ	strain
δ	deflection

CHAPTER ONE: INTRODUCTION

1.1 Background

Metal cutting or Machining is an important manufacturing operation in our day to day life[5]. Mainly the main deal of machining process is to create a surface with a specified shape and smooth surface finish preventing tool wear and thermal damage which leads losses of property, time consuming and geometric inaccuracy of the finished part. The thermodynamic approach to the activity at the cutting edge attempts to account for the energy consumed. Research has concluded that at least 99 percent of the input energy is converted into heat by deformation of the chip and by friction of the chip and work piece with the tool material[3]. The interface at which the chip slides over the tool is normally the hottest region during cutting and the maximum temperature is recorded exactly at the tool and work piece contact line[9] and this temperature is dependent on the following parameters.

- Type of work piece material,
- cutting speed,
- feed rate
- depth of cut
- type of cutting, orthogonal,oblique,milling,drilling
- cutting angles(position of tool and work piece)
- Tool geometry, coolant, and many other variables.

Due to the interaction of the chip and tool, which takes place at high pressures and temperatures higher heat energy creates, this energy is the cause for tool wear and damage. The life of the tool is predicted, depending on temperature and pressure which leads to bend or melting of the cutting tool[19].

1.2Types of metal cutting

The Most important machining operations in our day to day activities are

- Turning
- Drilling
- Milling

And there are other machining operations which are not common in our day to day activities like, Shaping and planning, Broaching and Sawing.

1.2.1 Turning

Single point cutting tool removes material from a rotating work piece to form the desired shape and surface finish: the case of lathe machine as shown in figure 1.1.

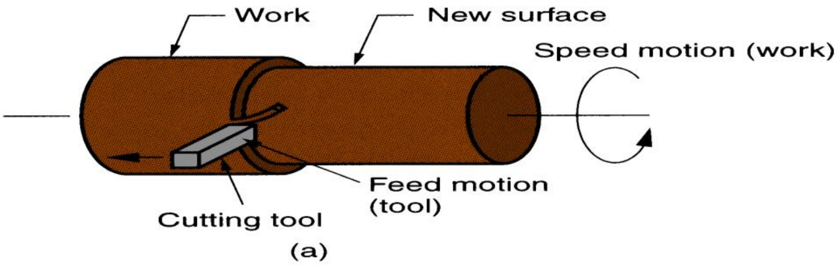

Figure 1.1: turning operation[10]

1.2.2 Drilling

This type of metal cutting operation is usually Used to create a round hole, by means of a rotating tool (drill bit)on fixed work piece that has two cutting edge shown in figure 1.2.

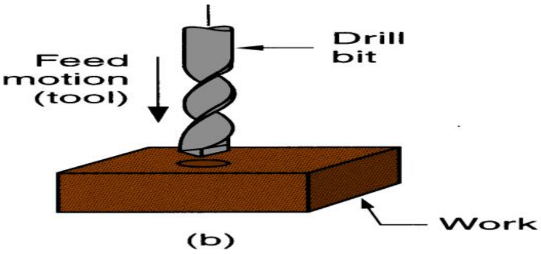

Figure1. 2:drilling operation**[10]**

1.2.3 Milling

This type of metal cutting operation is done by Rotating multiple-cutting-edge tool slowly, relative to work piece to generate plane or straight surface with small cutting thickness.

There are two types of milling, peripheral milling and face milling.

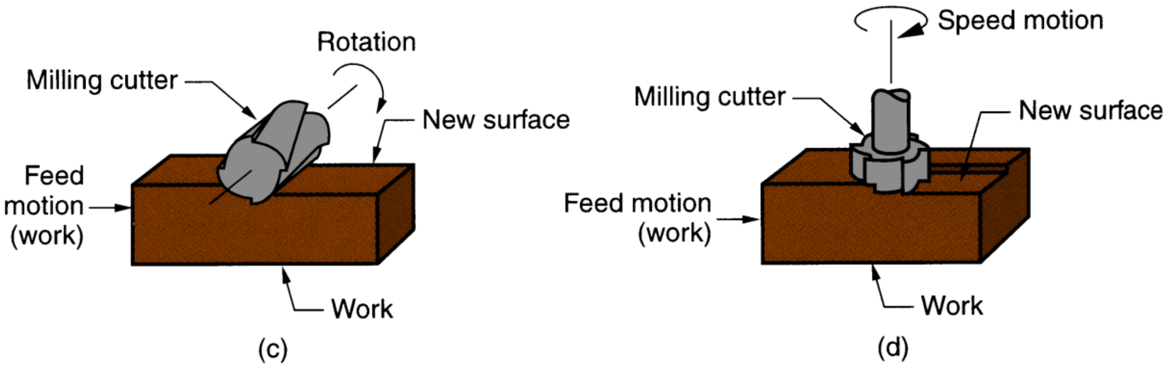

Figure 1. 3: Milling Orthogonal Cutting Model[10]

A simplified 2-D model of machining that describes the mechanics of machining fairly accurately[14].

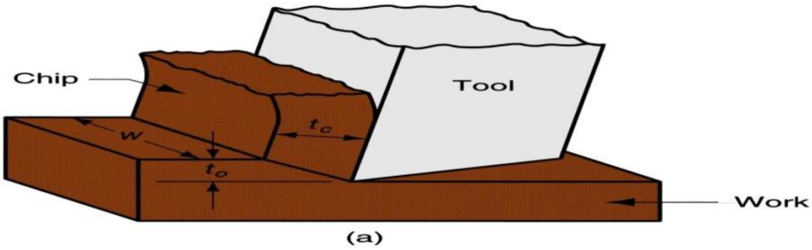

Figure 1. 4:simple 3-D model of orthogonal cutting[10]

1.3 finite element methods and variables in metal cutting

Finite element method is basically defined as dividing a continuum system to small elements (process of discretization) describing element properties as matrices and assembles them to reach a system of equations whose solutions argue the behavior of the total system[7].

FEM has a great use in modeling and simulation of orthogonal (2D) and oblique (3D) metal cutting process variables: Those metal cutting variables are[19]:

- temperature
- stress
- strain
- cutting force
- angle of cut(Φ) considering positive angle b/n work piece and tool

finite element method essentially consists of assuming a piecewise continuous function for solving and obtaining parameters of the functions such that reduces error in the solution by increasing number of elements, which mean as we go more number of elements we come up with an accurate solution for our system. Here the basic idea is to break up the geometry of the body into finite, simple shaped elements, thus the problem becomes solvable and it known applying more difficult steps make smaller error but more mathematical calculation will be carried out in order to find the solution. Mainly finite element method is Applicable on discretization on geometrical problems as Arc length and area of a circle, volume of a cylinder and sphere and for other complex geometries in real world phenomena.

It is clearly known that the heat transfer problem is very similar to the mechanics problem in terms of FEM analysis. The mechanics problem of displacement and force correspond to the heat transfer problem of temperature and heat flux, respectively FEM has a great use of modeling orthogonal (2D) and oblique (3D) metal cutting processes[6].

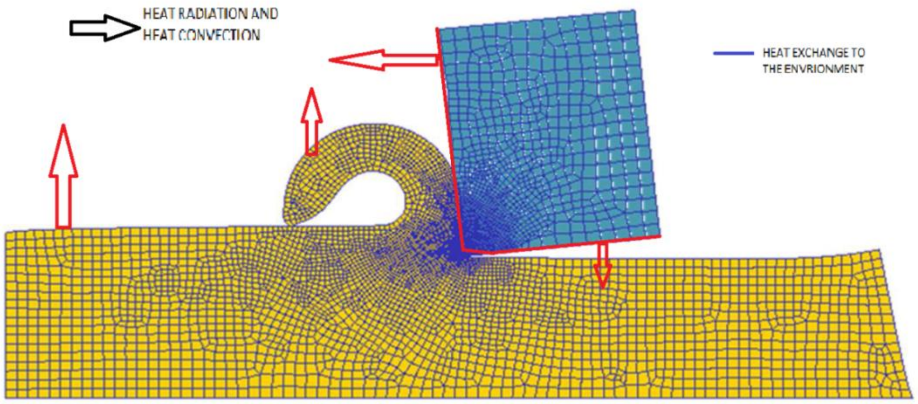

Figure1.5:FEM discretization and heat exchange to the surrounding due to boundary condition **[16]**

Three deformation zones in metal cutting process face different machining variables of metal cutting process including temperature distribution on each surface and the temperature exchange through radiation and conduction.

1. Primary shear zone (A-B in fig 1-6): The chip formation takes place firstly and mainly in this zone starting from the edge of the tool penetrates the work-piece. Material on this zone has been deformed by a concentrated shearing process in the main direction of cutting force.

2. Secondary shear zone (A-C in fig 1-6): The chip and the rake face of the tool are in contact b/n two points when the frictional stress on the rake face reaches a value equal to the shear yield stress of the work-piece material, material flow also occur on this zone.

3. Tertiary shear zone (A-D in fig 1-6): When the clearance face of the tool rubs the newly machined surface mainly deformation can occur on this zone.

In metal cutting process the heat transfer between the chip, the tool and the environment has a significant impact on wear mechanisms and hence on tool life and accuracy of the machined surface. The heat transfer at the tool-work piece interfaces commonly assumed to be governed by the interface heat-transfer coefficient. The interface heat transfer coefficient can be defined by the following equation[16].

$$h=\frac{Q}{\Delta T}$$

Where Q is the average heat flow and T is the temperature drop across the interface. It has been established that interface heat transfer coefficient is a function of several parameters, the dominant ones being contact pressure, interstitial materials, macro and micro geometries of the contacting surfaces, temperature and the type of lubricant or containment and its thickness For the FE modeling of metal machining processes, the thermal boundary conditions at the tool-chip interface are usually formulated in terms of the interface heat transfer coefficient. The interface heat transfer coefficient is an important input parameter to quantify the transfer of heat between the chip and the tool, and to accurately predict the temperature distribution within the cutting tool. In the application of interface heat transfer coefficient to the chip formation simulations, very high values of ‘h’ were used based on the assumption of perfect contact[3].

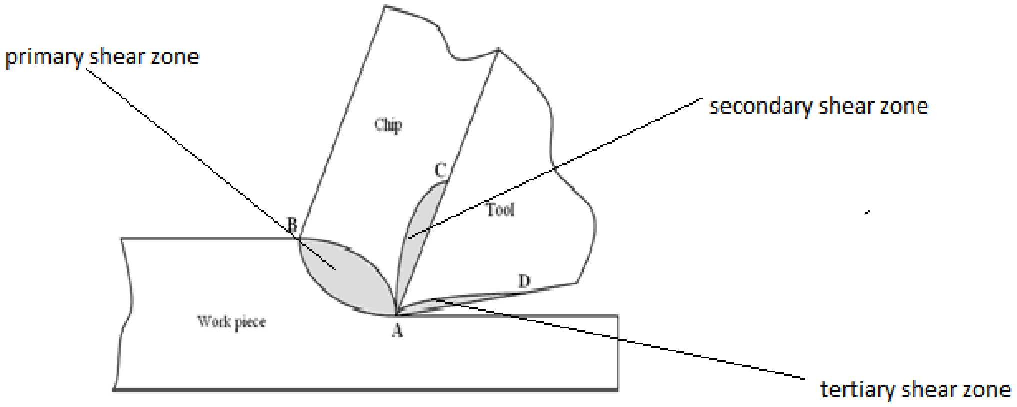

Figure1. 6: The three metal cutting zones **[3]**

1.4 Statement of the problem

Friction and plastic deformation are the cause of high heat generation, increasing the temperature of tool and work piece even above working service temperature, due to maximum speed and depth of cut, resulting failure of tool and undesired surface finish and investigating of temperature, strain and stress using experimental method is time consuming, expensive and not easily available.

1.5 Objective of the study

1.5.1 Main objective

The main role of the thesis is to simplify complex process of predicting variables such as temperature, cutting forces, strain and stress distributions and predicting tool life by simulating and modeling using finite element method than experimental method which is difficult to do so.

1.5.2 Specific objective

The specific objective of the thesis is showing the relation between variable parameters in metal cutting process using ANSYS software. The following relations are considered

- evaluating the effect of depth of cut and cutting speed on temperature gradient
- evaluating the effect of depth of cut and cutting speed on total deformation
- evaluating the effect of depth of cut and cutting speed on elastic strain
- evaluating the effect of depth of cut and cutting speed on von-mises stress
- evaluating the effect of feedrate and frequency ontemperature,strain,deformation and stress.

1.6 Methodology

In this stage all necessary data regarding milling, work piece and tool material properties, are collected from literatures and finite element analysis will be conducted at different parameters of depth of cut and speed.

1.6.1 Primary data collection

- The type of cutting and its principles will be studied from related literatures'.
- The work piece and tool materials and useful quantities describing their mechanical properties will considered.

1.6.2 Analytical solutions for temperature

The heat energy induced to the cutting process will be calculated from the power given to the cutting tool. In addition, the maximum temperature to be attained by the contact region will be calculated and the results will be recorded for later use in comparing it with the result obtained from the finite element analysis[18].

1.6.3 Finite element analysis

The finite element model of the work piece and the tool will be constructed using solid works and imported to the ANSYS 15 workbench for further analysis. The primary data collected in the previous steps will be an input to the finite element analysis.

To minimize the uncertainty arising the following assumptions are made

- Material for the FEA will be made to correspond to AISI1045 as work piece and uncoated tungsten as tool.
- The work material considered as fixed and the tool material moves with some velocity(V).
- The sounding temperature is assumed as 22c^o all times.

The finite element analysis will be conducted and the results analyzed as follows.

- The constructed finite element model will be imported to ANSYS workbench.
- Material will be selected as described above and be meshed properly
- The thermal and structural loads applied properly
- The temperature and stress distributions resulting from the superposition of the structural and thermal analysis will be collected from ANSYS 15 workbench outputs as tables, graphs and diagrams.
- These procedures will be repeated for each condition.

1.6.4 Analysis of the results obtained

The results from the finite element analysis will be analyzed and the contribution of feed rate, depth cut and velocity on cutting force, strain, stress and temperature investigated.

Then the result of this analysis will be evaluated and compared with the results of similar studies conducted by other researchers, Finally, the result of this analysis will be stated briefly so that it can be a reliable source to be used later in the conclusion stage.

1.6.5 Discussion on findings

The Results from the finite element analysis will be presented in tables, graphs and diagrams obtained from the superimposition of the transient structural and thermal Ansys workbench analysis.

1.6 Significance of the research

First and for most the risk arising from fall part of any equipment should be minimized significantly and the human causality and property loss associated with it should be avoided. Furthermore, the maintenance and replacement costs will be significantly minimized and the metal working companies will be benefited by implementing the recommendations and suggestions made at the end of this research. Moreover, the results of this research can be used in the future studies.

CHAPTER TWO:LITERATURE REVIEW

2.1 Introduction

Work piece and cutting tools suffer for high temperature values, thermal shock, fatigue, abrasion high stress and strain and chemical induced wear because of high heat generated due to friction and plastic deformation resulted from cutting variables and material type. This rise in temperature brings failure of the tool and lack of desired output inducing thermal crack, tensile residual stresses, strain and deformation[13].

2.2 Failure due to overheating

In metal cutting process due to high heat generation in primary and secondary shear zones high temperature is obtained even until melting point of the work piece material. This high temperature causes the following phenomena's.

- It reduces strength of the tool and formation of wear in the process, leads to Shorten tool life and cutting accuracy.
- Causes thermal distortion and un wanted shape may obtain.
- Causes large dimensional change in work piece which is result of thermal expansion so as making of control dimensional accuracy difficult parameter.

  When a material particle moves across the primary deformation zone the temperature rise is given by the formula[3].

$$T_p = \frac{1-\Lambda p}{\rho c v t w} \quad (2.1)$$

From Energy balance energy out is equal to energy in

Λp= Fraction of primary heat which goes to the work piece

P= Density of the material

C= Specific heat of a material

t, w =Uncut thickness and width of cutting condition

2.2.1 Thermal cracks

Heating allows producing small cracks which potentially progresses towards the failure of any machined product. Many thermal cracks can be removed, but care must be taken to make sure that the cracks have been completely eliminated.

2.2.2 Induced Tensile residual stresses

A very important category of tool failure is by the presence of tensile residual stresses at the contact region of tool and work piece. These compressive residual stresses are very useful for the tool to withstand fatigue stresses for the repeated work. However, the overheating reverses it to tensile stress. In the presence of tensile residual stresses, small thermal cracks may be sufficient to cause the sudden fracture of the tool[14].

2.2.3 Cutting Force

Most of the time cutting force acting on a tool is measured experimentally. But it is also important to predict quantity of cutting force and how different cutting parameters are affecting cutting force even before setting up the machining operation due to following reasons[1].

- In order to design of mechanical structure of cutting machine which will withstand cutting force and thrust force effectively.
- To determine power consumption during machining process. This will help in selecting suitable motor drive.
- To predict tool life.
- To increase productivity.

The important force in milling process is the cutting force; this force is thought of as a 3D vector that is represented by three components, namely, the power component, the radial component and the axial component in the tool coordinate system. Out of these three components, the greatest force normally is the power component, which is often we called the cutting force in cutting operation. This force is highly importance component of total force R. Force R is also resolved along the direction of tool motion into Fc, termed as the cutting force, and into F_T, the thrust force[8].In experimental determination of the cutting force, there are two hard problems: First and foremost is that the cutting force cannot be measured with reasonable accuracy although this fact has never been honestly admitted by the specialists in this field. The experiments were carefully prepared (the same batches of the work piece (steel AISI 1045), un coated tungsten tools) under the supervision of National Institute of standards and Technology (NIST) and replicated at four different most advanced metal cutting laboratories in the world(6). Interestingly, although extraordinary care was taken while performing these experiments, there was significant variation (up to 50%) in the measured Cutting force across these four laboratories. If less care is taken and no laboratory conditions are available then the accuracy of cutting force measurement would be much worse. Second, many tool and cutting inserts manufacturers (almost all manufacturing companies) do not have adequate dynamometric equipment to measure the cutting force. Many dynamometers used in this field are not properly calibrated because the known literature sources did not present proper experimental methodology for cutting force measurements using piezoelectric dynamometers. Therefore, they make practical calculations of the cutting force, another approach has to be thought should be proposed[8].

2.3 Related literatures

Many researchers have been conducting researches focused on improving the performance of the metal cutting process under different conditions. The efforts of these researchers cover wide range of issues related to the tool wear, thermo-mechanical behavior of the work piece and tool to improve design of tools geometry for a better residual stress distribution and temperature analysis of friction materials on thermo mechanical properties etc.

2.3.1 Velocity

They conduct two basic models of thought in their approach to the analysis of basic metal cutting mechanics;

1. Thin zone model which describe the cutting process at high cutting speeds condition.
2. Thick zone models which describe the cutting process at low cutting speeds condition.

2.3.1.1 Thin Zone Model

Piispannen , Merchant, Kobayashi and Thomsen, have favored the thin-plane (or thin zone) model, Merchant (1945) developed an analysis for thin-zone model having the following assumptions(12):

I) Tool tip is sharp, and no rubbing occur between the tool and the work piece.

ii) Deformation is always two dimensional.

iii) Stresses on the shear plane are uniformly distributed.

iv) Resultant force R applied at the shear plane is equal, opposite and collinear to the force R applied to the chip at the tool-chip interface.

This approach has two doubts. First, his assumption used minimum energy principle; this principle is not supported by exact evidence. Second, the differentiation assumes β and τ are Constants but β is not a constant and it is dependent of shear angle when β is the angle between the resultant force and the normal force. The resultant force R can be related to the other forces such as friction force F along the rake face or the power force FP in the direction of motion. Since this force is a vector quantity which can change in magnitude and direction, it is better to consider the two force components F_P along the work velocity and F_Q perpendicular to work velocity. These forces are

$$F_p = \frac{\tau t b cos(\beta-\alpha)}{\tau t b sin\phi cos(\phi+\beta-\alpha)} \tag{2.2}$$

$$F_q = \frac{\tau t b sin(\beta-\alpha)}{\tau t b sin\phi cos(\phi+\beta-\alpha)} \tag{2.3}$$

where τ is the shear stress on the shear plane assumed uniform over this plane and equal to shear yield stress of the work-piece material, $\boldsymbol{\phi}$ is the shear angle, α is the tool rake angle, t is the unreformed chip thickness, b is the width of cut, and β is the angle between the resultant force and the normal to the rake face. This angle represents the friction angle between the tool and chip.

Salomon and later Vaughn have discussed an interesting, in fact somewhat unusual, machining situation, which is known as ultrahigh speed machining. This is a metal cutting operation at cutting speeds in excess of 100 meters per min (Vaughn has tested up to speeds of 6096 meters per revolution).After a certain critical speed, which depends on the material being cut, the nature of the deformation is altered, giving a decrease in forces and temperatures, with further increase in speed. Vaughn has attributed this to a modified shear process, called adiabatic shear. At the very high speeds, it is suggested that limited time for heat flow, restricts the thermal energy generated by plastic flow to a preferred zone, causing weakening of this zone and additional shearing at low values of shear stress.

2.3.1.2 Thick model

Palmer and Oxley, and Okushima and Hitomi , have based analyses on a thick deformation region. They studied metal cutting at low cutting speeds and they derived slip line fields by using modified Hacky relationships. The Following assumptions are made in their analysis;

i) The Hacky relationships do not consider stress discontinuity or singularity at the tool tip.

ii) They assumed that the chip and tool were not in contact at the tool tip.

This analysis is used unrealistic assumptions such as no contact between the tool tip and chip. Another weak point of this analysis is that the deformation cannot be predicted analytically. During a metal cutting operation, high temperatures are generated because of Plastic deformation of work piece material and friction along the tool-chip interface. Determination of temperatures in tool, chip and work piece is important for process Efficiency because these temperatures have a great influence on the rate of tool wear[5].

Figure2.1 (a): was performed at different cutting speeds and at f=0.16mm/rev, γ =-5o, and at the same distance from the cutting edge (x=1.8643mm). It indicated from that at the speed of 103.2 m/min, the maximum temperature is 548oC, while at the speed of 250 m/min maximum temperature is 720C^{o}. In the cutting process when high cutting speed was used maximum stresses are obtained, and these stresses are more concentrated in the tool tip which may cause plastic deformation of tool edge. High temperatures are generated in the contact area because of plastic deformation of work piece material and friction along the tool/chip interface. When the cutting speed increases from 103.2 m/min to 250m/min, the increase in temperature was equal to 21.9%, which indicated that the tool-work piece interface temperature is closely connected to the cutting speed[12].

Figure2.1: (b) is drawn for temperature versus time at three values of the cutting speed, it is indicated from tha the maximum temperature is about (976$_{o}$C at interval of time=0.001093 ms) for v=200m/min, (T_{max}=759.2 $_{o}$C at t=0.001447 ms) for v=150 m/min and (T_{max}=659 C^{o} at t=0.00212 ms) for v=103.2 m/min, with increasing in the cutting speed, maximum temperature increased and the time in which high temperature occurred reduced. Power consumed in metal cutting was largely converted into heat, which leads to increase the heat generation near the cutting edge of the tool, so high value of temperature obtained[12].

Available experimental evidence indicates that the thick-zone model may describe the cutting process at very low speeds, but at higher speeds most evidence indicates that a thin shear plane is approached. Thus it seems that thin-zone model is likely the most realistic for practical cutting conditions. In addition, it leads to far simpler mathematical treatment than does the thick-zone model. For these two reasons the analysis of the thin zone has received far more attention and is more complete than that of the thick zone.

2.3.2 Temperature

It is known that determination of exact temperature rise in the tool–chip interface is recognized as an important factor in achieving the best cutting performance in metal cutting process that is the reason why several researchers have become interested in determining the temperature histories on the rake face of cutting tools. Many of temperature measurement techniques have been developed over the years are experimental techniques to determine the temperature distribution of the tool chip interface, although direct measurements of temperatures at the tool–chip–work piece interfaces are very difficult due to the cutting movement and the small contact areas involved. Due to these experimental difficulties finite element method is used to model; and simulate temperatures of contact. Approximately 98% of the energy in machining is converted into heat this can cause temperatures to be very high at the tool chip interface and the remaining energy (about 2%) is retained as elastic energy in the chip[17].The temperature distribution in different nodes on the tool has different value**.** The maximum node temperature is obtained exactly in the middle contact between the work piece and tool. The highest temperature of the tool surface and located at a distance nearby the tool tip, this was due to high heat generation in the contact region between tool and work piece. As the node is far of the cutting edge, it has temperature lower than the nearest node to the contact area due to heat transfer parameters

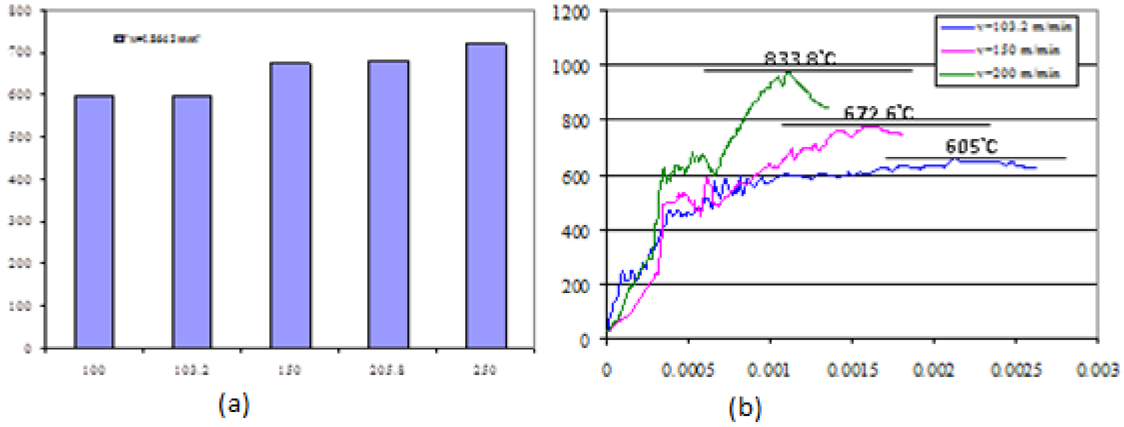

Figure 2.1:a)Temperature vs. cutting speed at f=0.16mm/rev

b) Temperature vs. time at different cutting speed

The temperature distributions in the work piece and chip during orthogonal machining that is in case of milling operation are obtained numerically using the Galarkins approach of finite element method. The effect of a number of process variables such as speed, feed rate, coolant type, rake angle, tool flank wear and tool material type on the temperatures is crucial[12].

2.3.3 feed rate

The distribution of temperature and heat flux along the interface predicted for different feed rate is shown in **figure2.2(a)**. As the feed rate increases, the section of chip increases and consequently friction increases, this lead to increase cutting forces, especially in thrust direction. It is observed that the region of high stresses in the thrust direction turns inward as the feed increases, which may result in increase in temperatures generated, so the temperature at interface increases. As the feed rate increases from 0.16 mm/rev to 0.25mm/rev, the temperature increases in a 13.82%. The effect of feed rate on the heat flux can be shown in **Figure2.2 (b):** it was clear from that figure when the feed rate increased high temperature generated due to cutting large pieces from the metal in one revolution, which transmitted as a heat flux between tool and work piece[12]

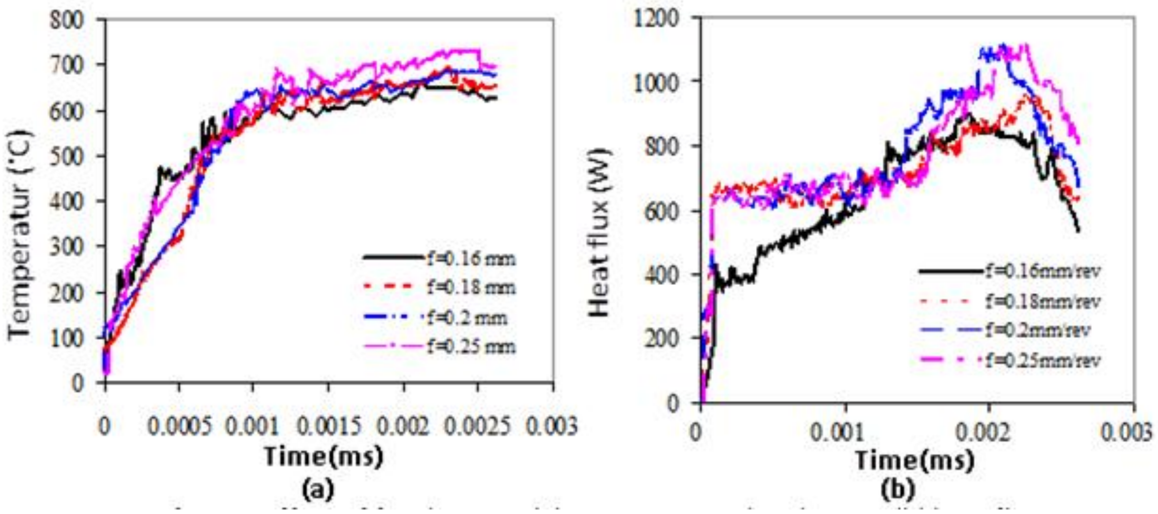

Figure 2.2: The effect of feed rate(a)on Temperature (b)heat flux

2.3.4 Rake angle

The rake angle is one of the most important parameters, which determine the tool and work piece contact area temperature stress and strain. There is generally an optimum value rake angle for cutting condition, increasing of the rake angle over its optimum value has a negative effect on the tool performance and accelerates the tool wear. Three different rake angles (-5º,0º, 5º) are considered .The effect of different rake angles on temperature distribution was shown in **Figure2.3(a) .** Maximum temperature is reaches to 656 $_{o}$C, 605 $_{o}$C and 593 $_{o}$C when rake angle is equal to -5º, 0º and 5º respectively. It can be noticed with a reduction in the rake angle, promotes a longer contact length and hence a larger contact area with more heat conducting into the tool, therefore high heat will be generated, so the temperature increases when the negative rake angle is used. On the other side by increasing the positive rake angle (higher shear angle produces), the cutting forces were decreased; the reason is that the tool can plunge into the work piece easily(12).

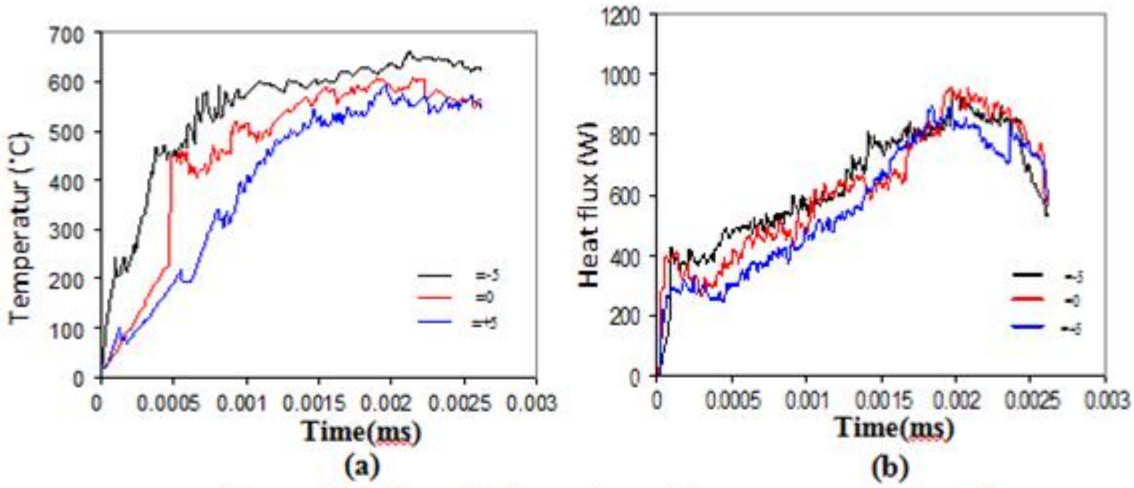

Figure 2.3: The effect of rake angle on (a)temperature (b) heat flux.

2.3.5 Tool shape

Geometry affect local temperatures distribution in the cutting tool. The tool geometry must designed to cut various work piece metals by forming chips in a smooth way, also providing a strong cutting edge. Insert geometry for finishing will have an area comprising smaller feeds and depths while at the other end, a rough-turning geometry will have a large feed and depth values. The finishing insert uses the geometry at the corner of the insert while the roughing one uses a relatively long part of the main cutting edge. The tool shape details arrange and have the same noise radius and height, the different between these tools is the shape. The effect of the shape of tool on temperature and heat flux behavior drawn in **Figure2.4 ,** at the beginning of cutting process TNMA has the largest value of temperature than the other shapes, when cutting process progress VNMA has the large value of temperature and TNMA has the lowest value. At the ending of cutting TNMA has the large value of maximum temperature than the other shapes of tool.

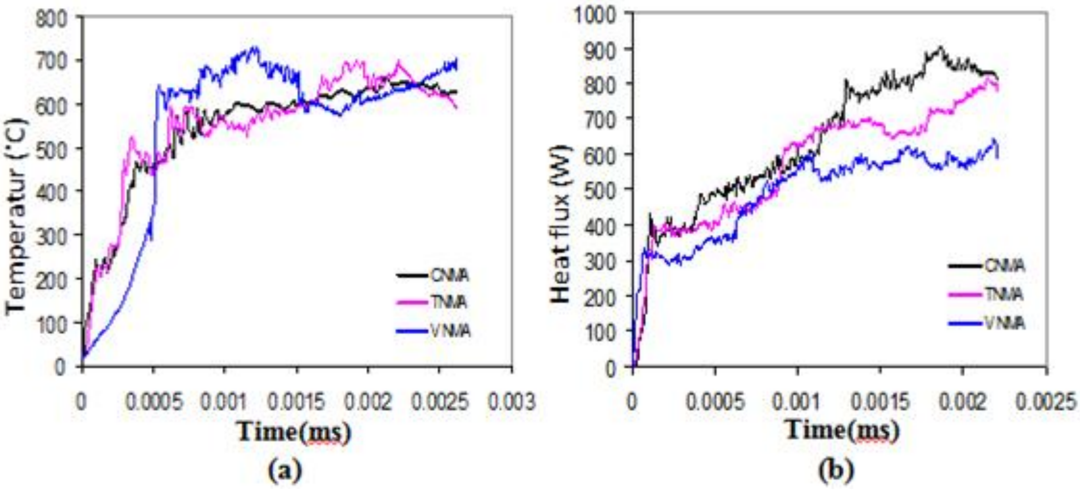

(a)

(b)

Figure 2.4:The effect of tool shape on (a)temperature (b) heat flux

2.3.6 Work piece material type

Effect of Work piece Material on Temperature Distribution and Heat Flux Four curves have been plotted for different materials (these materials were selected because of their suitability and widely used in the model by previous researcher) as shown in Figure 2.5 (a) and (b)[12]. The temperature dependent properties should be considered when calculating the cutting temperature, so the thermal properties of the work piece such as the thermal conductivity and specific heat as functions of (T) are shown .The heat capacity for the four materials equal, so they behavior depending on thermal conductivity. For the same range of temperature AISI1025 and AISI1030 have the same behavior of thermal conductivity, while AISI1045 has a larger value at a lower temperature, AISI 316h has a lower thermal conductivity than other materials. Thermal conductivity of these four materials was depending on temperature and effect on the temperature distribution in the contact region, so the curves oscillated and overlap with each other depending on variation of their thermal properties[12].

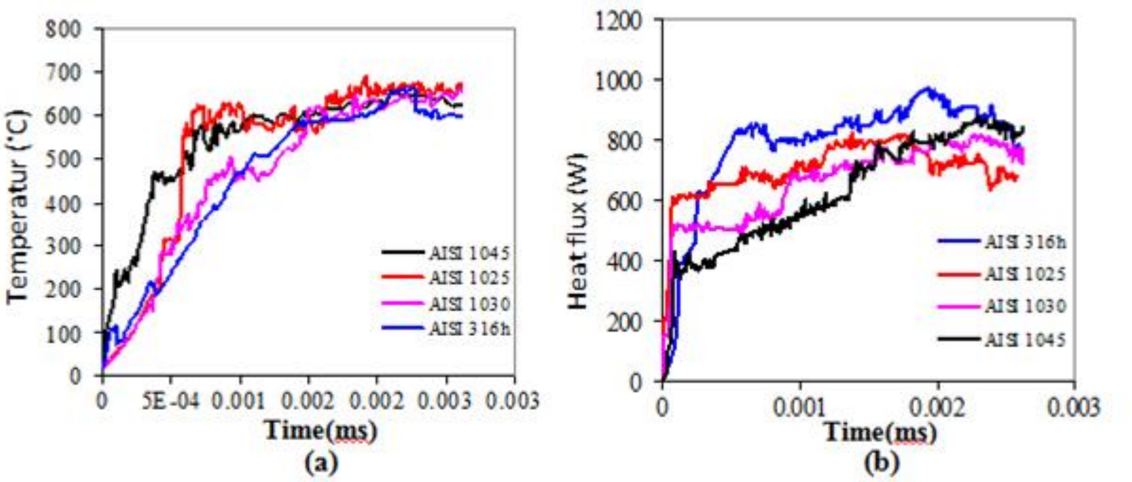

Figure 2.5:a) The effect of work piece material on (a)temperature (b) heat flux

Effect of Tool Material On Temperature Distribution And Heat Flux

Figure2.6 presented the values of temperature **(a)** and heat flux **(b)** for different tool materials. It is easy to understand that the Tic coating induces the lowest temperature rise and heat flux due to the fact that coating tool leading to decrease of the tool–work piece contact area, decrease of the thickness of the secondary shear zone[12].

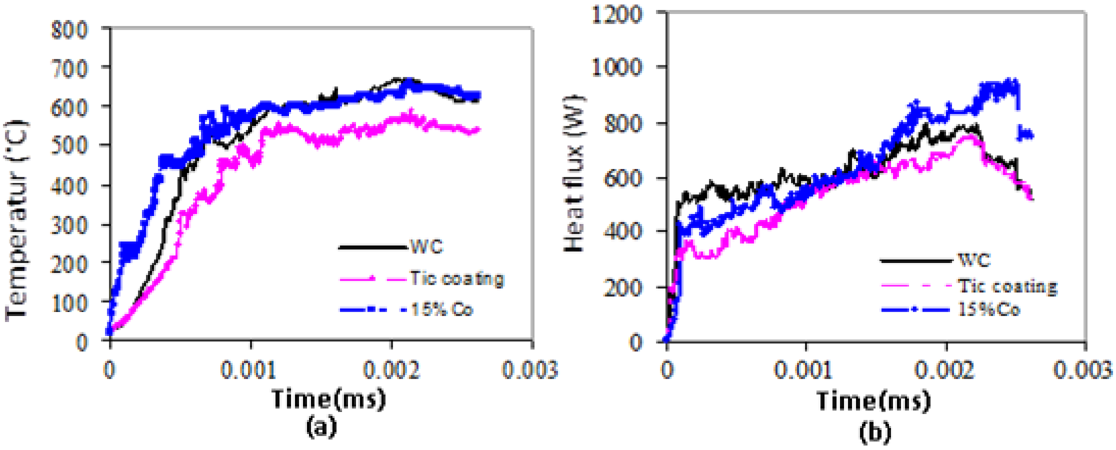

Figure 2.6: The effect of tool material on (a)temperature (b) heat flux

2.4 lubricant selections

Temperature in metal cutting can be controlled by Application of cutting fluid (coolant, changing the cutting condition by reduction of cutting speed and/or feed, Selection of proper cutting Geometry like Positive tool orthogonal rake angle.

Function of cutting fluids

- Lubrication system
- Reduction of cutting force and energy in the process
- Cooling conditions
- Chip removal
- Improves product surface finish

The cutting fluid should posses the following properties

- It should have high thermal conductivity and high specific heat
- It should posses good lubricating properties
- It should be odorless
- Non-corrosive to work and machine non-toxic to operating
- It should have low viscosity to permit free flow of the liquid

Types of cutting fluids

Cutting fluids may be water based or oil based Oil based cutting fluids are Chlorinated oil, Mineral oils, Fatty oils, Sulphurized oil and Soluble oils.

CHAPTER THREE:NUMERICAL AND ANALYTICAL SOLUTIONS

3.1 Numerical solutions

In many practical machining situations, finding the temperature in a solid body is the most importance in terms of the maximum allowable temperature, In this study, the derivation of the finite element equations was carried out using Variation method as well as Gala kin method for the three dimensional heat conduction equation. The governing differential equation for transient temperature is given as[20];

$$Ni(\frac{\partial}{\partial x}\left(k1(t)\frac{\partial T}{\partial x}\right)+\frac{\partial}{\partial y}\left(k2(t)\frac{\partial T}{\partial y}\right)+\frac{\partial}{\partial z}\left(k3(t)\frac{\partial T}{\partial z}\right)-\rho cp\frac{\partial T}{\partial t})\,d\Omega \tag{3.1}$$

Where k1, k2, k3 are thermal coefficients of the cutting process in x, y, z direction respectively.

3.1.1 Material properties

Thermal Conductivity

Conduction is the process by which heat flows from a region of higher temperature to a region of lower temperature within a medium. The Thermal Conductivity in this case is the ability of the material to conduct heat within an object's boundary. Temperature dependent!

Thermal Expansion

Defines the material's tendency to grow and shrink with changes in temperature. Temperature dependent!

Heat Capacity

The Heat Capacity for a given material is the measure of the change in internal energy per degree of temperature change. Temperature dependent!

Emissivity

The emissive power (E) of a body is the total amount of radiation emitted by a body per unit area and time. The Emissivity (e) of a body is the ratio of E/Black body where Black body is the emissive power of a perfect black body.

Table3. 1:Percentage material composition of AISI1045[9]

Carbon (C)	**Manganese (Mn)**	**Silicon (Si)**	**Phosphorus (P)**	**Sulfur (S)**
0.42-0.50	0.60-0.90	0.15-0.35	0.035	0.040

Table3. 2:Percentage material composition of un coated tungsten[9]

Tungsten **Wc**	**Nickel** **Ni**	**iron** **fe**
0.89-0.91	0.05-0.075	0.03-0.055

3.1.2 Object boundary conditions

1. Object condition

2 .interior object condition

3. Environment object condition

Object condition

There are three parameters to be considered under this condition.

I friction In metal cutting process there are two component forces frictional and normal force, and there are two frictional forces these are friction between tool and chip and friction between tool and work piece.

II object velocity or movement in this condition the tool is moving with velocity VC in x direction and it is fixed in y direction while the workspace is considered as fixed in both directions[11].

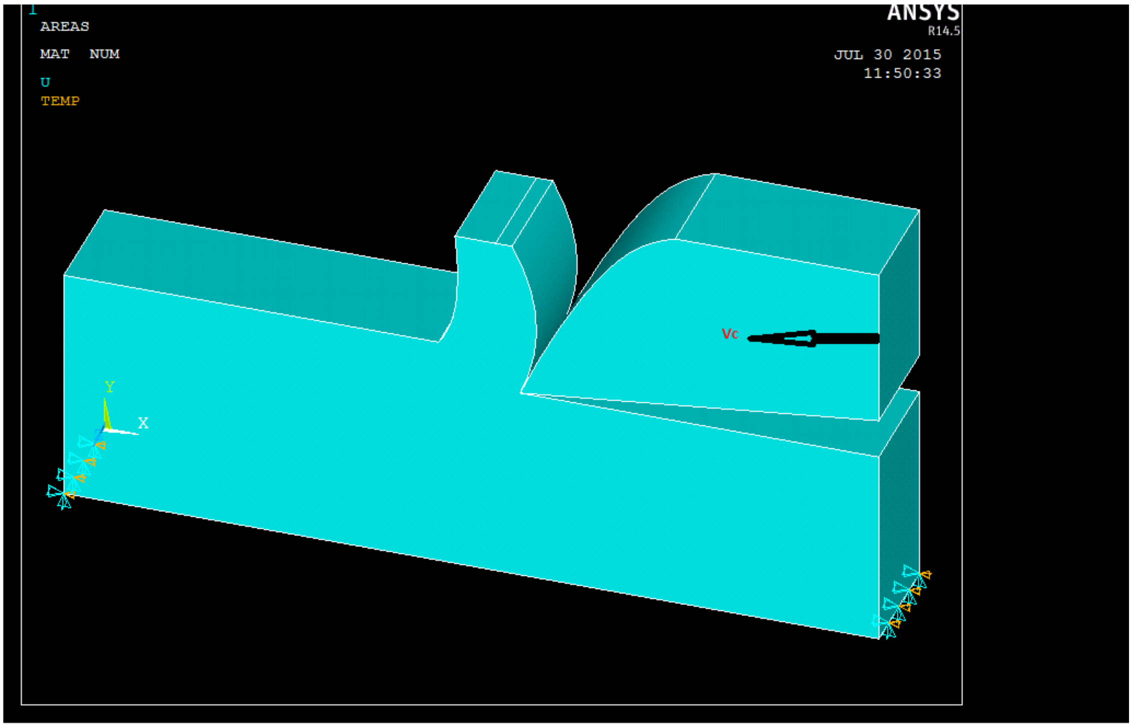

Figure 3.1 : Velocity boundary condition

III heat transfer: the process of cutting have high temperature at the tool tip so as there is heat transfer from the tool and workspace at the tip to the other side.

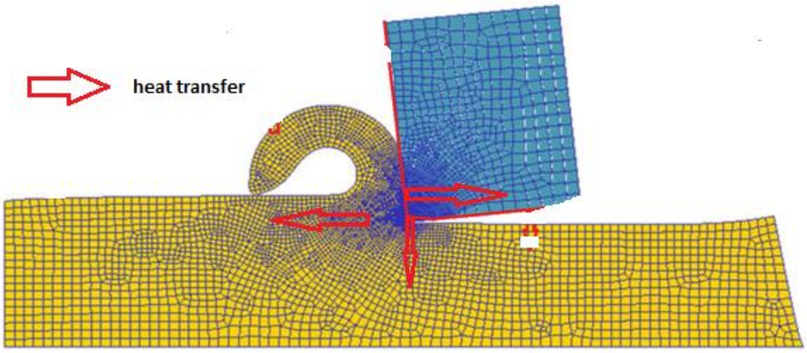

Figure 3.2: Heat transfer boundary condition[7]

Interior object conditions

This includes frictional force and internal heat transfer from the tool tip towards each side.

Environment object condition

Since the process is exposed to the environment there is always heat convection and heat radiation in all directions.

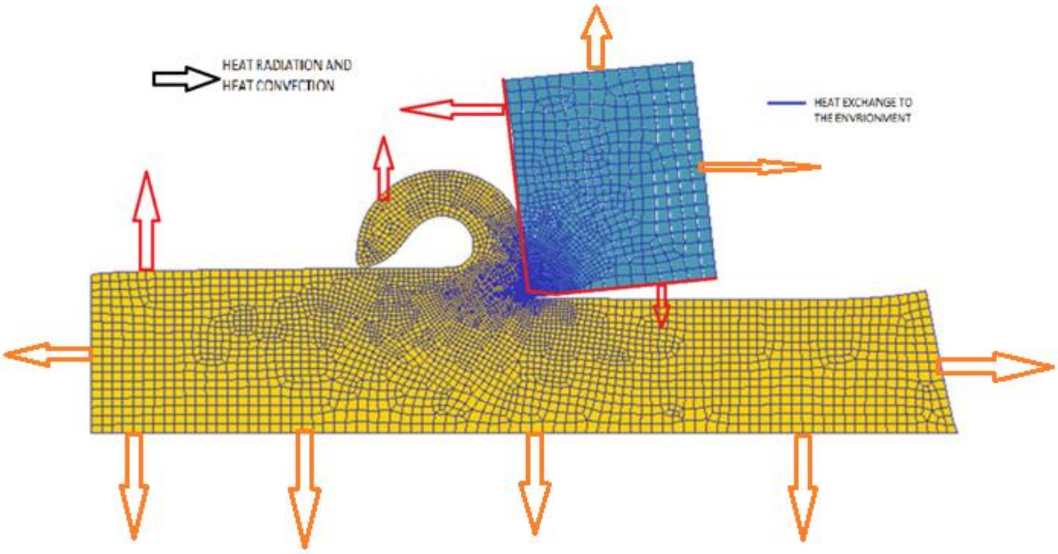

Figure 3.3: Environment boundary condition

T=T∞ on the surface=22 C^O

$$-k\partial T\frac{\partial T}{\partial n} = h\infty(T - TC) \qquad (3.2) \quad on\ Sc$$

$$-k\partial T\frac{\partial T}{\partial n} = h\infty(T - T\infty) \qquad (3.3) \quad on\ SH$$

$$-k\partial T\frac{\partial T}{\partial n} = 0 \qquad (3.4)\ on\ So$$

For the heat transfer calculations, the following assumptions are made:

i) The contact between the tool and the chip is thermally perfect. Hence a very large value of the interface heat transfer coefficient (h) is used and it is fixed to 1000 kW/m^2

ii) The boundaries that are sufficiently away from the cutting zone remain at the room temperature (T=22ºC)

iii) The chip and the tool loss heat due to heat convection (h=10 W/m2 ºC) on the free surfaces on the work piece.

iv) Heat loss due to radiation is very small and it is neglected.

Let have the transient temperature analysis

3.1.3 Galarkins approach

The application of the Galarkin's method for the transient equation subjected to appropriate boundary and initial conditions is addressed. The temperature is discredited over the analysis area as follows[18]:

$$T(x,y,z,t)=\sum_{i=0}^{n} Ni(x,y,z)Ti(t) \tag{3.5}$$

Where Ni are the shape functions in n number of nodes in an element and T(t)is time dependant nodal temperatures. Then the gala kin method gives.

$$\int Ni(\frac{\partial}{\partial x}\left(k1(t)\frac{\partial T}{\partial x}\right)+\frac{\partial}{\partial y}\left(k2(t)\frac{\partial T}{\partial y}\right)+\frac{\partial}{\partial z}\left(k3(t)\frac{\partial T}{\partial z}\right)-\rho c_p\frac{\partial T}{\partial t})\, d\Omega \tag{3.6}$$

Applying integration by parts on the three terms of the Equation and inserting boundary conditions we get the following.

$$-\int \frac{\partial Ni}{\partial x}\left(k1(t)\frac{\partial T}{\partial x}\right)+\frac{\partial Ni}{\partial y}\left(k2(t)\frac{\partial T}{\partial y}\right)+\frac{\partial Ni}{\partial z}\left(k3(t)\frac{\partial T}{\partial z}\right)-\rho cp\frac{\partial T}{\partial t})\, d\Omega+\int NiK1(t)\frac{\partial T}{\partial x}ldTij+$$
$$\int NiK2(t)\frac{\partial T}{\partial y}mdTij\int NiK3(t)\frac{\partial T}{\partial z}ndTij \tag{3.7}$$

Over the domain of Tij

Note that from this Equation;

$$=\int NiqdTi-\int Nih(T-Ti)dTij \tag{3.8}$$

On substituting the spatial approximation from Equation, finally it becomes

$$\int (k1(T)\frac{\partial Ni}{\partial x}\frac{\partial T}{\partial x}Ti(t)+\int k2(T)\frac{\partial Ni}{\partial y}\frac{\partial T}{\partial y}Ti(t)+\int k3(T)\frac{\partial Ni}{\partial z}\frac{\partial T}{\partial z}Ti(t)$$
$$-Ni\,\rho cp\frac{\partial T}{\partial t})d\Omega\int -Ni\,\rho cp\frac{\partial Ni}{\partial t}T(t)d\Omega$$
$$-\int NiqdTij-\int Nih(T-Ta)dTij=0$$

(3.9)

Where i and j represent the nodes, and it can be written in a convenient form as;

{C}{$\frac{\partial T}{\partial t}$}+ {K/T}={f} (3.10)

Where

[Cij]=$\int \rho cpNiNj\, d\grave{}\Omega$ (3.11)

[Kij]=$\left[\int (k1(T)\frac{\partial Ni}{\partial x}\frac{\partial NJ}{\partial x}(Ti) + \int k2(T)\frac{\partial Ni}{\partial y}\frac{\partial Nj}{\partial y}(Ti) + \int k3(T)\frac{\partial Ni}{\partial z}\frac{\partial Nj}{\partial z}(Ti)\right] d\grave{}\Omega +$
$\int hNiNj\, dt$ (3.12)

[f]=$-\int qNidTij +$
$\int NihTadT$ (3.13)

In matrix form

[C]= $\int \rho cp[N]^T[N]d\grave{}\Omega$ (3.14)

[K]= $\int [B]^T[D\backslash B]d\grave{}\Omega + \int h[N]^T[N]dT$ (3.15)

The thermal conductivity matrix becomes;

$$D = \begin{bmatrix} K & 0 & 0 \\ 0 & K & 0 \\ 0 & 0 & K \end{bmatrix}$$

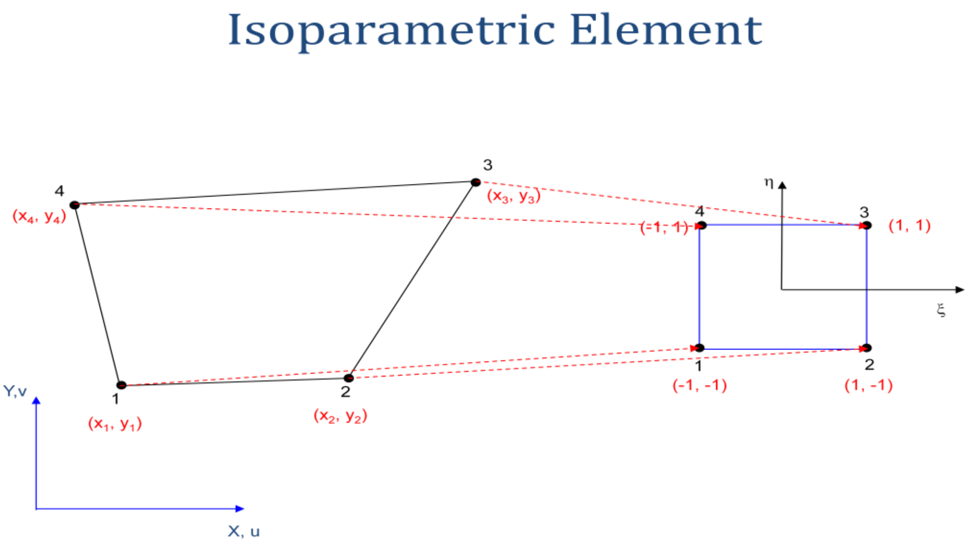

Figure 3.4: The shape function for solid node 55 quadrilateral element[15]

$$N1=\frac{1}{4ab}(x-x_2)(x-x_4) \tag{3.16}$$

$$N2=-\frac{1}{4ab}(x-x_1)(x-x_2) \tag{3.17}$$

$$N3=\frac{1}{4ab}(x-x_4)(y-y_2 \tag{3.18}$$

$$N4=\frac{1}{4ab}(x-x_3)(y-y_1) \tag{3.19}$$

$$N1=-\frac{1}{4}(1-\xi)(1-\eta) \tag{3.20}$$

$$N2=-\frac{1}{4}(1+\xi)(1-\eta) \tag{3.21}$$

$$N3=-\frac{1}{4}(1-\xi)(1+\eta) \tag{3.22}$$

$$N4=-\frac{1}{4}(1+\xi)(1+\eta) \tag{3.23}$$

Nodal shape functions for displacement is given as follows

$$\begin{bmatrix} u \\ v \end{bmatrix} = \begin{bmatrix} N1 & N2 & N3 & N4 & 0 & 0 & 0 & 0 \\ 0 & 0 & 0 & 0 & N1 & N2 & N3 & N4 \end{bmatrix} \tag{3.24}$$

The displacement and strain relationships:

$$\varepsilon_x=\frac{\partial u}{\partial x}=\frac{\partial u}{\partial \xi}.\frac{\partial \xi}{\partial x}+\frac{\partial u}{\partial \eta}.\frac{\partial \eta}{\partial x} \tag{3.25}$$

$$\varepsilon_y=\frac{\partial v}{\partial y}=\frac{\partial v}{\partial \xi}.\frac{\partial \xi}{\partial y}+\frac{\partial v}{\partial \eta}.\frac{\partial \eta}{\partial y} \tag{3.26}$$

$$\begin{bmatrix} \varepsilon_x \\ \varepsilon_y \\ \varepsilon_{xy} \end{bmatrix} = \begin{bmatrix} \frac{\partial u}{\partial x} \\ \frac{\partial v}{\partial y} \\ \frac{\partial u}{\partial y}+\frac{\partial v}{\partial x} \end{bmatrix} = \begin{bmatrix} \frac{\partial \xi}{\partial x} & \frac{\partial \eta}{\partial x} & 0 & 0 \\ 0 & 0 & \frac{\partial \xi}{\partial y} & \frac{\partial \eta}{\partial y} \\ \frac{\partial \xi}{\partial y} & \frac{\partial \eta}{\partial y} & \frac{\partial \xi}{\partial x} & \frac{\partial \eta}{\partial x} \end{bmatrix} . \begin{bmatrix} \frac{\partial u}{\partial \xi} \\ \frac{\partial u}{\partial \eta} \\ \frac{\partial v}{\partial \xi} \\ \frac{\partial v}{\partial \eta} \end{bmatrix} \tag{3.27}$$

But it is not easy to find $\frac{\partial \xi}{\partial x}$ and $\frac{\partial \eta}{\partial x}$ therefore Coordinate transformation should be taken for simplification.

$$\frac{\partial u}{\partial \xi}=\frac{\partial u}{\partial x}\cdot\frac{\partial x}{\partial \xi}+\frac{\partial u}{\partial y}\cdot\frac{\partial y}{\partial \xi} \quad (3.28)$$

$$\frac{\partial u}{\partial \eta}=\frac{\partial u}{\partial x}\cdot\frac{\partial x}{\partial \eta}+\frac{\partial u}{\partial y}\cdot\frac{\partial y}{\partial \eta} \quad (3.29)$$

$$\begin{bmatrix}\frac{\partial u}{\partial \xi}\\ \frac{\partial u}{\partial \eta}\end{bmatrix}=\begin{bmatrix}\frac{\partial x}{\partial \xi} & \frac{\partial y}{\partial \xi}\\ \frac{\partial x}{\partial \eta} & \frac{\partial y}{\partial \eta}\end{bmatrix}\cdot\begin{bmatrix}\frac{\partial u}{\partial x}\\ \frac{\partial u}{\partial y}\end{bmatrix} \quad (3.30)$$

$$\begin{bmatrix}\frac{\partial x}{\partial \xi} & \frac{\partial y}{\partial \xi}\\ \frac{\partial x}{\partial \eta} & \frac{\partial y}{\partial \eta}\end{bmatrix} \quad (3.31)$$

=J Jacobin matrix

$$\frac{\partial x}{\partial \xi}=\Sigma\frac{\partial Ni}{\partial \xi}xi\,\frac{\partial y}{\partial \xi}=\Sigma\frac{\partial Ni}{\partial \xi}yi \quad (3.32)$$

$$\frac{\partial x}{\partial \eta}=\Sigma\frac{\partial Ni}{\partial \eta}\mathrm{xi}\frac{\partial y}{\partial \eta}=\Sigma\frac{\partial Ni}{\partial \eta}yi \quad (3.33)$$

$$\begin{bmatrix}\frac{\partial u}{\partial x}\\ \frac{\partial u}{\partial y}\end{bmatrix}=[J]^{-1}\begin{bmatrix}\frac{\partial u}{\partial \xi}\\ \frac{\partial u}{\partial \eta}\end{bmatrix} \quad (3.34)$$

$$\boldsymbol{\Sigma}\mathrm{x}=\frac{\partial u}{\partial x}=J_{11}^{*}\,\frac{\partial u}{\partial \xi}+J_{12}^{*}\,\frac{\partial u}{\partial \eta} \quad (3.35)$$

When $J_{11}^{*}\ and\ J_{12}^{*}$ first row coefficient of jacobian matrix

$$\frac{\partial u}{\partial \xi}=\Sigma\frac{\partial Ni}{\partial \xi}\mathrm{ui}\quad\text{and}\quad\frac{\partial u}{\partial \eta}=\Sigma\frac{\partial Ni}{\partial \eta}ui \quad (3.36)$$

The element stiffness matrix will be

$$[k]=\int[B]^{T}[E][B]dV=\int_{-1}^{1}\int_{-1}^{1}[B]^{T}[E][B]t|J|d\xi d\eta$$

$$[\mathrm{K}]=\int[B]^{T}[D\backslash B]d\Upsilon+\int h[N]^{T}[N]d\Upsilon \quad (3.37)$$

The gradient matrix is given by;

$$g=\begin{bmatrix} \frac{\partial T}{\partial x} \\ \frac{\partial T}{\partial y} \\ \frac{\partial T}{\partial z} \end{bmatrix}=\begin{bmatrix} \frac{\partial Ni}{\partial x} & \frac{\partial Nj}{\partial x} & \frac{\partial Nk}{\partial x} \\ \frac{\partial Ni}{\partial y} & \frac{\partial Nj}{\partial y} & \frac{\partial Nk}{\partial y} \\ \frac{\partial Ni}{\partial z} & \frac{\partial Nj}{\partial z} & \frac{\partial Nk}{\partial z} \end{bmatrix} \tag{3.38}$$

$$B=\begin{bmatrix} \frac{\partial Ni}{\partial x} & \frac{\partial Nj}{\partial x} & \frac{\partial Nk}{\partial x} \\ \frac{\partial Ni}{\partial y} & \frac{\partial Nj}{\partial y} & \frac{\partial Nk}{\partial y} \\ \frac{\partial Ni}{\partial z} & \frac{\partial Nj}{\partial z} & \frac{\partial Nk}{\partial z} \end{bmatrix} \tag{3.39}$$

3.2.1Analytical solution for maximum cutting temperature

Since this is a thermo-mechanically coupled model, there are also thermal boundary conditions defined. First of all, the work piece is losing heat to the environment, which is assumed to be at 20 °C, at a rate of 0.4 N/mm.°C. Work piece loses heat to the environment due to convection according to the following formula.

$$q = h \cdot (T_w - T_0) \tag{3.40}$$

where, h is the convection heat transfer coefficient of the work piece (0.4 N/(mm.°C)), T_w is the work piece surface temperature, and T_o is the ambient temperature (20 C°).

3.2.2 Analytical Model for frictional force

The heat generated during friction, its distribution to the work piece, tool and chip then to the surrounding air are of importance in the thermal analysis.

The heating power generated between the contacting surfaces is given by:

$$q(r) = f_f r v \tag{3.41}$$

Where:

$f_f = the\ frictional\ force\ per\ unit\ contact\ area$

$v = the\ velocity\ of\ the\ tool$

$r = the\ radius\ of\ the\ tool$

The frictional force per unit contact area can be calculated as:

$$f_f = \frac{\mu F_N}{A} \tag{3.42}$$

Where: F_N $the\ normal\ force$

$\mu = the\ friction\ coefficient$

$A = contact\ surface\ area$

The heat conduction is a time dependent phenomena that can be computed using transient heat transfer equations as follows.

$$\rho c_p\left(\frac{\partial T}{\partial t}\right) + \nabla(-k\nabla T) = Q - \rho c_p u \nabla T \tag{3.43}$$

Where the material properties for the wheel and block are:

$\rho = density\ of\ material$

$k = Thermal\ conductivity$

$c_p = specific\ heat\ capacity$

$u = velocity\ field$

$Q = heating\ power\ per\ unit\ volume$

3.3 Cutting Force and Thrust Force analysis

The determination of the cutting force is based upon the calculation of power Pc spent in machining process and is calculated as follows;

$$\boldsymbol{P_c = F_c * v_c} \tag{3.53}$$

This power dictates the energy required for cutting, cutting temperatures, plastic deformation of the work material, machining residual stress and other parameters. In this work machining of medium carbon steel AISI 1045 (the ultimate tensile strength = 655 MPa, the tensile yield strength = 375 MPa) is considered as work piece material resulted, greater tool life, lower required power, cutting temperature, machining residual stresses than those obtained in the machining of stainless steel AISI 316L (Ϭr= 517 MPa; $\boldsymbol{\tau}$y = 218 MPa). The prime reason is that any kind of strength of the work material in terms of its characteristic stresses cannot be considered alone without corresponding strains, which determine the energy spent in deformation of the work material. Only when the stress and corresponding strain are known, other parameters-outcomes of the metal cutting process can be calculated.

3.3.1 Proposed methodology for cutting force calculation

The proposed methodology is based on the definition of the metal cutting process proposed by and the model of energy partition in the metal cutting system based on this definition. According to this model, the power balance in the cutting system can be written as[14]

$$P_c = \mathrm{P_{pd}} + \mathrm{P_{fr}} + \mathrm{P_{ff}} + \mathrm{P_{ch}} + \mathrm{P_{mn}} \qquad (3.54)$$

From which the cutting force is calculated

$$\frac{\mathrm{P_{pd}+P_{fr}+P_{ff}+P_{ch}+P_{mn}}}{\mathrm{v}} = \mathrm{Fc} \qquad (3.55)$$

Where Ppd is the power spent on the plastic deformation of the layer being removed, $\mathrm{P_{fr}}$ is the power spent on the tool-chip interface, $\mathrm{P_{ff}}$ is the power spent on the tool-work piece interface, $\mathrm{P_{ch}}$ is the power spent in the formation of new surfaces, $\mathrm{P_{mn}}$ is the energy spent due to the combined influence of the minor cutting edge.

3.3.1.1 Plastic Deformation

The power spent on the plastic deformation of the layer being removed, Ppd , can be calculated from the chip compression ratio and parameters of the deformation curve of the work material as follows.

$$P_{pd} = \frac{\mathrm{K}(1.15\ \ln\varsigma)^{\mathrm{n}+1}}{\mathrm{n}+1} vAw \qquad (3.56)$$

Where K is the strength coefficient ($\mathrm{N/m^2}$) and n is the hardening exponent of the work material, ς is the chip compression ratio (Astakhov, 2004, 2006), Aw is uncut chip cross-sectional area ($\mathrm{m^2}$)[12].

Aw = dw*f, dw is the depth of cut (m), f is the cutting feed per revolution (m/rev).

For AISI1045 from property table we have
K=1.34Gpa,n=0.25

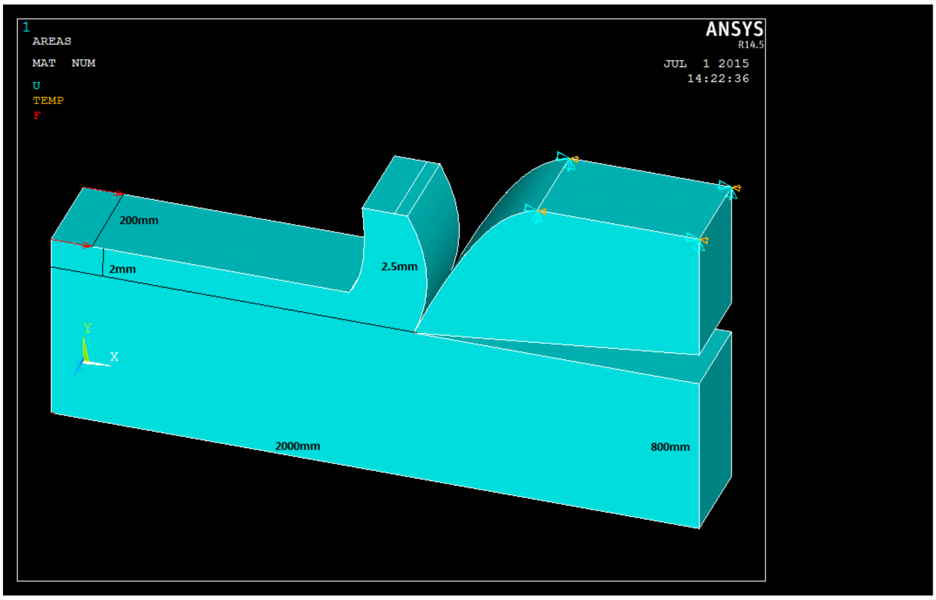

Figure 3.5:assumption in dimensions of cutting process

From the cutting model assumption we have

Aw=dwf=2mm for dw and 20mm for width

$A_w=0.00004m^2$

3.3.1.2 Friction at the Tool-Chip Interface

The power spent due to friction at the tool-chip interface is calculated as

$$P_{fR} = \boldsymbol{\tau}_c l_c b_{1T} \frac{v}{\varsigma} \tag{3.57}$$

Where $\boldsymbol{\tau}c = 0.28\sigma R$ is the average shear stress at the tool-chip contact (N/m^2)

σ_R is the ultimate tensile strength of the work material (N/m^2),

Lc is the tool-chip contact length (m),

b_{1T} is the true chip width (m).

$\sigma_R = 0.585Gpa, \tau_c = 0.28 * 0.585Gpa$ =0.1638Gpa

The tool-chip contact length is assumed as, Lc=5mm (assumption)

B_{1T}=2.5mm ,V=1m/s

$P_{fr} = \tau_c l_c b_{1T} \frac{v}{\varsigma} = 0.1638Gpa * 0.005m * 0.0025m \frac{1m/s}{1.25}$ =163.8w

3.3.1.3 Formation of New Surfaces

The power spent in the formation of new surfaces, P_{ch} is calculated as the product of energy required for the formation of one shear plane and the number of shear planes formed per second, i.e.,

$$P_{ch} = E_{fr} * f_{cf}. \tag{3.58}$$

Where f_{cf} is the frequency of chip formation, i.e., the number of shear planes formed per second, E_{fr} is the energy of fracture per a shear one shear plane. The frequency of chip formation determines how many shear planes form per second of machining time. This frequency depends primarily on the work material and the cutting speed as discussed by Astakhov (1998=1999). Figure 4 provides some data for common work materials.

The work of fracture per a shear plane is[14].

$$E_{fr} = E_{ch} * A_{fr} \qquad (3.59)$$

Where E_{ch} is the cohesive energy (J/m2) (Shet and Chandra, 2002), Afr is the area of fracture (m2).The area of fracture is the area of the shear plane determined.

F_{cf} is assumed to be 1 kHz

A_{fr} =0.0025m*0.002m=0.000005m2

E_{ch} =42000J/m2 from property table

E_{fr}=0.000005*42000=0.21J

P_{ch} = 0.21J* 1 KHz=210w

3.3.1.4 Friction at the Tool-Work piece Interface

The power spent due to friction at the tool-work piece interface is calculated as

$$\mathbf{P_{fF} = F_{fF} * v} \qquad (3.60)$$

Where F_{ff} is the friction force on the tool–work piece interface.

$$F_{ff} = 0.625\boldsymbol{\tau}y\boldsymbol{\rho}c\ l_{ac}\sqrt{\frac{Br}{sina}}$$

where $\boldsymbol{\tau}_y$ is the shear strength of the tool material (N/m2), $\boldsymbol{\rho}$c is the radius of the cutting edge (m), $\boldsymbol{\alpha}$ is the normal flank angle (deg), l_{ac} is the length of the active part of the cutting edge (the length of the cutting edge engaged in cutting) (m).

$Br=\frac{cos'\Upsilon}{\varsigma-sin'\Upsilon}$

where ′Y is the normal rake angle (deg) assumed to -6 deg and $\boldsymbol{\alpha}$ is the normal flank angle (deg)=6, $Br=\frac{\cos(-6)}{1.25-\sin(-6)}=0.734$

$\boldsymbol{\tau}_y$=283Gpa for un coated Wc

$\boldsymbol{\rho}$c=0.05mm (assumption) and Lac=0.04mm

F_{ff}=0.625*283Gpa *0.00005* 0.00004*$\sqrt{\frac{0.734}{sin6}}$ =933.9N

P_{ff}= Fff*v=933.9N*1m/s=933.9w

$$F_c = \frac{P_{pd}+P_{fr}+P_{ff}+P_{ch}+P_{mn}}{v} \quad (3.61)$$

$$F_c=\frac{800w+163w+933.9w+210w+0}{1m/s}=2{,}107\text{N}$$

Table 3.3: Property table for cutting process[16]

Property	AISI1045	Un coated wc
Bulk Film temperature coefficient(w/mk)	15	110
Bulk modulus(Gpa)	163	400
Coefficient of thermal expansion(m/k)	0.000015	0.0000071
Compression strength(Mpa)	420	6833
Density(kg/m3)	7700	15880
Ductility	0.012	0.0074
Elastic limit (Mpa)	210	530
Endurance limit (Mpa)	450	420
Energy content(MJ/kg)	122	200
Hardness (Mpa)	170	3600
Maximum service temperature(k)	923	1050
Melting point(k)	1793	3193
Poisons ratio	0.29	0.31
Tensile strength (Mpa)	585	530
Thermal conductivity (w/mk)	51.9	88
Shear modulus (Gpa)	80	283
Specific heat capacity (J/kgk)	433	960
Youngs modulus (Gpa)	200	600

Table3. 3:input parameters for AISI1045[16]

Variable	Symbol	Unit	Value
Depth of cut	d_w	M	0.002
Cutting feed per edge	F	m/edge	0.0004
Strength coefficient	K	Gpa	1.34
Hardening exponent	N		1.6
Chip compression	Ç		1.25
Ultimate tensile strength of the work material	Ϭr	Gpa	0.585
Normal rake angle	$\boldsymbol{\alpha}$	Deg	-6
Shear strength of the work material	$\boldsymbol{\tau}_y$	Gpa	283
Normal flank angle	α^*	Deg	6
Cohesive energy per unit fracture area	E_{ch}	J/m2	42000
Frequency of chip formation	F_{cf}	Hz	1000

Table 3.4:cutting force from experiment and from the proposed methodology

Cutting Speed (m/s)	Feed (mm/edge	Depth of cut (mm)	Frequency (kHz)	Cutting force calculated through the measured power (N)	Cutting force calculated using proposed methodology (N)
1	0.20	3	1.0	1580	1608
1.5	0.20	3	1.6	1348	1389
3	0.2	3	3.0	1348	1389
4	0.2	3	4.0	1076	1104
1.5	0.3	3	1.6	873	945
1.5	0.4	3	1.6	1562	1606
1.5	0.2	2	1.6	1640	1676
1.5	0.2	5	1.6	940	998

As we see from table3.5 both the cutting force from experiment and from the proposed methodology increases when the velocity decreases, this shows the inverse relation b/n them.

Table 3.5:The effect of velocity

velocity	Depth of cut=1mm		Depth of cut=1.5mm		Depth of cut=2mm	
	Cutting force[N]	Thrust force[N]	Cutting force[N]	Thrust force[N]	Cutting force[N]	Thrust force[N]
1	1707	171	1907	191	2107	211
1.5	1637	164	1837	184	2036	204
2	1602	161	1802	181	2012	202
2.5	1582	159	1781	179	1985	199
3	1567	158	1767	177	1967	197

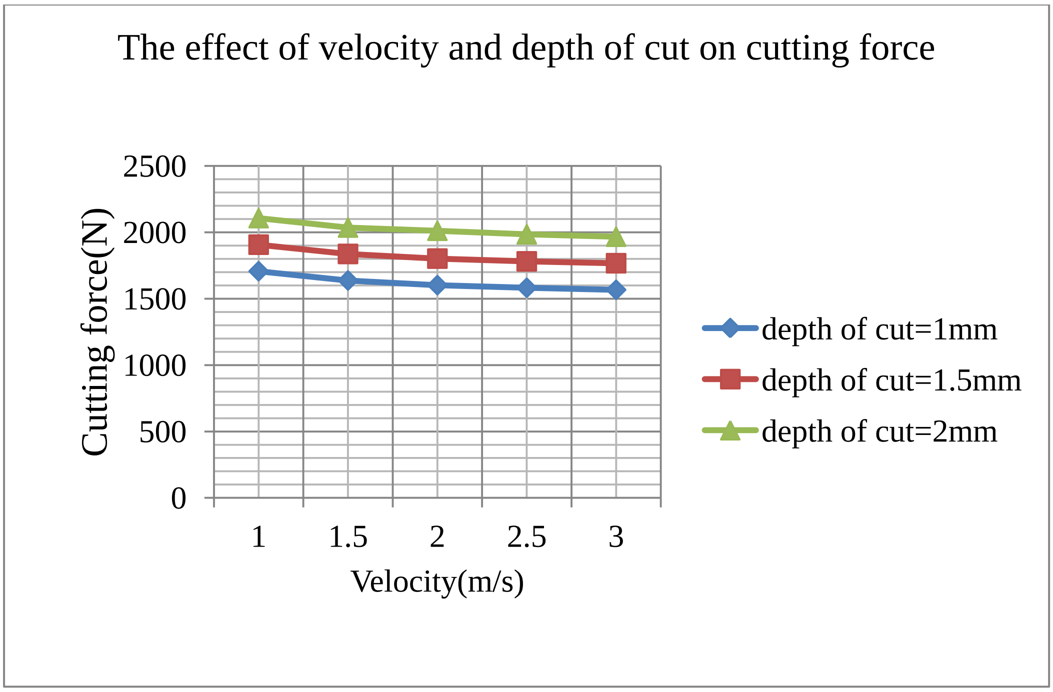

Figure 3.6:cutting force and velocity at different depth of cut having feed=0.2mm

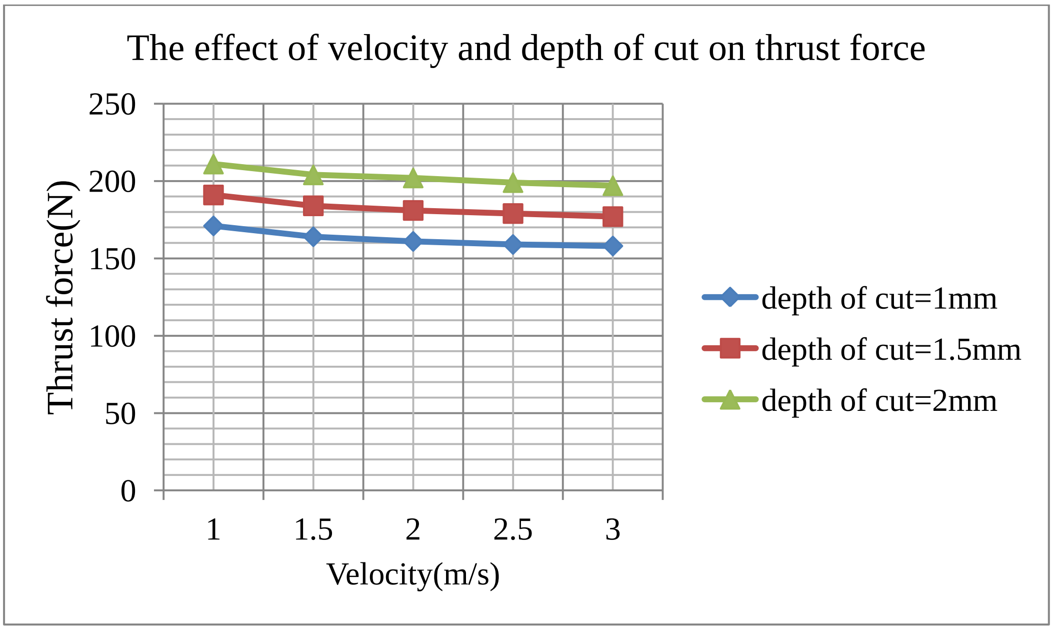

Figure3.7: Thrust force and velocity at different depth of cut having constant feed=0.2mm/edge

Table 3.6: The effect of feed on cutting force and thrust force

Feed rate	Velocity=1m/s		Velocity=1.5m/s		Velocity=2m/s	
	Cutting force[N]	Thrust force[N]	Cutting force[N]	Thrust force[N]	Cutting force[N]	Thrust force[N]
0.1mm	1697	170	1626.9	164	1591	160
0.15mm	1892	188	1821	182	1786	179
0.2mm	2087	210	2016.9	201	1981	199
2.5	2282	229	2211	222	2176	218
0.3m	2477	248	2406	241	2371	238

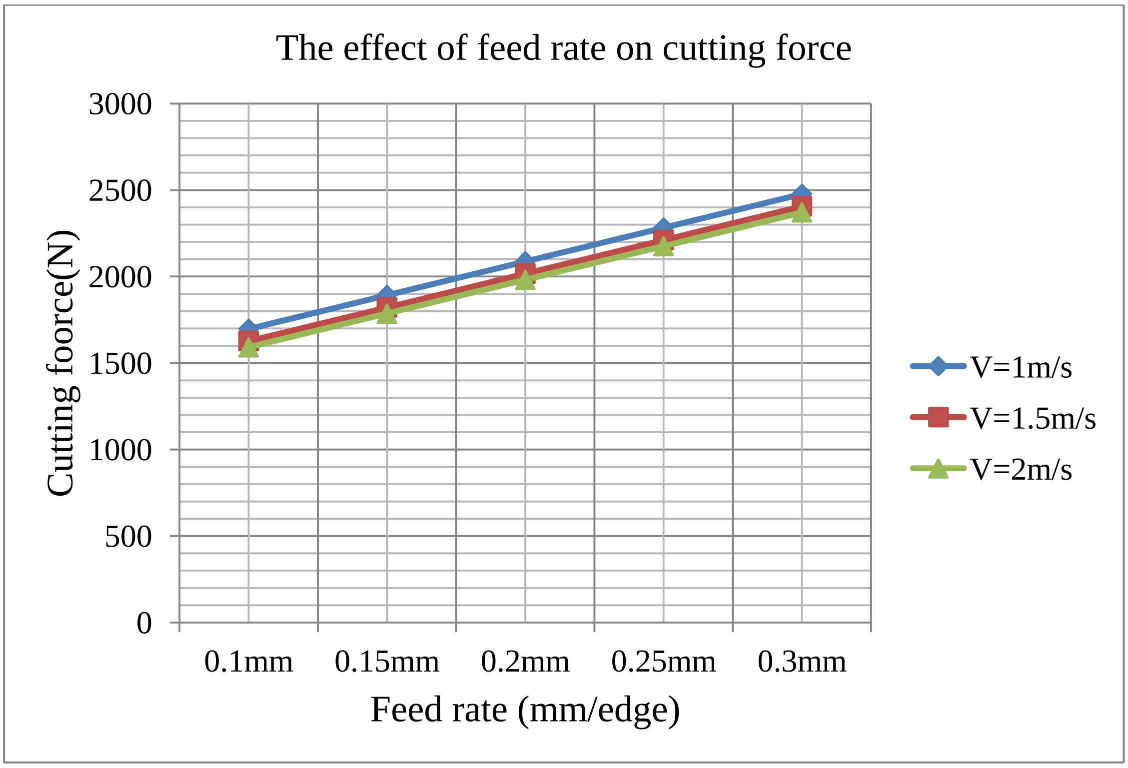

Figure 3.8: The effect of feed on cutting force having constant depth of cut=2mm

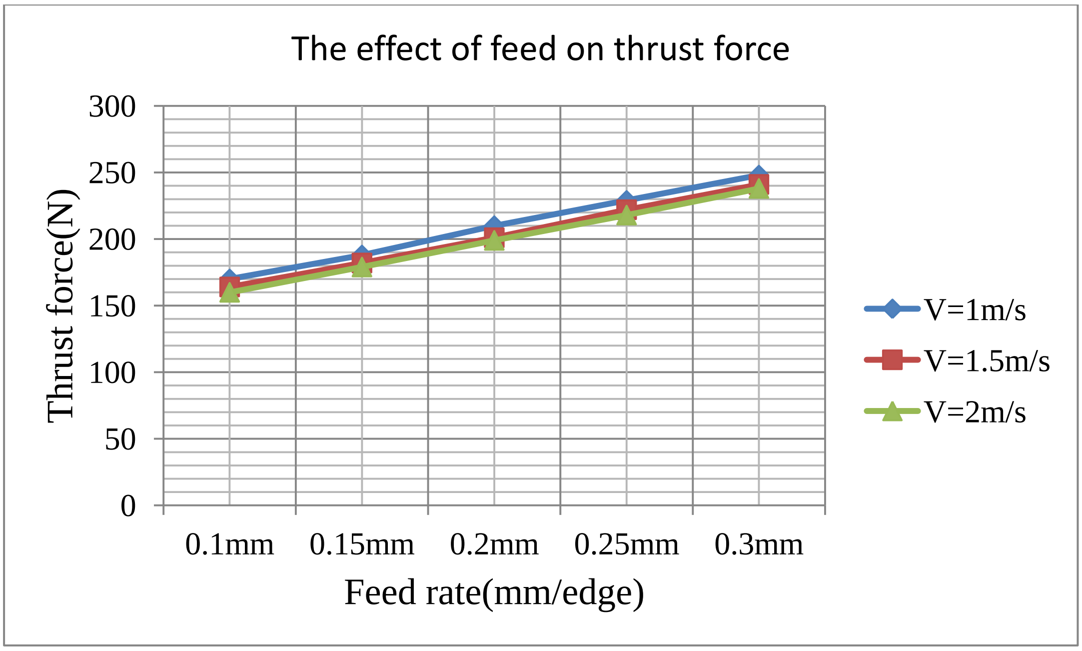

Figure 3.9: The effect of feed on thrust force having constant depth of cut=2mm

Thrust force analysis using the methodology proposed

Vector addition of Fc and Ft = resultant R is given by

$tan\Phi = \frac{Ft}{Fc}$, Ft=$F_c$tanΦ=F_c tan6^o=0.10517

Table3. 7: Thrust force calculated

Cutting Speed (m/s)	Feed (mm/edge)	Depth of cut (mm)	Thrust force calculated using the methodology (N)
1	0.20	3	162
1.5	0.20	3	138
3	0.2	3	139
4	0.2	3	113
1.5	0.3	3	96
1.5	0.4	3	162
1.5	0.2	2	169
1.5	0.2	5	10.6

3.4 Shear Stress and strain distribution

3.4.1 Shear stress distribution in metal cutting

3.4.1.1 Structural Stress analysis due to cutting force

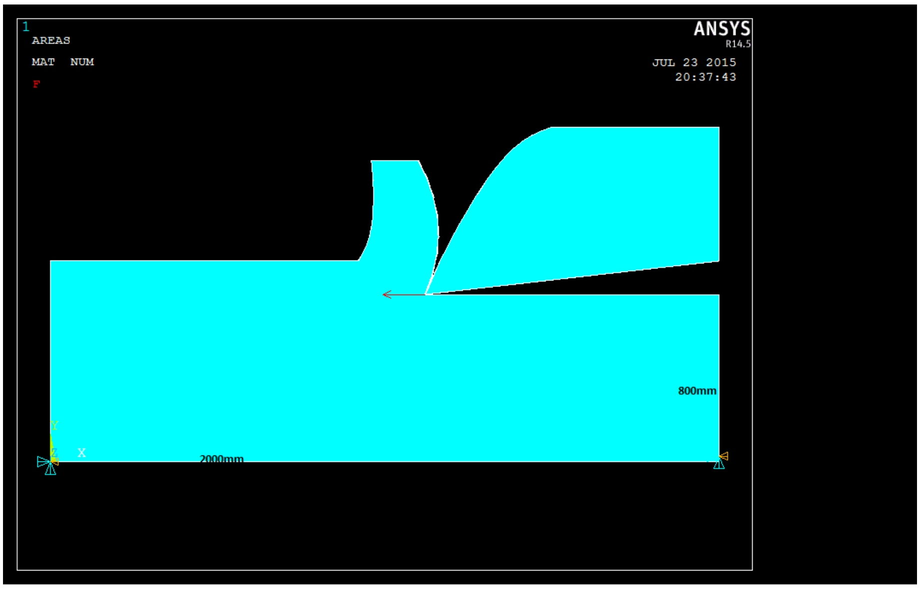

Figure 3.10: Given parameters are for the process of stress calculation

Length L=200mm,Width, w =200mm,Height, h=800mm.Fc=2008N,E=200Gpa

$$I = \frac{W \ast h^3}{12} = \frac{0.2 \ast 0.8^3}{12} = 0.00853m4$$

$$6 = \frac{M \ast C}{I} = \frac{2008 \ast 0.4}{0.00853} = 94.16kpa$$

$$\varepsilon = \frac{6}{E} = \frac{94160}{200000000000} = 0.00000047$$

$$\delta = \frac{ML^2}{2EI} = \frac{2008 \ast 2^2}{2 \ast 200000000000 \ast 0.00853} = 0.000002354m$$

=2.354µm

Where

E, young modulus Ϭ, stress Ɛ, strain δ, deflection I, moment of inertia and M, cutting force

3.4.1.1 Stress and strain analysis due to high temperature

$$\sigma_f=\sigma o.T(T)\left(1+\frac{\varepsilon_p}{\varepsilon_o}\right)^{1/n} \qquad (3.62)$$

where, n is the hardening exponent, T is the current temperature, σo is the initial yield stress at the reference temperature T_0, ε_p is the reference plastic strain, $T(T)$ is a thermal softening factor ranging from 0 to 1 and has a general representation depending on the work piece material of interest[22].

There are three different flow stress models on the finite element simulation and modeling of orthogonal cutting process on AISI 1045 steel using coated tungsten carbide (wc). material behavioral models in finite element modeling are elastic, ideal plastic, plastic with strain hardening and elastic plastic with strain hardening.

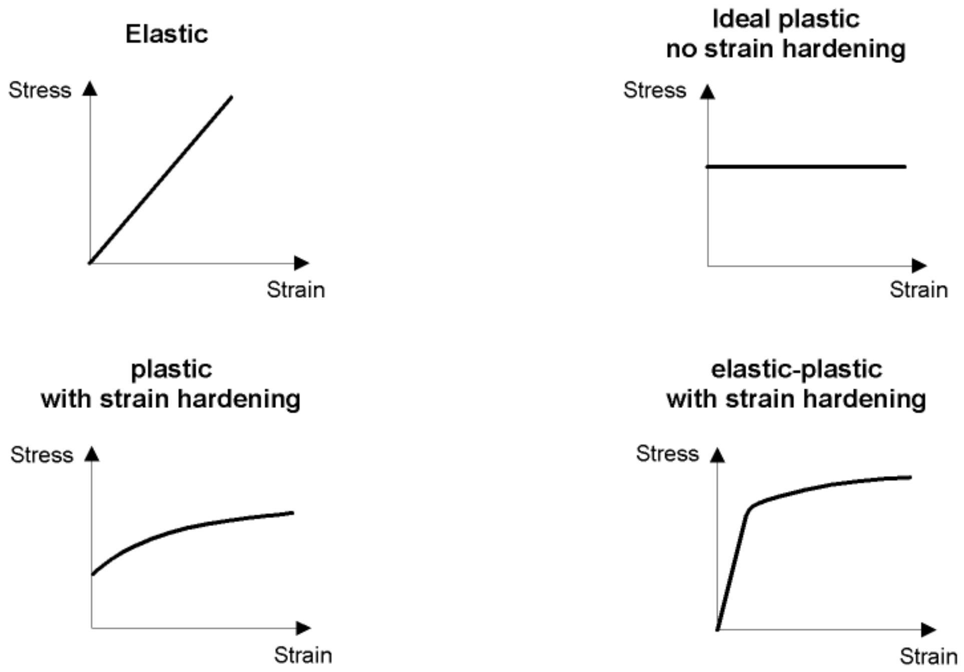

Figure 3.11:principle of stress theory[23]

Mathematically stress is defined as the ratio of force and area at which this force acts on

$$\sigma = \frac{F_s}{A_s} \qquad (3.63)$$

Where A_s = area of the shear plane

The flow stress or instantaneous yield strength is the stress at which work material starts to plastically deform. Temperature, strain, strain rate and metallurgical microstructure of the material are the main parameters to occur. The Oxley-C and MJ-C flow stress models were chosen for the investigation process to study the orthogonal cutting process of AISI 1045 steel material.

3.4.1.1.1Oxley18 and his co-workers

Developed the following material model by employing the stress-strain data of 0.16%, 0.33%, 0.49%, and 0.52% plain carbon steel generated from high speed Compression tests:

$$\sigma = \sigma_1 \varepsilon^n \qquad (3.64)$$

where σ_1 is the material flow stress at $\varepsilon=1$; and *n*, the strain-hardening index. Values of σ_1 and *n* are determined by using the velocity, modified temperature Tmod, which is defined as

$\mathrm{Tmod} = [1 - v \log10 (\varepsilon/\varepsilon_0)]\ T$

Where n and ε_0 are two constants for a given material and a range of testing conditions. This model has been utilized in the orthogonal cutting of low and medium carbon steel in conjunction with slip-line field analysis and as an analytical solution to predict cutting forces, average strain and strain rate in the primary shear zone[23].

3.4.1.1.2 Johnson-Cook Model

Johnson and Cook19 developed a constitutive equation for materials based on torsion and dynamic Hopkinson bar tensile tests over a wide range of strain rates and temperatures for a variety of engineering materials. Johnson and Cook established a material constitutive relationship as follows[23]:

$\sigma = [A + Be^{n}]\ [1+ C \ln (e/e_0)]\ [1- ((T - \mathrm{Troom})/(\mathrm{Tmelt} - \mathrm{Troom}))m]$ where σ is the Von-Misses flow stress; e, the equivalent plastic strain, e_0, the reference plastic strain rate; T, the temperature of the work material; Tmelt the melting temperature of the work material; and Troom, the room temperature. Coefficient A is the yield strength, the hardening modulus, C, the strain rate sensitivity coefficient; n, the hardening coefficient and m is the thermal softening coefficient. The strain rate ε is normalized with a reference strain rate ε_0.The material constants for the J-C model for AISI 1045 steel[23].

3.4.1.1.3 Modified Johnson-Cook Model

The Modified Johnson-Cook model can be expressed as follows.

$\sigma = B\varepsilon^{n}\ [1 + C \ln (\varepsilon/\varepsilon_0)]\ [(\mathrm{Tmelt} - T)/(\mathrm{Tmelt} - \mathrm{Troom})]+Ae^{-0.00005}[(T - 700)\ (T - 700)]$

where B and n are strength coefficient and strain hardening index, respectively. The first term of the Modified J-C equations represents the strain hardening behavior of the material. The second term which represents the effect of strain rate is assumed to be similar to that of

Johnson-Cook model with a reference strain rate (e_0) of 1000/s. The third term gives the temperature factor which varies for different materials. The Modified J-C model [equation (4)] considers the blue brittleness effect in low and medium carbon steel and gives a good approximation for the FE analysis of AISI 1045 steel. The material constants for the Modified J-C model for AISI 1045 steel[23].

3.5 Power calculations

A machining operation requires power, the power to perform machining has been been computed from the equation:

$$\boldsymbol{P_c = F_c * v_c}$$

Where P_c = cutting power; F_c = cutting force; and v = cutting speed.

3.6 Analytical heat flux calculation

Assuming that 10% of the heat is dissipated through radiation and convection and the heat partitioning parameter $\varepsilon = 0.75$, the instant heat flux can be calculated from equation[12]:

$$\dot{Q} = \frac{\varepsilon_1 * \varepsilon_2 * q}{A_b} \tag{3.65}$$

Where q is power, A_b contact area

3.6.1 Heat flux due to plastic deformation

Assuming that 10% of the heat is dissipated through radiation and convection and the heat partitioning parameter $\varepsilon = 0.75$, the instant heat flux can be calculated from equation:

$$\dot{Q} = \frac{\varepsilon_1 * \varepsilon_2 * q}{A_b} \tag{3.66}$$

Where q is power spent due to plastic deformation in primary zone

$Ppd = \frac{\mathrm{K}(1.15 \ln\varsigma)^{\mathrm{n}+1}}{\mathrm{n}+1} vAw$ is the power.

For AISI1045 from property table we have

K=1.34Gpa ,n=0.25 Here Aw=d*f where d, depth of cut and f feed rate

$$\xi = \frac{2.5}{2} = 1.25$$

$$Ppd = \frac{\mathrm{K}(1.15\ \ln\varsigma)^{\mathrm{n}+1}}{\mathrm{n}+1} vAw$$

Ab =20mm*2mm=$0.00004 m^2$

Table 3.8: Summary of calculated heat flux due to plastic deformation

velocity	Depth of cut=1mm		Depth of cut=1.5mm		Depth of cut=2mm	
m/s	Power[w]	Heat flux[w/m^2]	Power [w]	Heat flux[w/m^2]	Power[w]	Heat flux[w/m^2]
1	391	6598125	587	9905625	783	13213125
1.5	587	9905625	879	14833125	1174	19819687
2	783	13213125	1173	19794375	1566	26426250
2.5	978	16503750	1466	24738750	1956	33032812
3	1174	19811250	1759	29683125	2346	39639375

3.6.2 Heat flux due to friction at the tool and chip interface

The power spent due to friction at the tool-chip interface is calculated as[12].

$$\mathrm{P}_{\mathrm{fr}} = \boldsymbol{\tau}_{\mathrm{c}} \mathrm{l}_{\mathrm{c}} \mathrm{b}_{1\mathrm{T}} \frac{\mathrm{v}}{\varsigma}$$

Where $\boldsymbol{\tau}_c = 0.28\sigma_R$ is the average shear stress at the tool-chip contact (N/m^2)

σ_R is the ultimate tensile strength of the work material (N/m^2),

Lc is the tool-chip contact length (mm),

B1T is the true chip width (mm).

$\sigma_R = 0.585 Gpa$ For AISI1045

$\tau_c = 0.28 * 0.585 Gpa$ =0.1638Gpa

The tool-chip contact length is assumed as, Lc=0.5mm, B_{1T}=20mm

$$\dot{Q} = \frac{\varepsilon_1 * \varepsilon_2 * q}{A_b} \quad (3.67)$$

A_b=20mm*5mm=0.0001m^2

Table 3.9: Summary of calculated heat flux due to friction at the tool and chip interface

Velocity[m/s]	Power[w]	Heat flux[w/m^2]
1	131	884520
1.5	196.5	1326780
2	262	1769040
2.5	327.5	2211300
3	393	2653560

3.6.3 Heat flux due to new machined surface

$P_{ch} = E_{fr} * f_{cf}$

$E_{fr} = E_{ch} * A_{fr}$

A_{fr} =0.0025m*0.002m=0.000005m2

E_{ch} =42000J/m2 from property table for AISI1045

E_{fr}=0.000005*42000=0.21J

P_{ch} = 0.21J* fc_f

$$\dot{Q} = \frac{\varepsilon_1 * \varepsilon_2 * q}{A_b} \tag{3.68}$$

A_b=200mm*20mm=4000mm^2=0.004m^2

Table 3.10: Summary of calculated heat flux due to new machined surface

Frequency[Hz]	Power[w]	Heat flux[w/m^2]
1000	141.8	35437
1500	212.6	53155.5
2000	283.5	70874
2500	354.5	88592
3000	425	106311

CHAPTER FOUR:FINITE ELEMENT ANALYSIS

4.1 Introduction

The finite element method is a numerical procedure that can be applied to obtain solutions to a variety of problems in engineering. Steady, transient, linear, or nonlinear problems in stress analysis, heat transfer, fluid flow, and electromagnetism problems may be analyzed with finite element methods[20].

In the Pre-processing of finite element formulation, the process of dividing the big domain into finitely many building blocks (elements) that are connected at their nodes is carried out by defining them by approximate functions called shape functions. These discrete parts are then assembled together to represent the complete problem[2].

Boundary conditions and loads are also applied in the pre-processing stage. Then, analysis follows to solve system of linear or nonlinear algebraic equations and get nodal values of the quantities for the elements. Finally, in the Post processing, the nodal values are processed so that other values of interest at any other location and given time can be obtained depending on the type of the analysis[18].

4.2 Finite element analysis using Ansys-15.0

ANSYS software is generally used to analyze engineering problems that are too complex to compute by hand in the design and optimization of a system. Its capability to solve the finitely many equations defining the discrete elements created in the meshing process makes it the most suitable mathematical tool to be chosen. It implements the preprocessing, analysis and post processing stages to analyze a given system.

4.2.1 General procedures of ANSYS software

1) Preprocessing

In this part the desired geometry will be defined by using the various commands like key points, lines, areas, volumes etc or one can also import a model that is already constructed using solid works or catia as (iges, igs files). Material selection and meshing are also carried out. Then Meshing carried out, divide the whole object into many finite parts called elements that are connected at the nodes.

2) Solution

This is a stage all the constraints and loads are applied including analysis type and initial conditions and solutions are obtained. Choosing the analysis type, defining loads and controlling outputs by using the load step options are to be performed before solving the problem.

3) Post processing

This stage makes ANSYS software the most suitable mathematical tool to obtain the results of the analysis in a user-friendly manner. Stress distribution, temperature gradients, deformation, strain, etc are be obtained with colored contours that best describe the response of the system to the loading conditions stated in the solution stages. In addition, graphical and tabular outputs are available for the user to analyze and compare outputs corresponding to given set of inputs. Moreover the user is able to make any changes of inputs like material property, loading conditions, etc to obtain another set of outputs in the same project as in the case of optimization.

4.3 Analysis of the cutting variables using ANSYS -15.0

Ansys version 2012 is used to make the coupled transient structural and transient thermal analysis to see the effect of different variables on thermo-mechanical properties. The finite element model constructed using solid works is imported to the ansys15.0 workbench ASI1045 as work piece and tungsten as tool with their thermal and mechanical properties are considered.

Assumptions

- Material properties are isotropic and do not vary with temperature.
- The convective heat transfer coefficient is constant throughout the process.
- The radiative heat transfer is neglected as time is comparatively short and the magnitude is very small.
- The wear on the contact surfaces is negligible until the chip removed.

4.3.1Geometrical model

solid work 13 is used to generate the geometry. The contact areas of work piece and tool are properly placed so that the pressures corresponding to the cutting force and loads and fixed supports are applied during the analysis. The three dimensional model of the assembly is then saved as igs file for later use in the Ansys workbench.

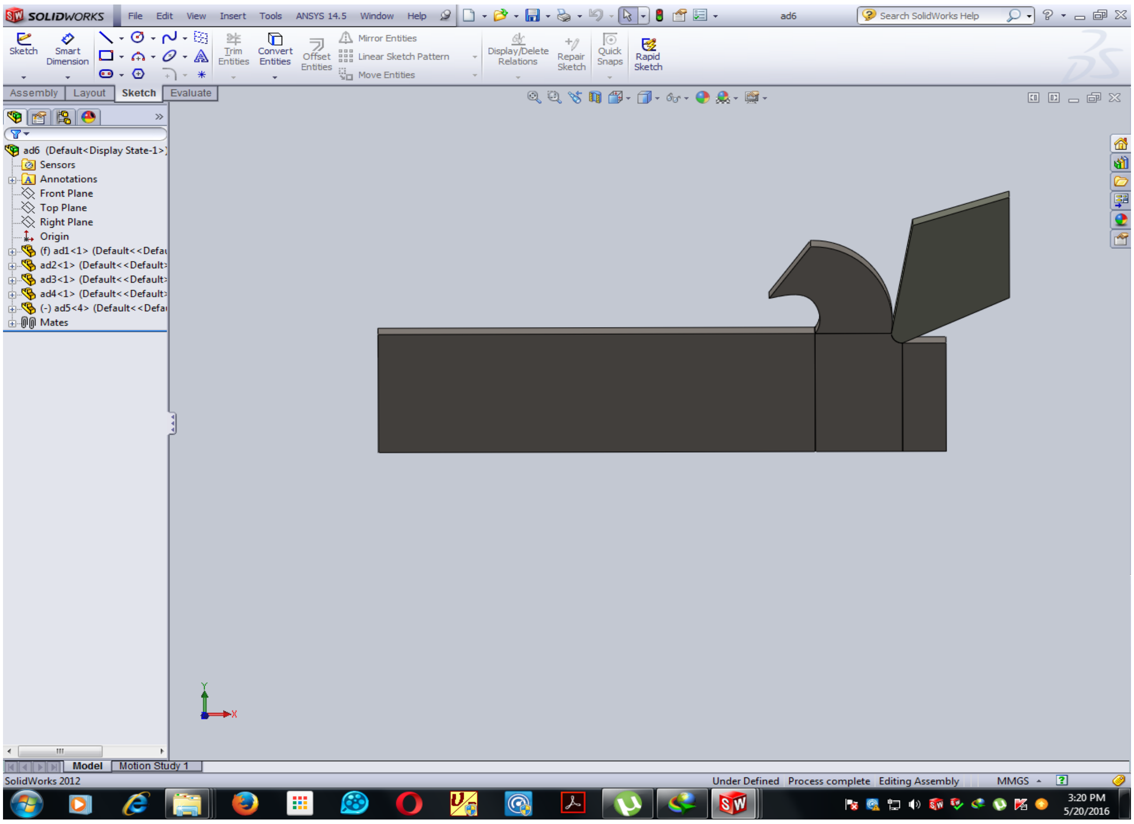

Figure 4.1: Finite element model constructed using solid works13

4.3.2 material property definition

The material properties used for the finite element analysis are summarized in table 4.1 as follows. here AISI1045 as work piece and tungsten as cutting tool are used.

4.3.3 Mesh generation

The finite element model needs to be divided into small building blocks called elements that are connected at finite points called nodes. In this particular analysis the model is divided into many small free rectangular elements using the automatic mesh generation command. The meshed wheel is shown in fig 4.2 below.

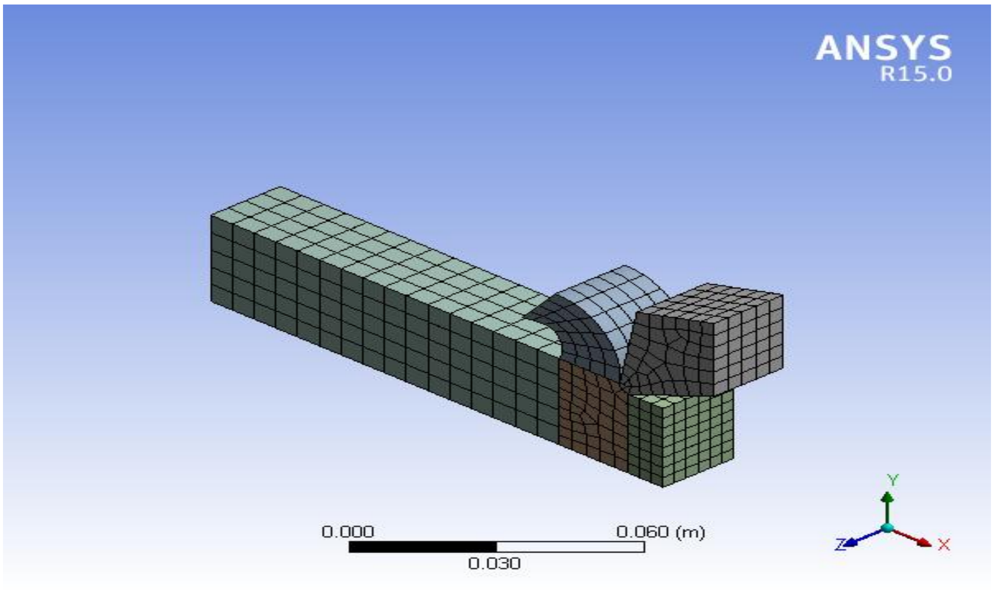

Figure 4.2: Mesh generation

4.3.4 Defining Boundary conditions and loads

After the meshing is completed it is very important first to define the initial boundary conditions so that the forthcoming analysis will have some references to begin with.

The boundary conditions set for this analysis are ambient temperature, initial wheel temperature, the convective heat transfer coefficient (film coefficient) and support conditions. Whereas the loads to be applied to the wheel are the heat flux, pressure at the contact areas with the brake block and with the rail, angular velocity and gravitational acceleration. Hence, the boundary conditions applied to this analysis are as follows.

- Ambient temperature=22^{o}C
- Initial wheel temperature=22^{o}c
- Film coefficients of work piece and tool
- Fixed support on the work piece and tool velocity is given

CHAPTER FIVE:RESULT AND DISCUSSION

5.1 introduction

The effect of cutting force, fixed support, feed rate and depth of cut on thermo-mechanical properties of the metal cutting process is analyzed using ANSYS 15.0 software. The temperature gradient, Von-misses stress distribution and total deformation are computed separately. Each analysis is made of elapsing time of 10seconds.

The results obtained from the combined transient thermal and structural analysis for each steps are presented and analyzed as follows. For all cases, the thermal and structural boundary conditions and loads are applied as illustrated in the figures5.1 below.

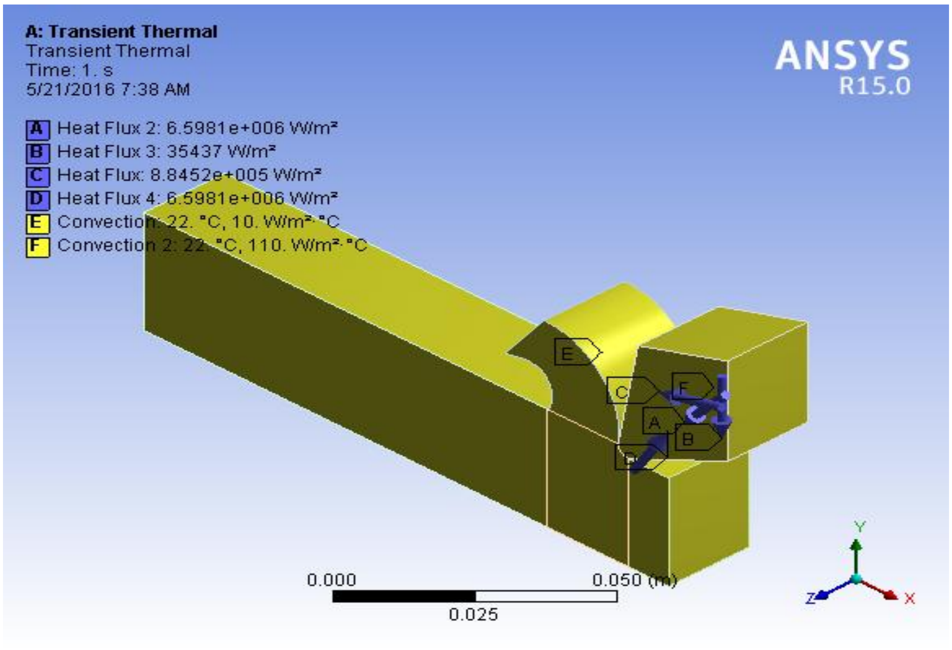

A: Transient Thermal
Transient Thermal
Time: 1. s
5/21/2016 7:38 AM

A Heat Flux 2: 6.5981e+006 W/m²
B Heat Flux 3: 35437 W/m²
C Heat Flux: 8.8452e+005 W/m²
D Heat Flux 4: 6.5981e+006 W/m²
E Convection: 22. °C, 10. W/m²·°C
F Convection 2: 22. °C, 110. W/m²·°C

Figure 5.1:applied loads for thermal analysis

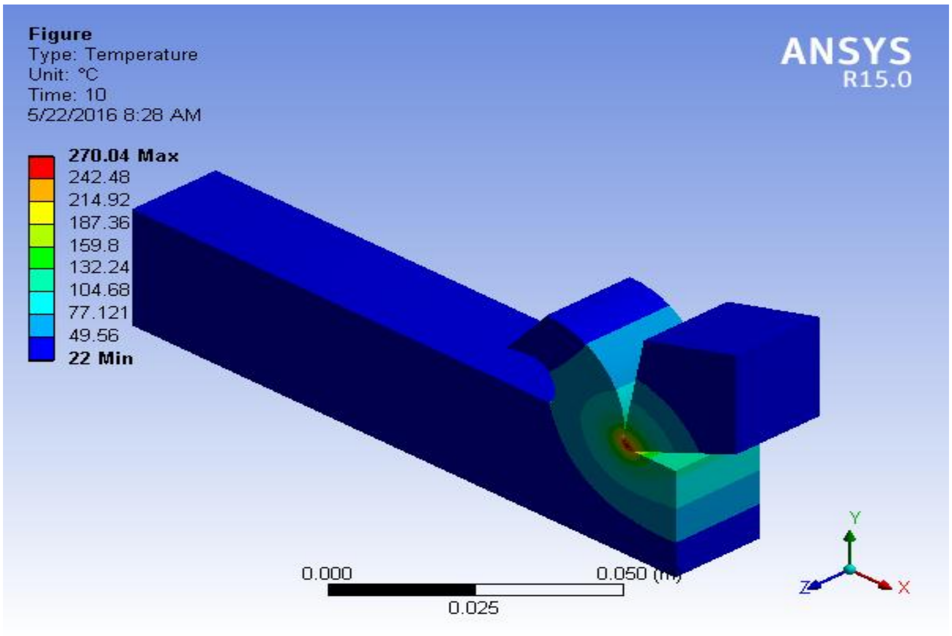

a) temperature

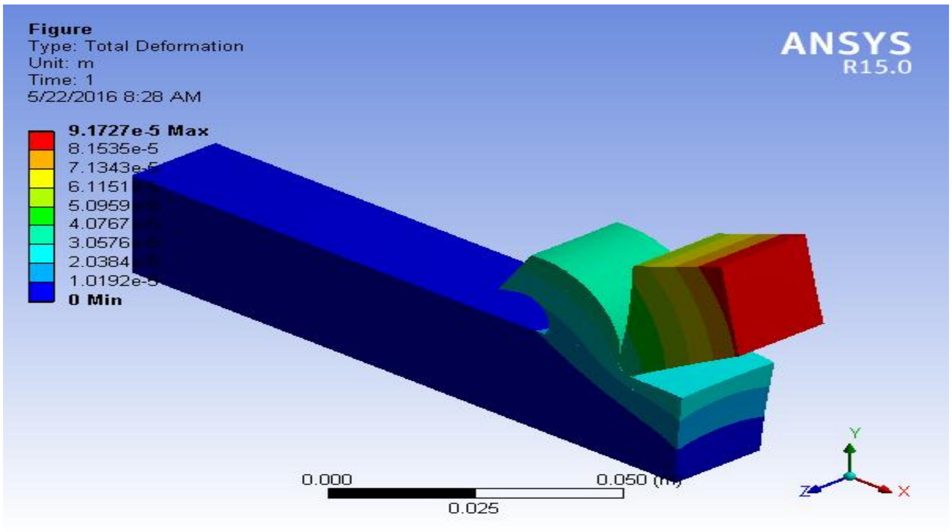

b)total deformation

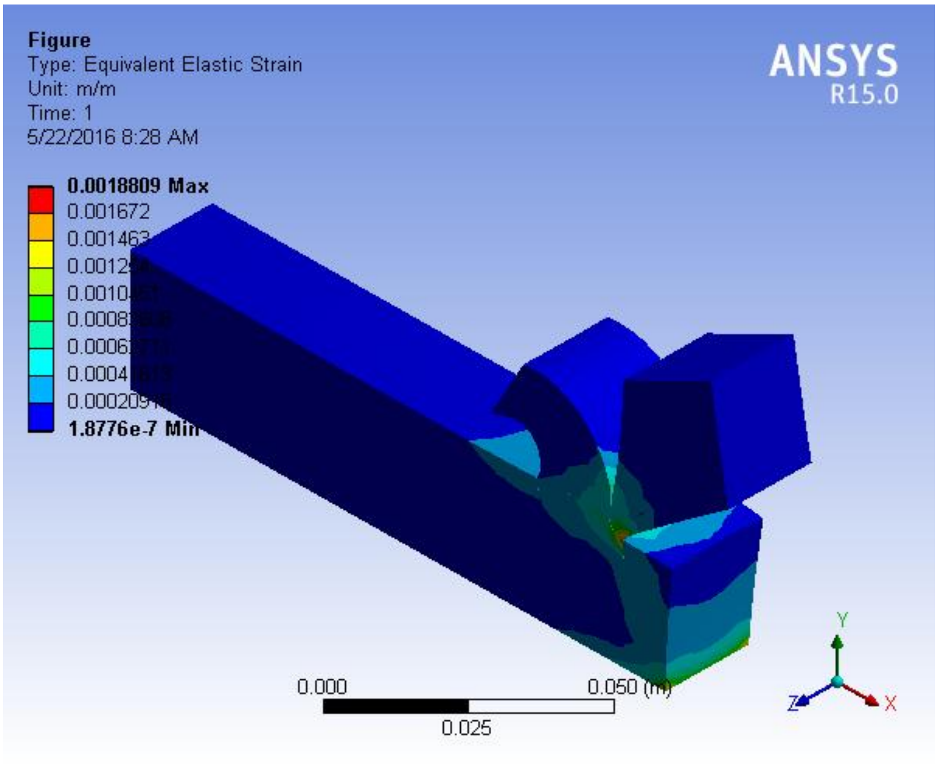

c)elastic strain

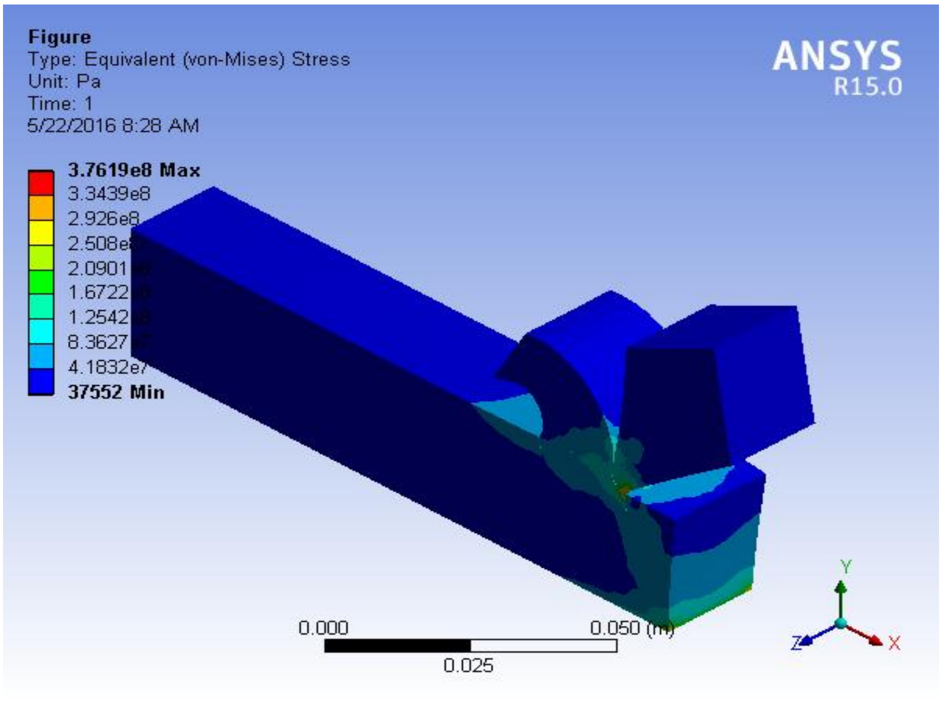

d)von-mises stress

Figure5.2:a)temperature b)total deformation c)strain d) stress at v=1m/s and d=1mm

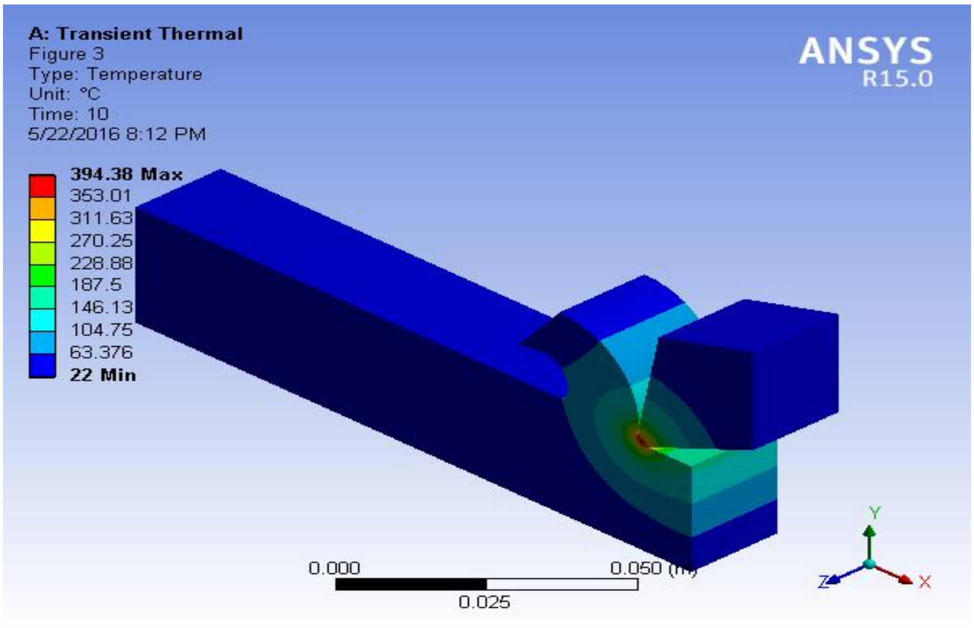

a)temperature

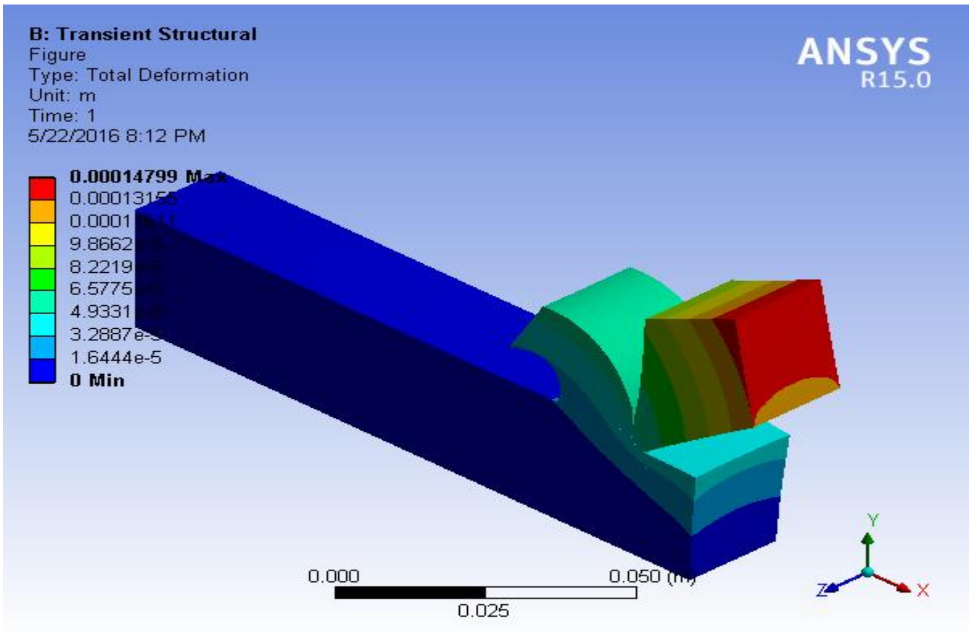

b)deformation

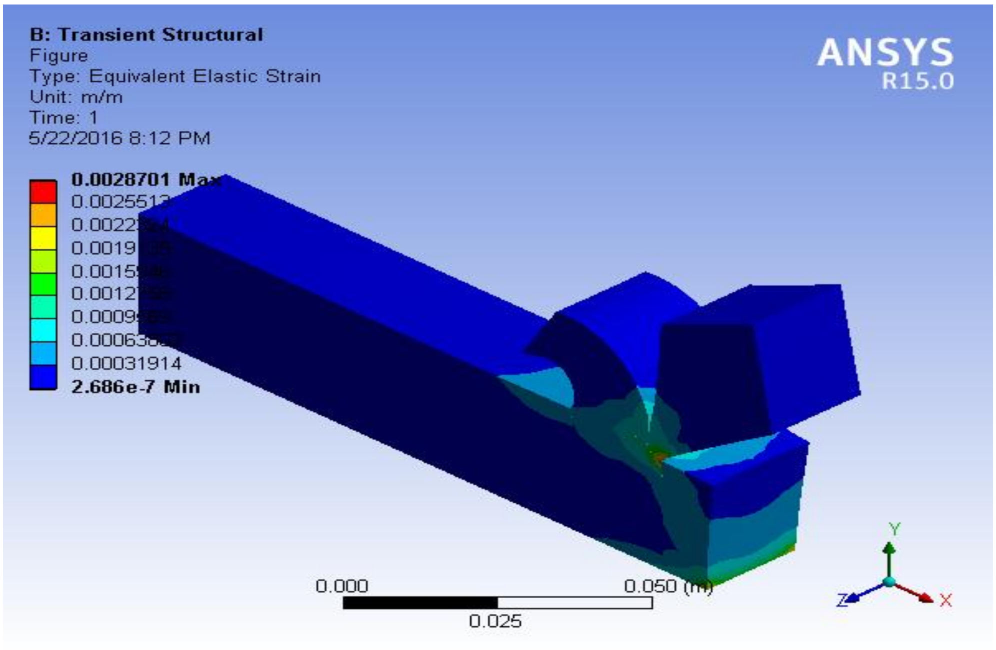

c)strain

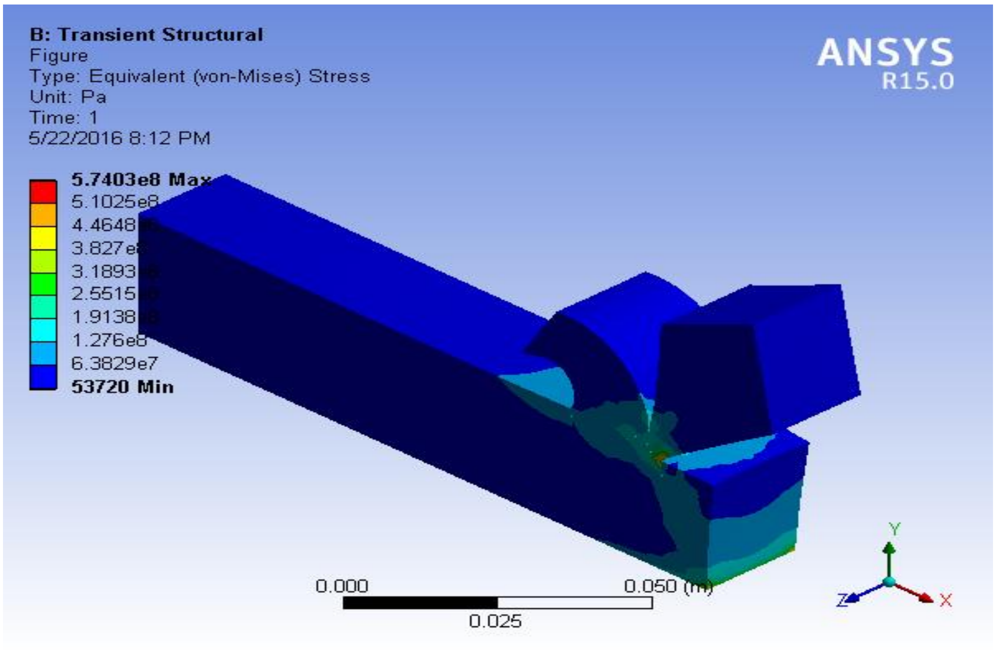

d)von-mises stress

Figure 5.3:a)temperature b)total deformation c) strain d) von-mises stress at v=1.5m/s and d=1mm

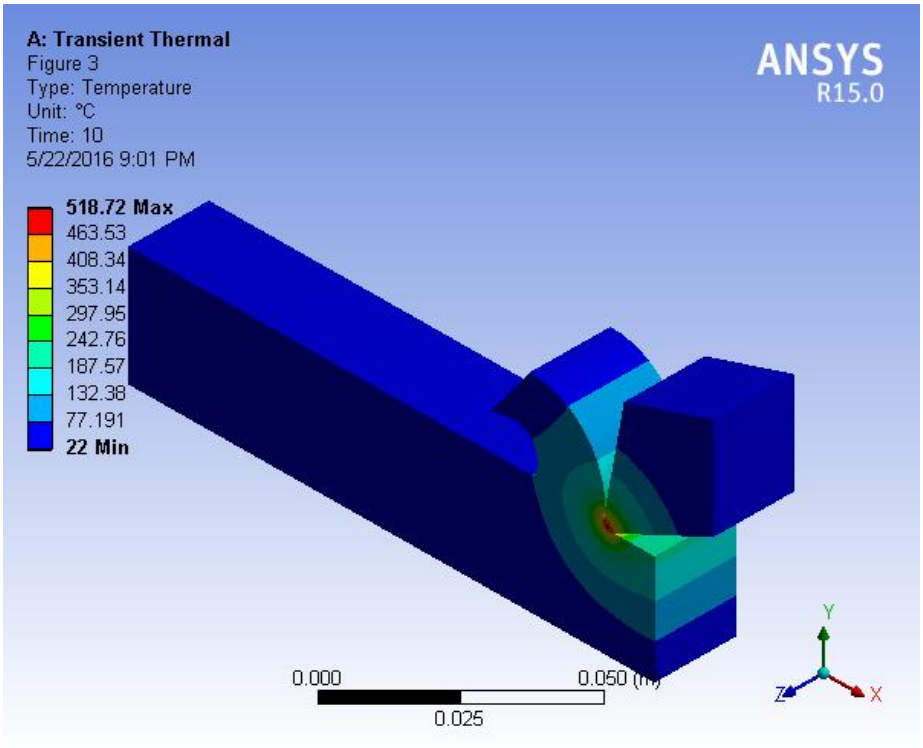

a)temperature

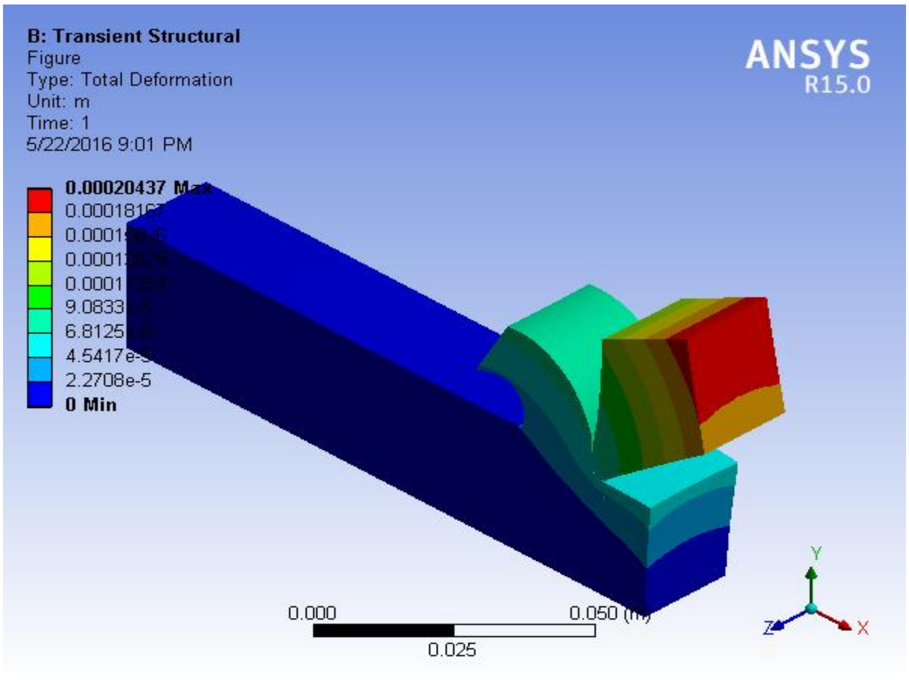

b)deformation

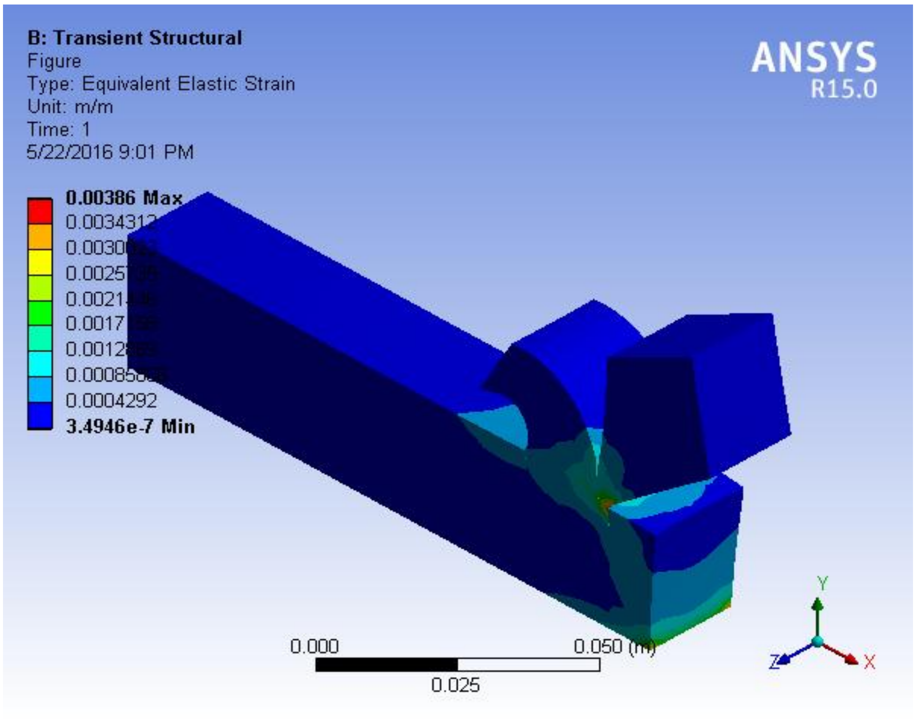

c)strain

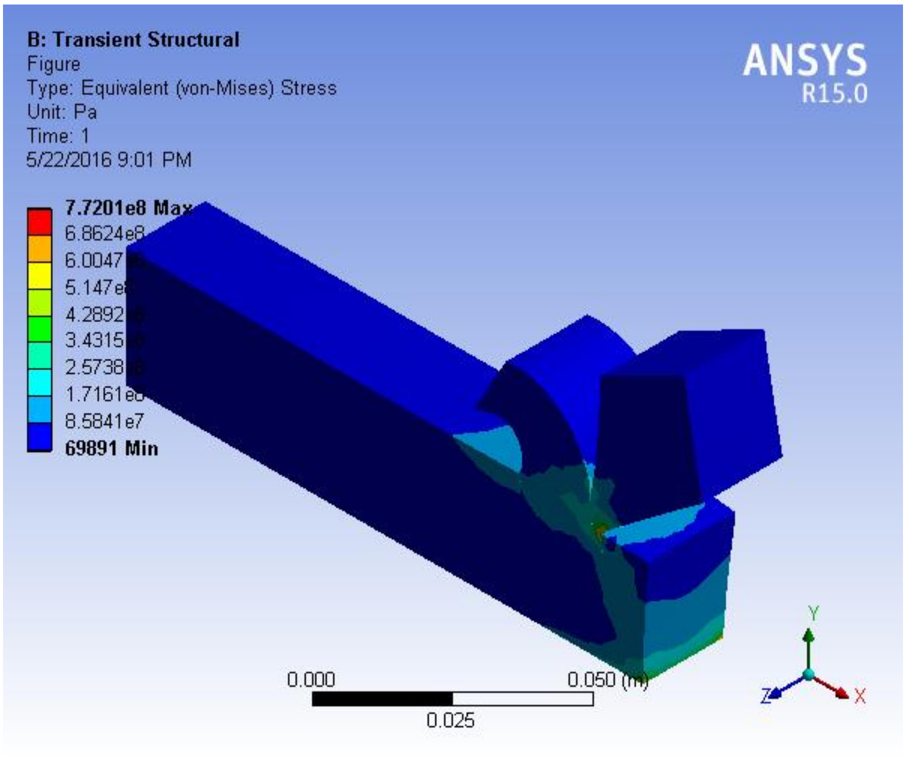

d)von-mises stress

Figure5.4:a)temperature b) total deformation c)strain d)von-mises stress at v=2m/s and d=1mm

Table 5.1:summary of results as possible and impossible conditions of the process

velocity	Depth of cut=1mm			Depth of cut=1.5mm			Depth of cut=2mm		
m/s	possible	Impossible	Reason	possible	impossible	Reason	Possible	impossible	Reason
1	✓			✓				x	high tensile stress
1.5	✓				x	high tensile stress		x	High temperature and stress
2		X	High tensile stress		x	High temperature and stress		x	High temperature and stress
2.5		X	High tensile stress		x	Large temperature and stress		x	High temperature and stress
3		X	High temperature and stress		x	Large temperature and stress		x	High temperature and stress

CHAPTER SIX:CONCLUSION, RECOMMENDATION AND FUTURE WORKS

6.1 Conclusion

In this dissertation, a three dimensional finite element model has been developed using ANSYS software to predict the temperature distribution ,total deformation, elastic strain and von-mosses stress at different cutting speed and depth of cut. A transient thermal analysis assuming as Gaussian distribution heat source with temperature-dependent material properties has been used to investigate the temperature distribution and stress distribution. Finite element modeling was carried out for temperature-dependent material properties.

Certain parameters such as depth of cut, cutting speed, federate, the latent heat, heat flux, the percentage of discharge energy transferred to the tool have made this study nearer to real process conditions. metal cutting variables like depth of cut, feed rate, cutting force and cutting speed and their effects on temperature, total deformation, strain and stress are analyzed.

When the cutting force is 1200N,cutting speed 1m/s at depth of cut 1mm the maximum temperature is 270^{O}C obtained from transient thermal analysis. however the resulting total deformation, elastic strain and Von-misses stress are obtained from the coupled Thermo-mechanical analysis, those are 5.91e-5Pa, 0.00188,3.762e8pa respectively.

The maximum temperature obtained at speed of 3m/s and 1mm depth of cut is 766^{O}C,which is above the working service temperature of the material (650^{o}c) so as it melts due to high speed even if the depth of cut is small.

The maximum temperature obtained from speed of 3m/s and 2mm depth of cut which is 1671.7^{O}C and The corresponding von-misses stresses is2.3169 e9Pa . There is huge difference when we compare it to the values resulting from depth of cut 1mm and speed of 1m/s(270^{O}C maximum temperature and 3.762e8Pa Equivalent stress).

Therefore, those cutting parameters has significant contribution to both overheating and mechanical failure due to stress conditions of desired products and production machines.

The maximum temperature corresponding to 1.5mm depth of cut and 1.5m/s speed is (578^{O}C), the corresponding von-misses stress (8.67e8Pa) is much higher than the ultimate tensile strength of both work piece and tool materials. Consequently, it is evident that every cutting parameter(depth of cut, cutting speed,feedrate and cutting force) directly related to maximum temperature and maximum stress resulting overheating and wear. To put it in a nut shell, the heat and stress generated during machining parameters (depth of cut ,cutting speed and federate)are factors of increasing temperature,deformation,strain and stress and deteriorate the tool fast.

6.2 Recommendations

Continuous assessment on machining and cutter wear should clearly investigated. operators should always be given proper trainings that enable them to have a very good judgment capability while performing machining operation so that the phenomenon of overheating and wear are minimized.

The use of CNC mounted systems will also improve the performance of the machining operation considering the above cutting parameter as feed of CNC. this minimizes the chance of overheating .In addition, inspecting the whole length of the work piece is necessary since there is micro-structure changes due to heat and other load factors on it and may not be uniform.

6.3 Future Work

- It is very important to set up workshop experiment and collect first hand temperature data. the results obtained could be compared to those obtained at the end of this thesis.
- Analysis of the micro-structural changes incurred during machining process due to high temperature is also another vital investigation that reveals the extent of damage caused by the overheating on desired products and machine part.
- In addition, different tools with different work piece materials should be investigated and should clearly set to work, and environment temperature changes should consider from place to place.

Appendix

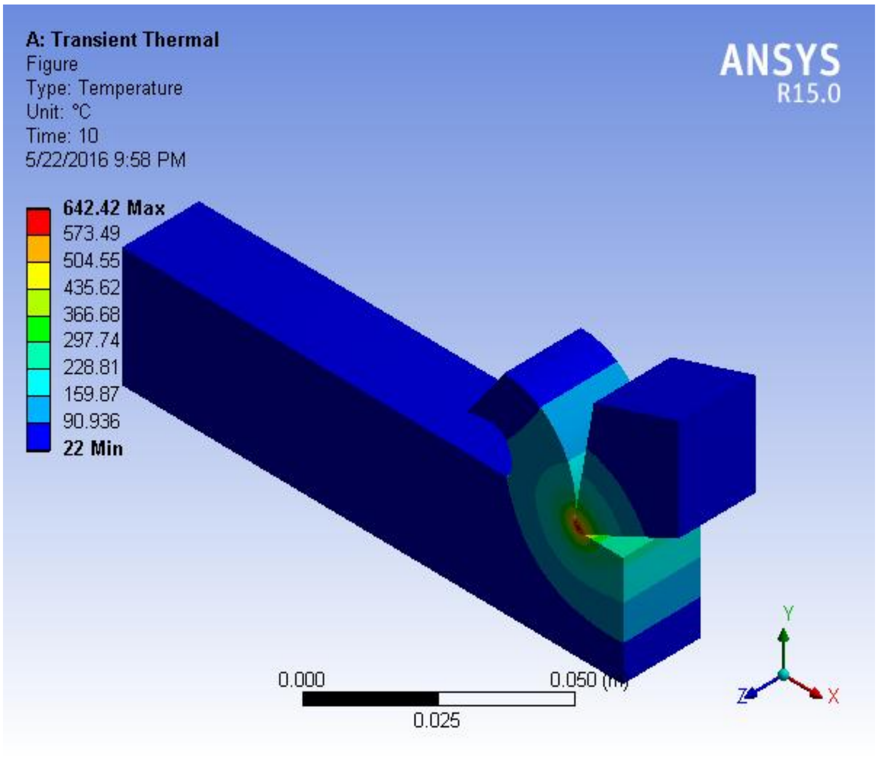

A: Transient Thermal
Figure
Type: Temperature
Unit: °C
Time: 10
5/22/2016 9:58 PM

a)temperature

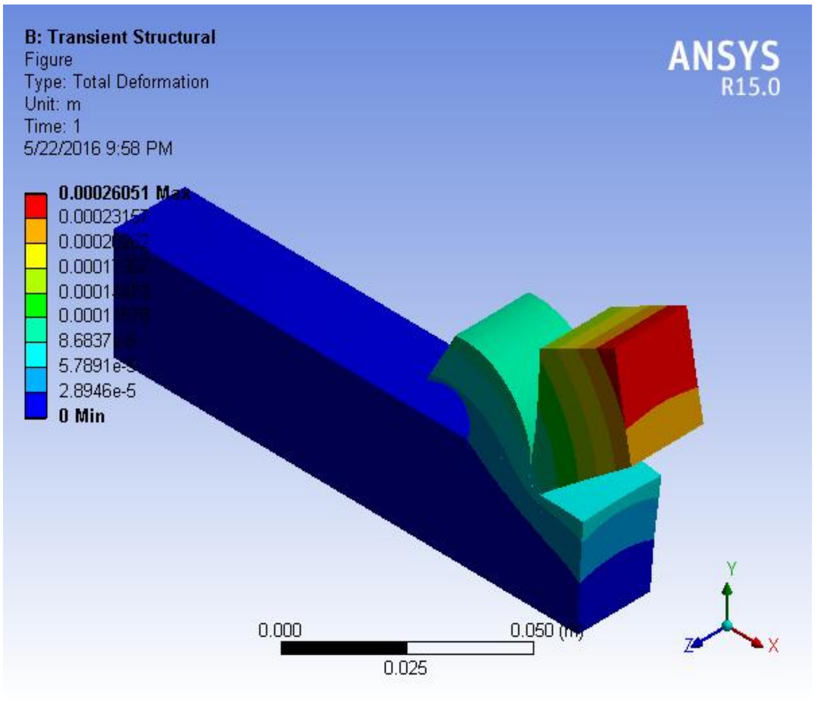

B: Transient Structural
Figure
Type: Total Deformation
Unit: m
Time: 1
5/22/2016 9:58 PM

b)deformation

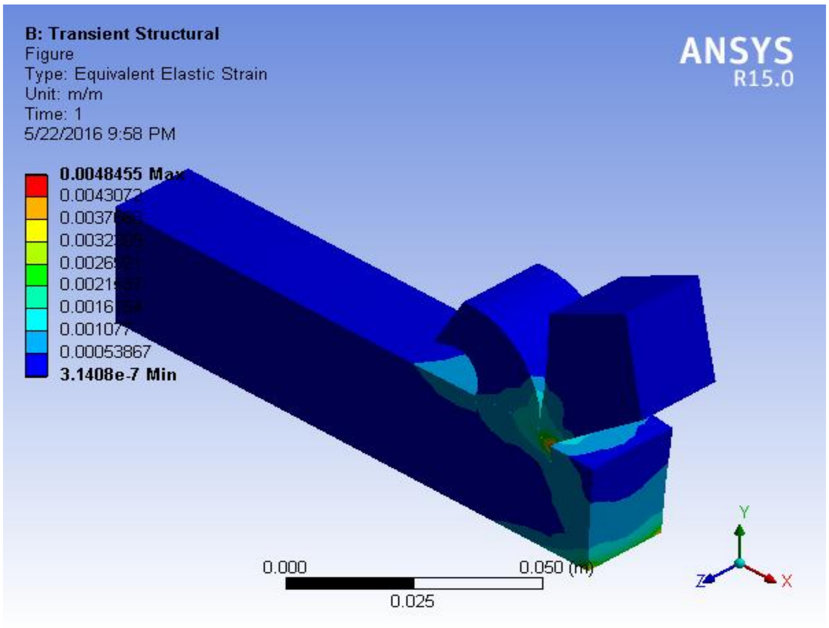

c)strain

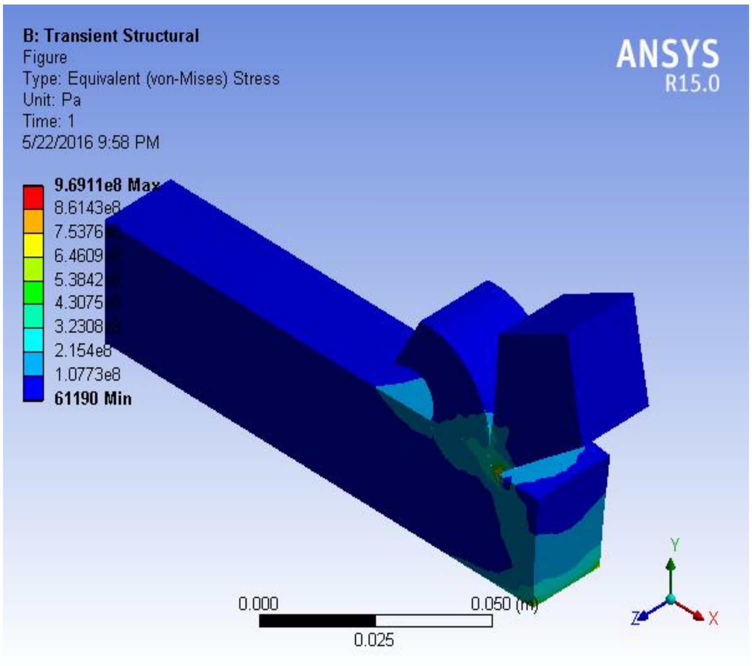

d)von-mises stress

Figure 5.5:a) temperature) total deformation c)strain d) von-mises stress at v=2.5m/s and d=1mm

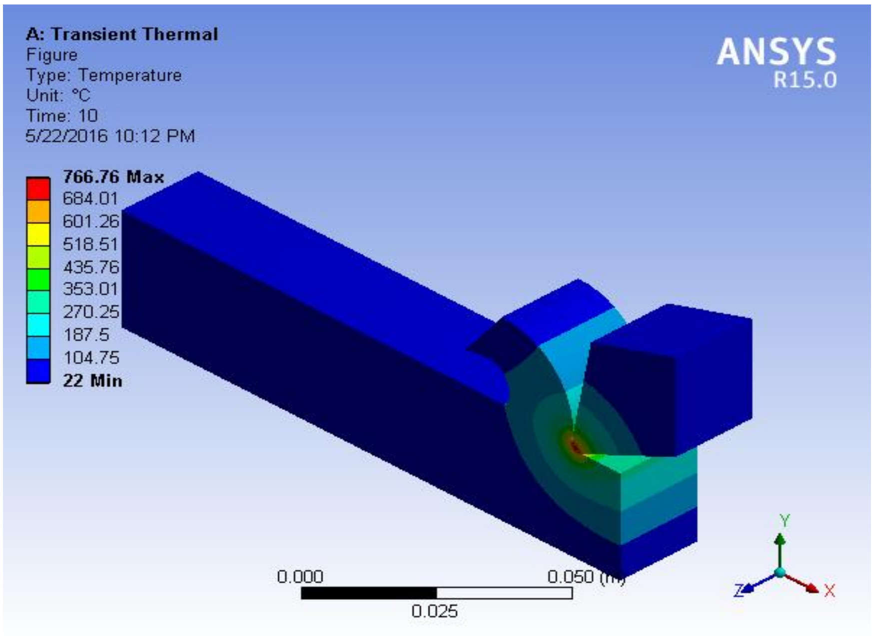

a)temperature

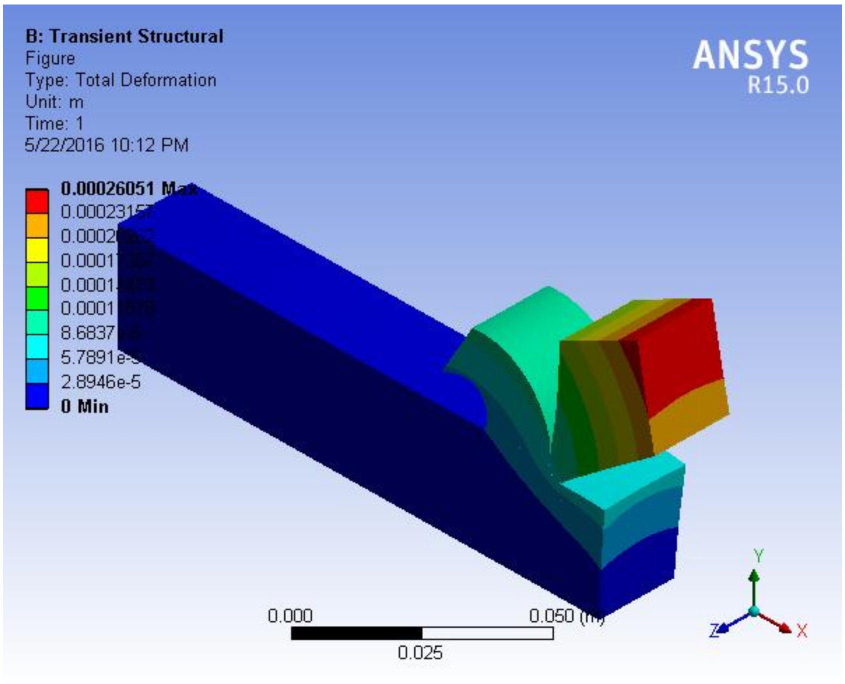

b)deformation

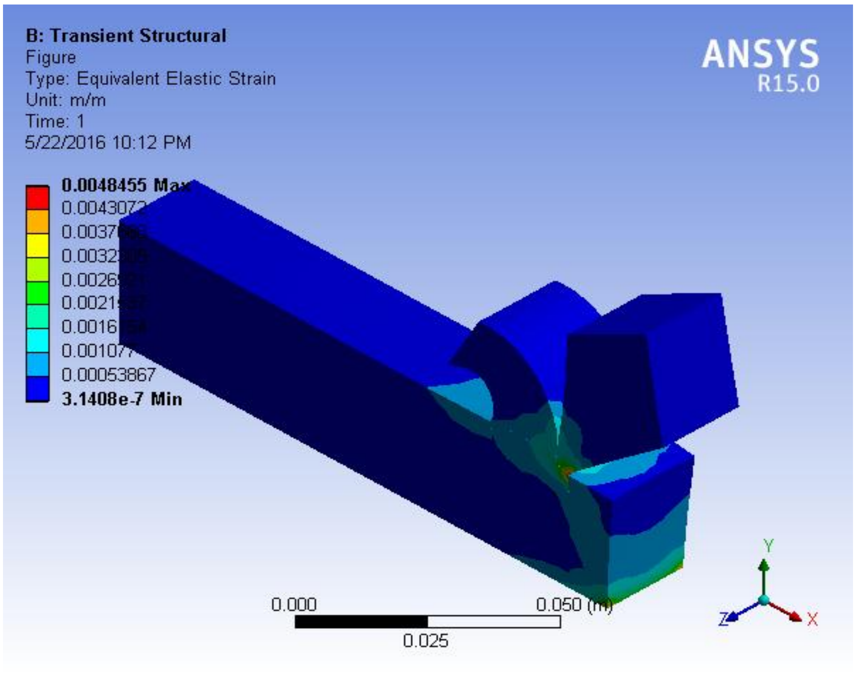

c)strain

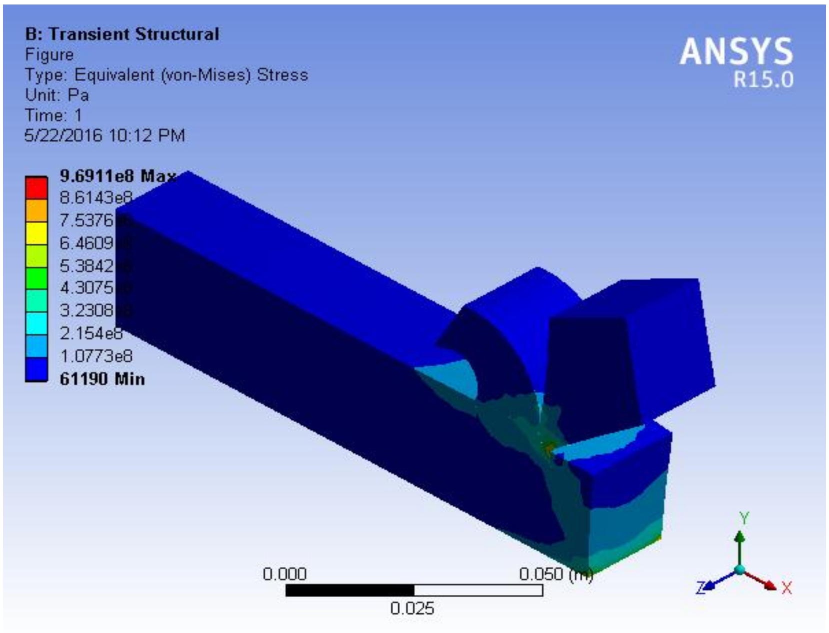

d)von-mises stress

Figure 5.6:a) temperature b) total deformation c)strain d) von-mises stress at v=3m/s and d=1mm

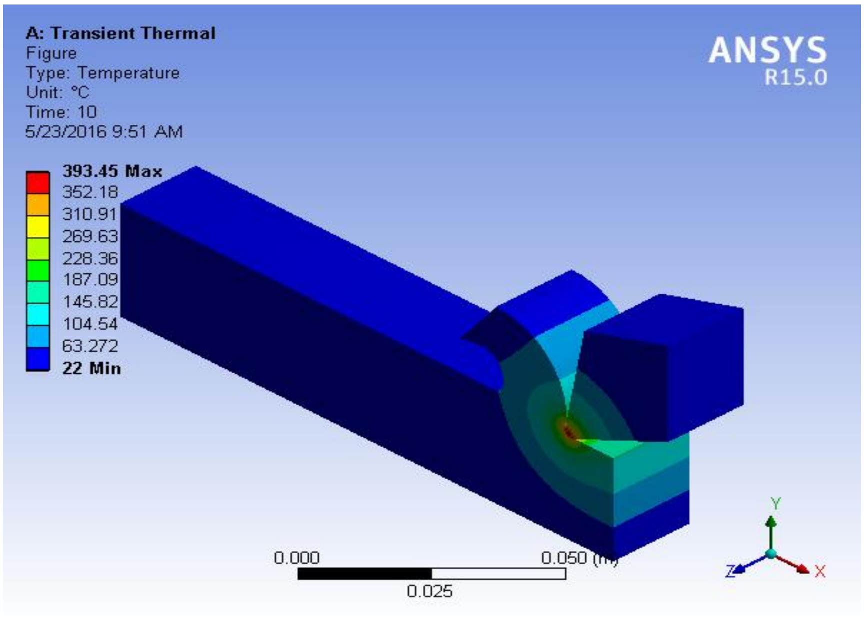

a)temperature

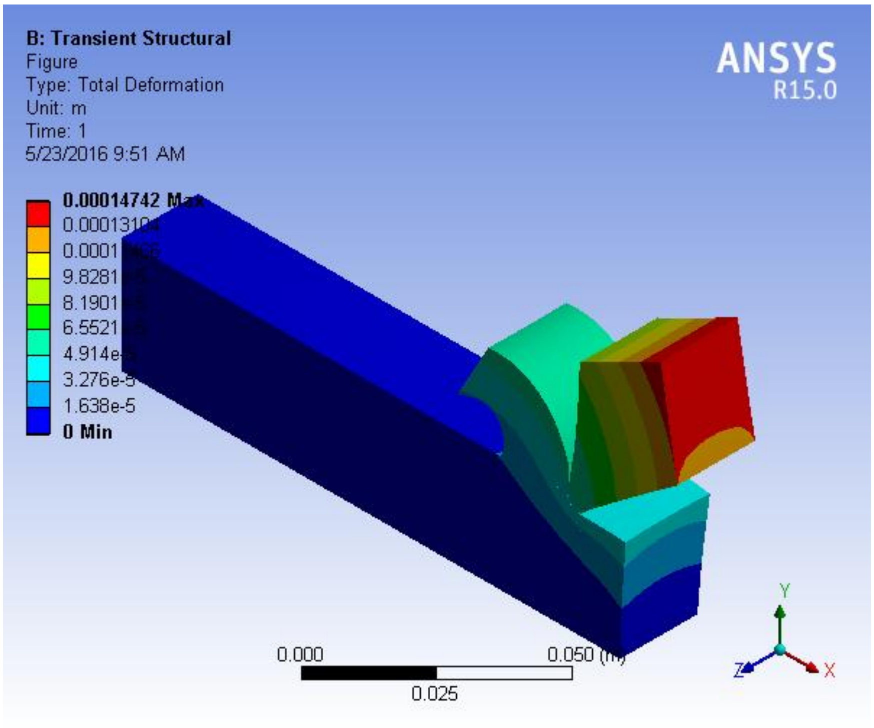

b)deformation

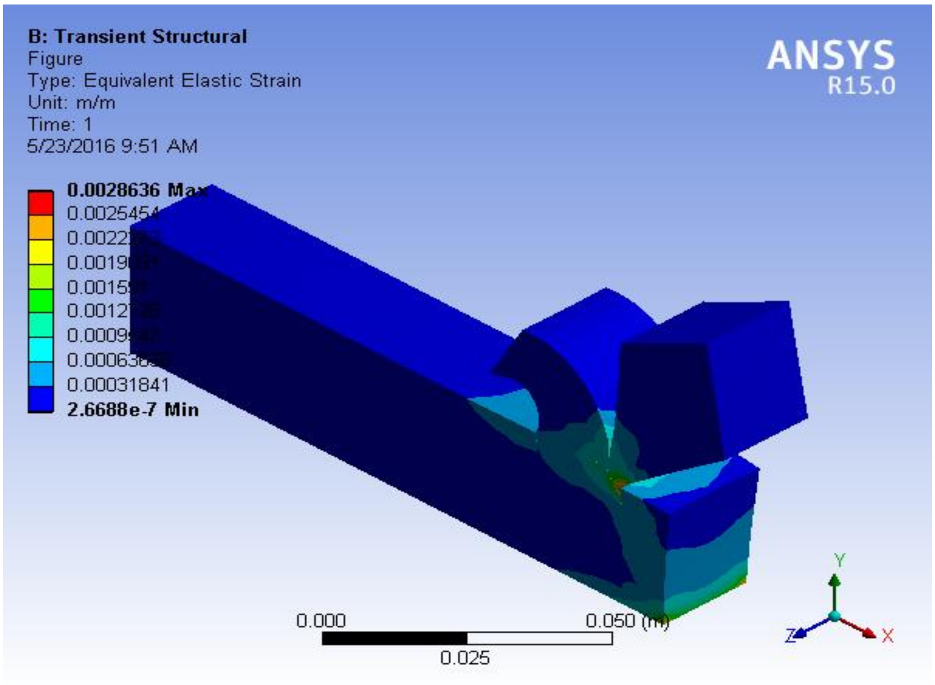

c)strain

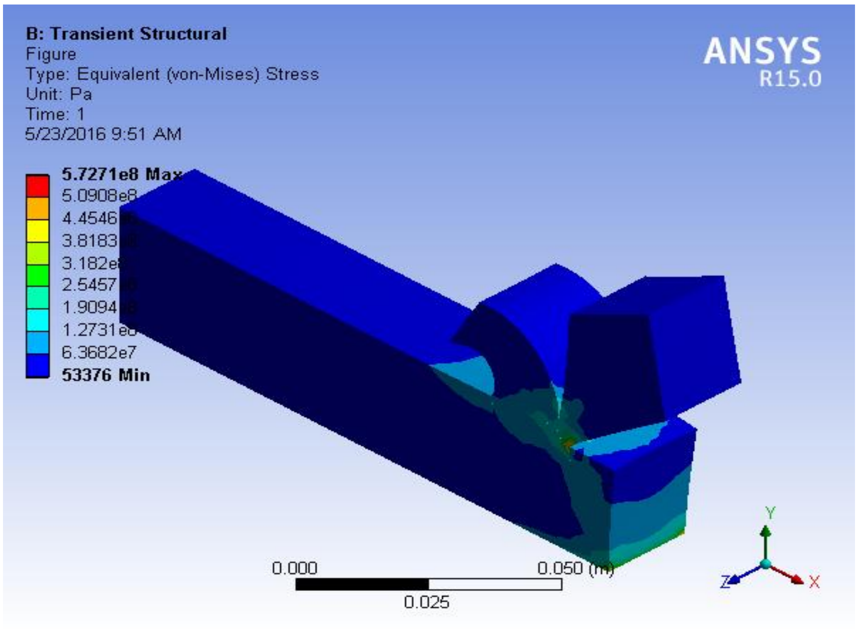

d)von-mises stress

Figure 5.7:a) temperature b)total deformation c)strain d) von-mises stress at v=1m/s and d=1.5mm

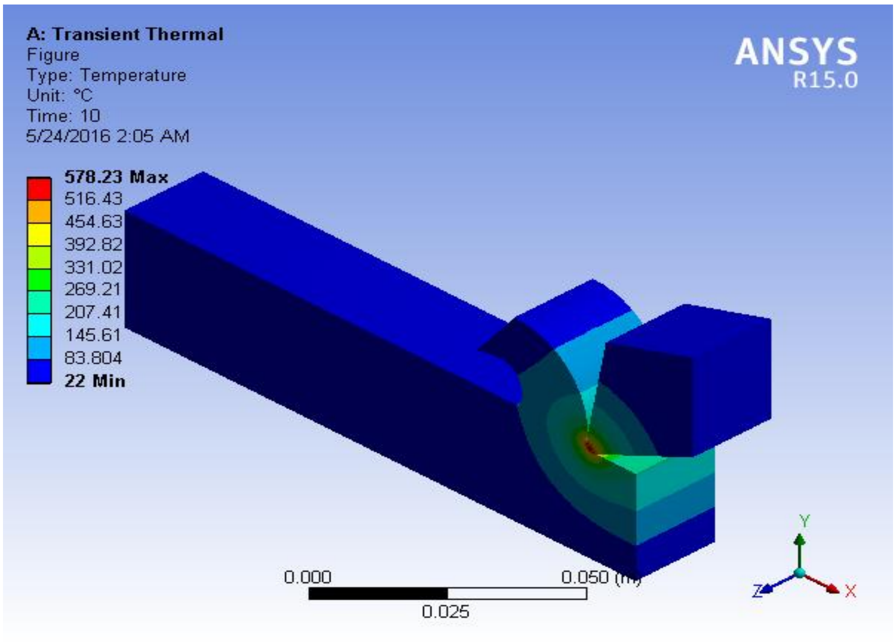

a)temperature

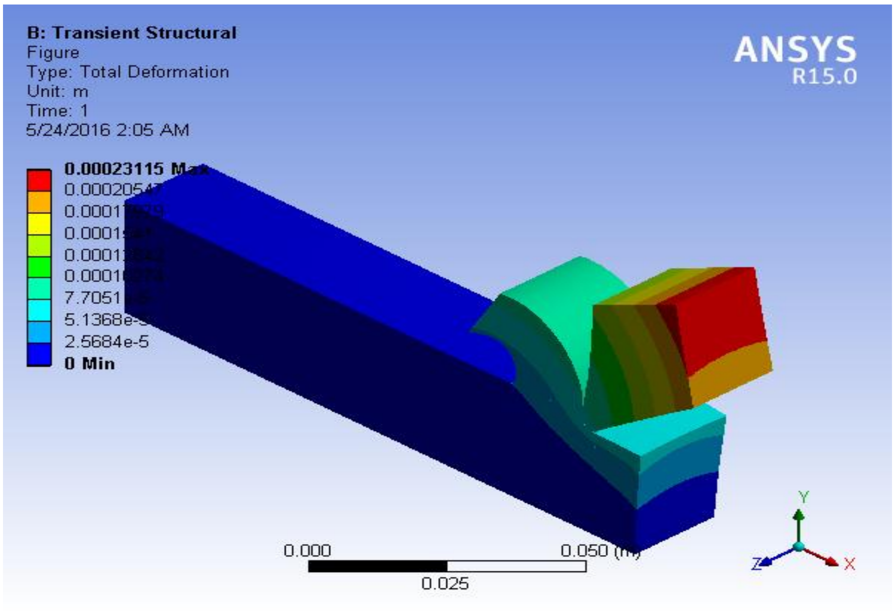

b)deformation

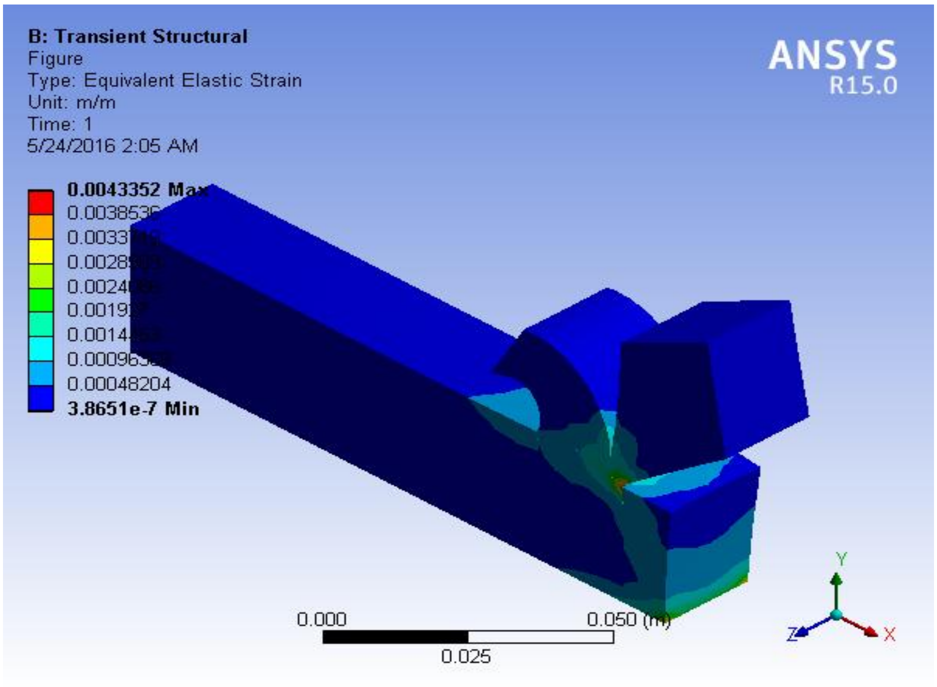

c)strain

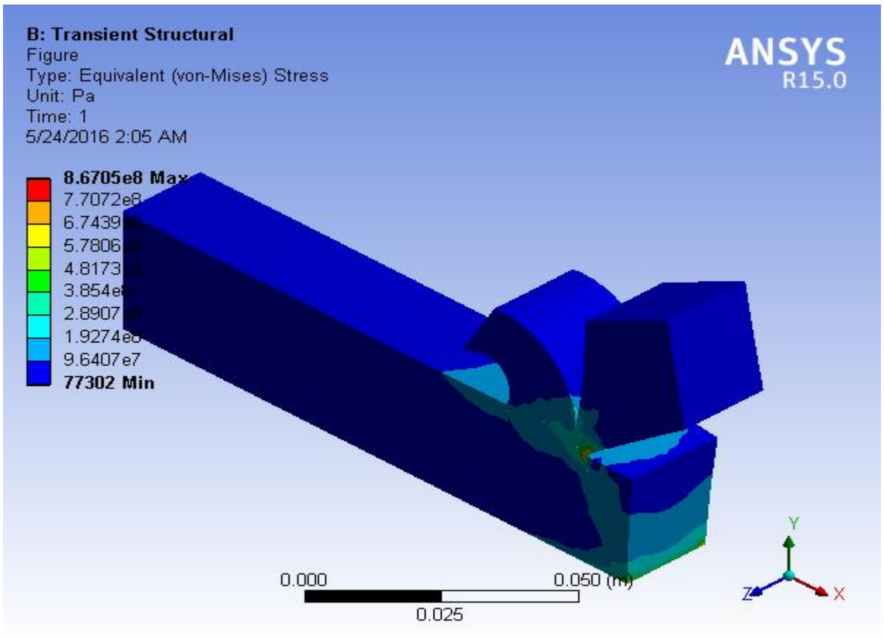

d)von-mises stress

Figure 5.8: a) temperature b)total deformation c)strain d) von-mises stress at v=1.5m/s and d=1.5mm

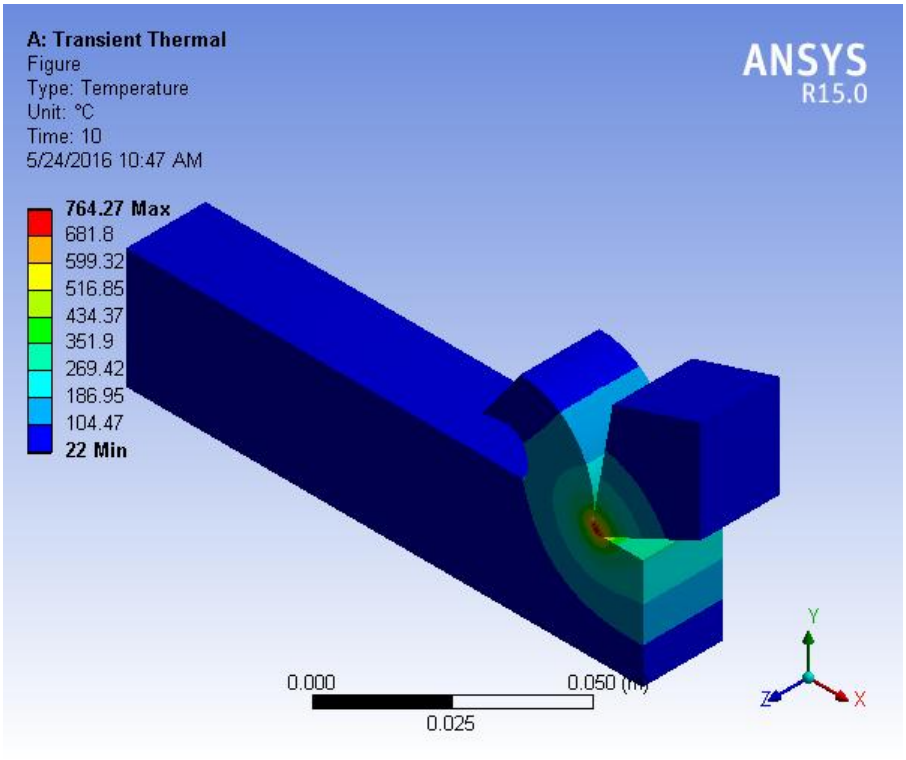

a)temperature

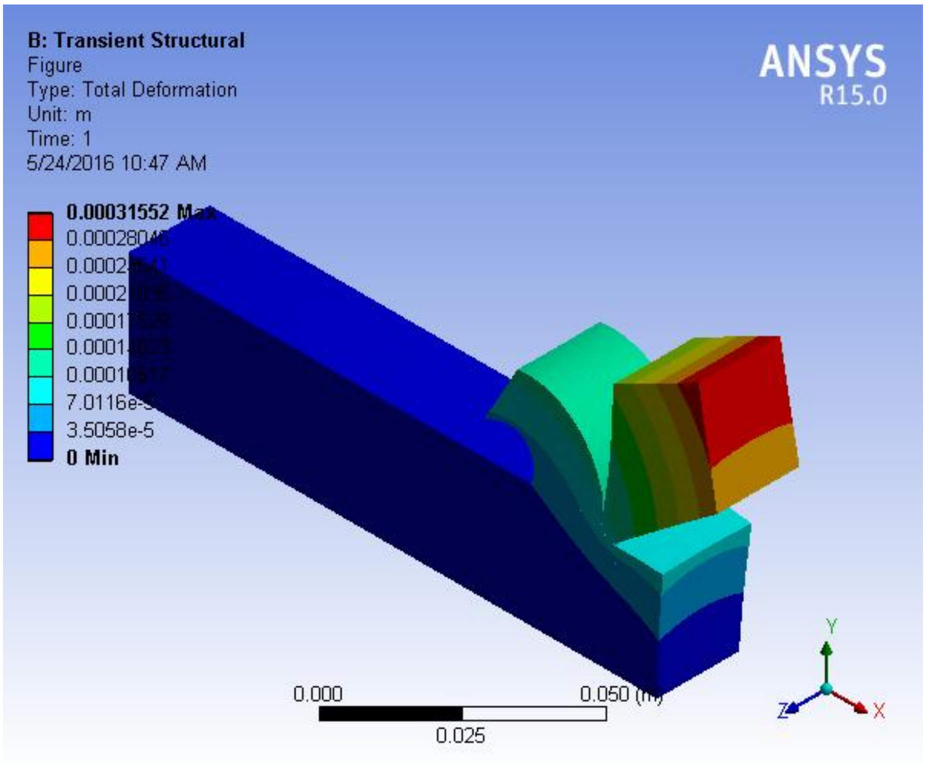

b)deformation

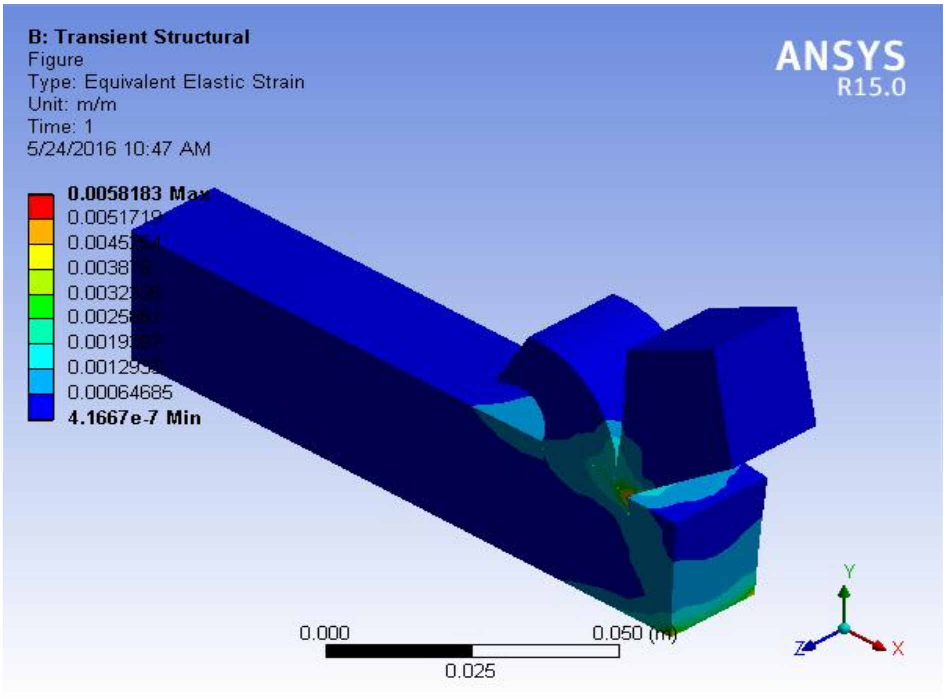

c)strain

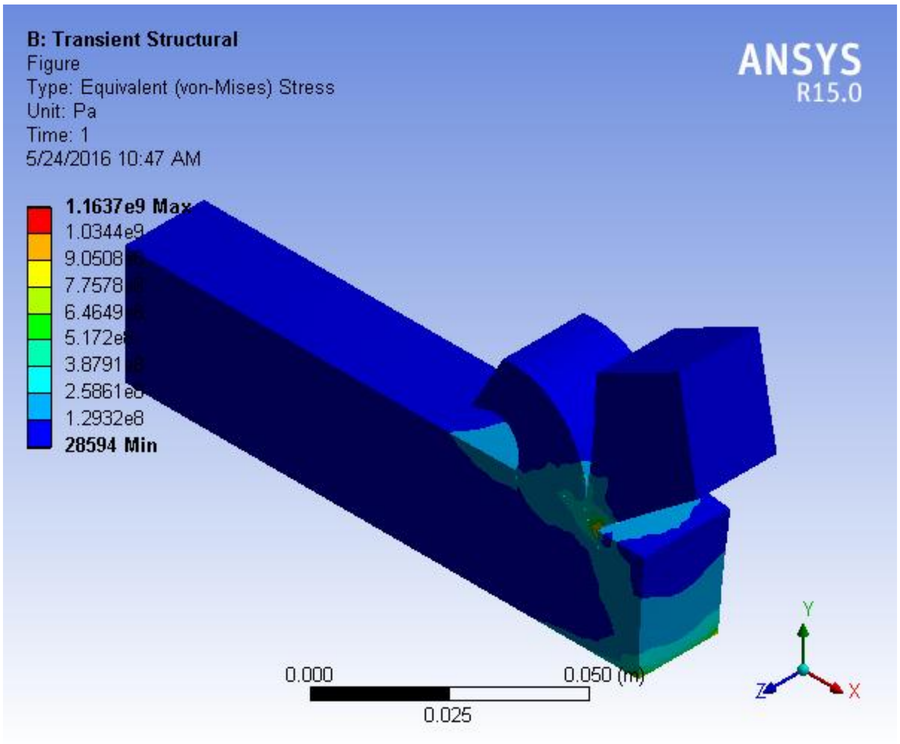

d)von-mises stress

Figure 5.9: a) temperature b)total deformation c)strain d) von-mises stress at v=2m/s and d=1.5mm

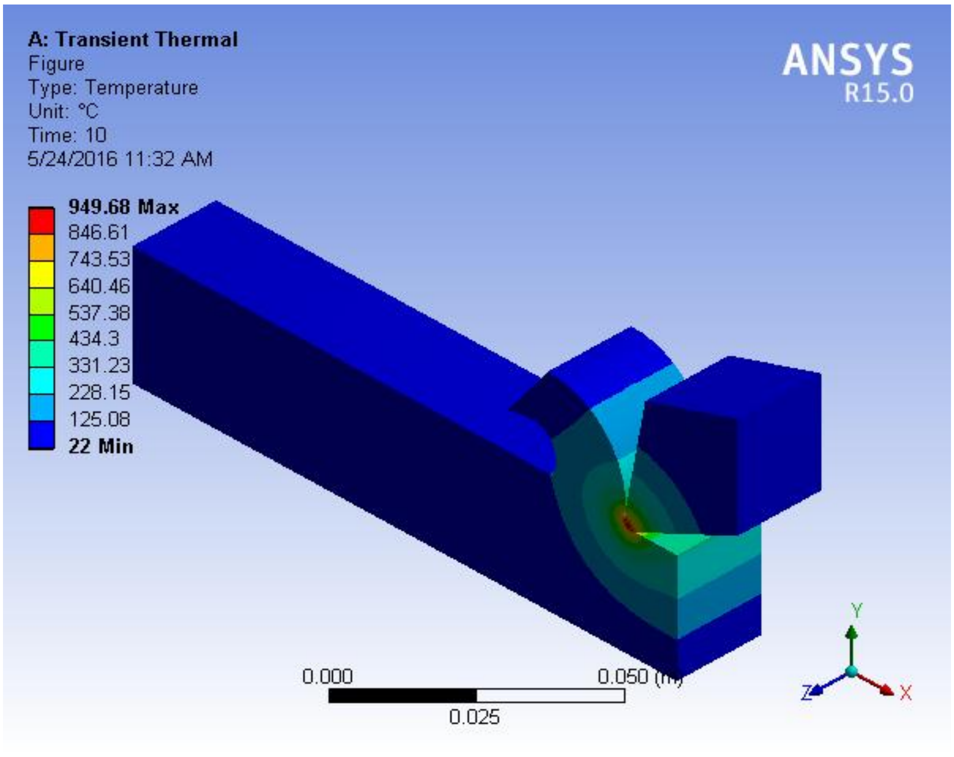

a)temperature

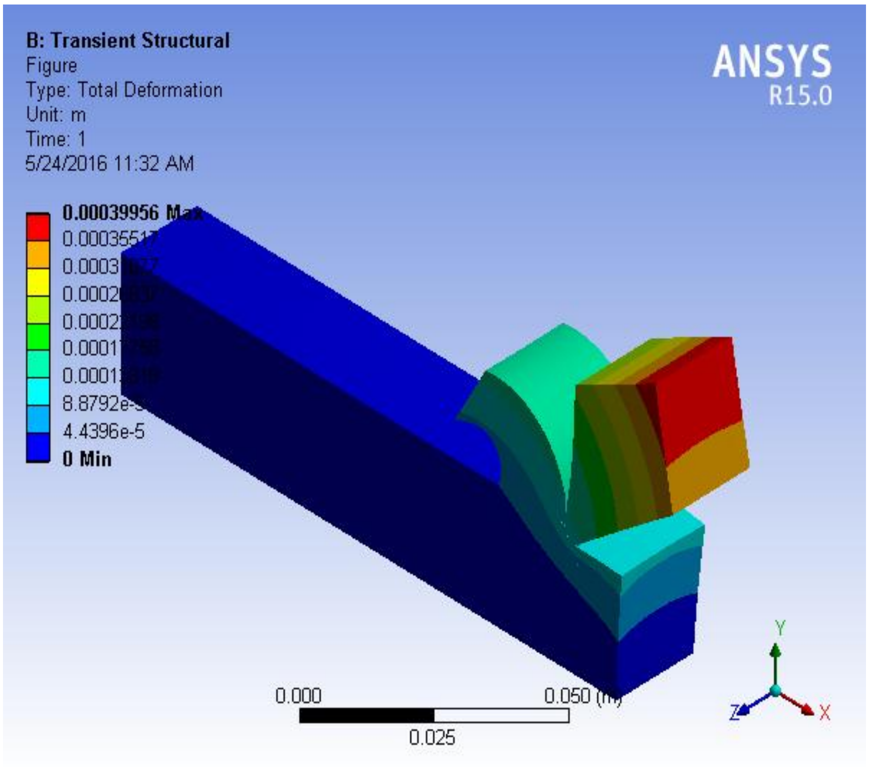

b)deformation

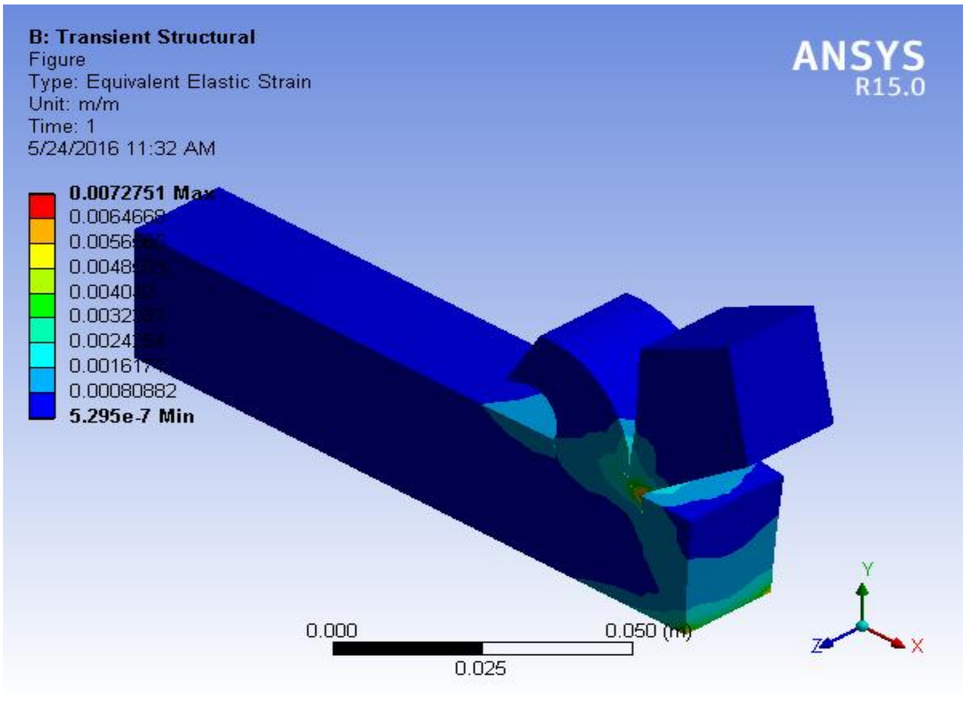

c)strain

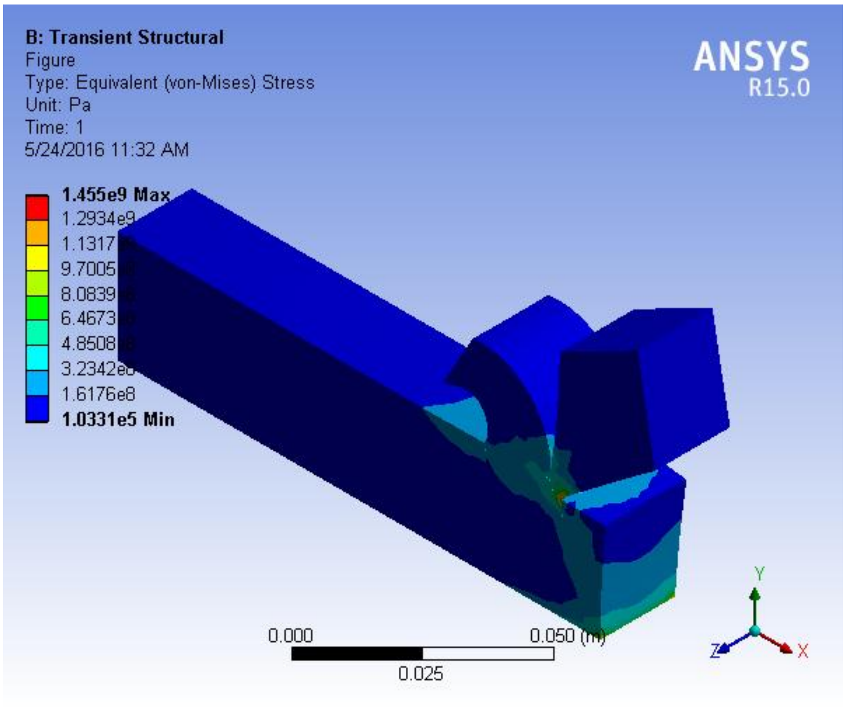

d)von-mises stress

Figure 5.10:a) temperature b)total deformation c)strain d) von-mises stress at v=2.5m/s and d=1.5mm

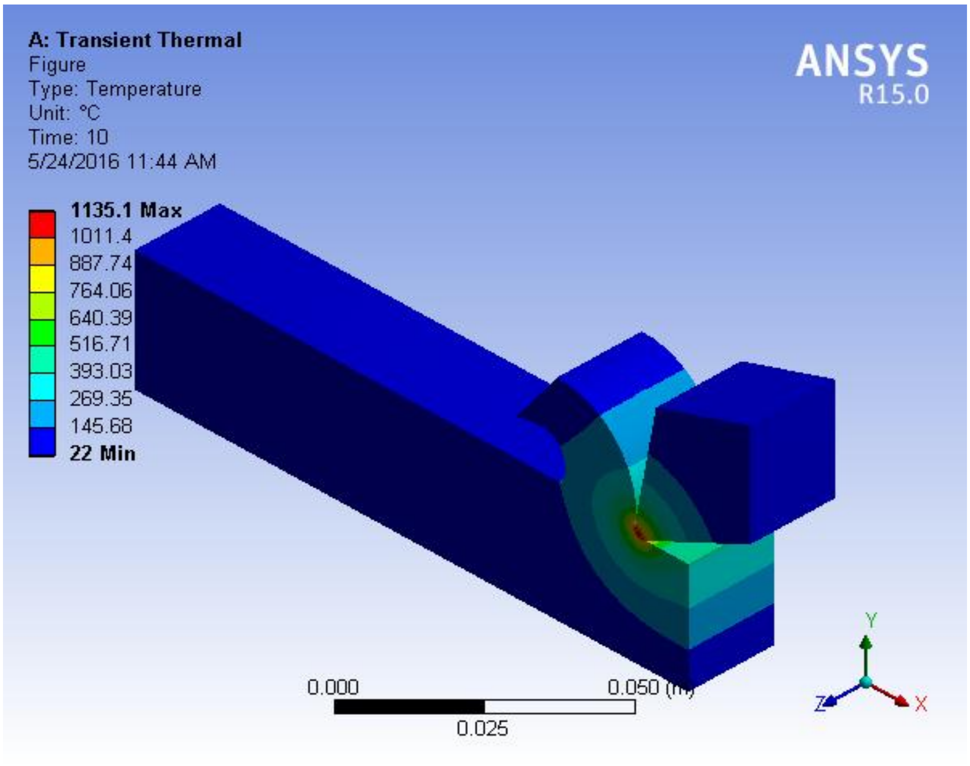

a)temperature

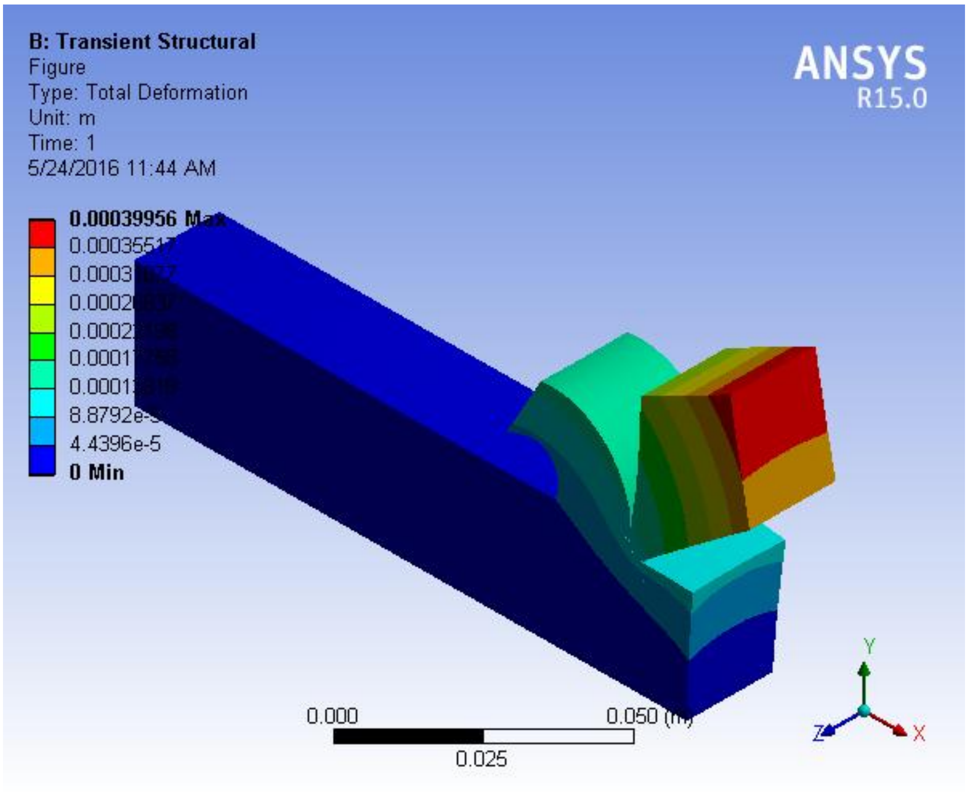

b)deformation

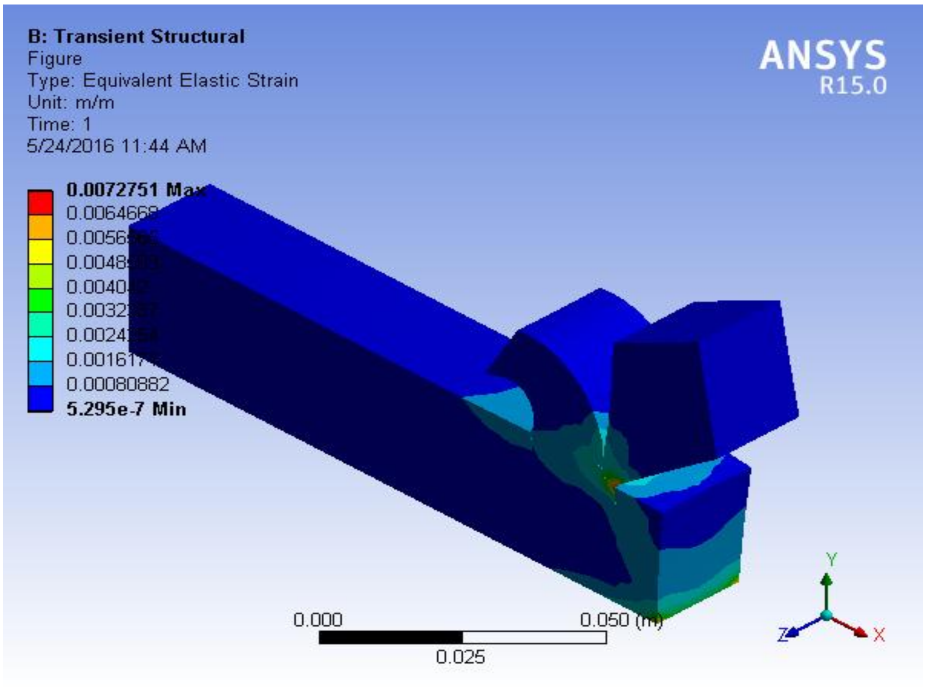

c)strain

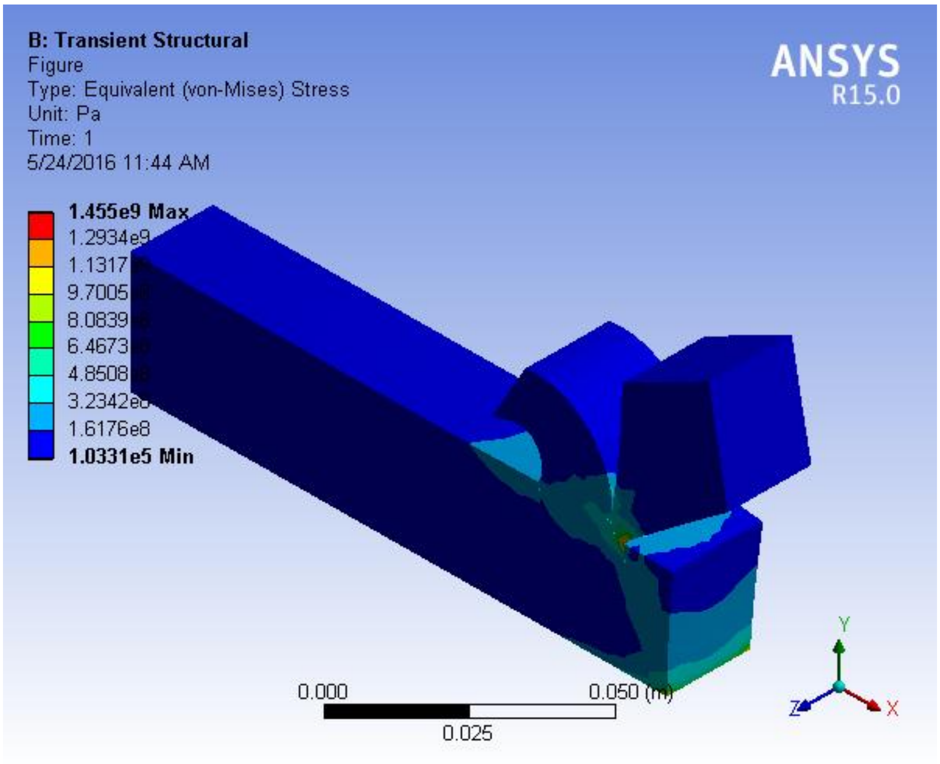

d)von-mises stress

Figure 5.11: a) temperature b)total deformation c)strain d) von-mises stress at v=3m/s and d=1.5mm

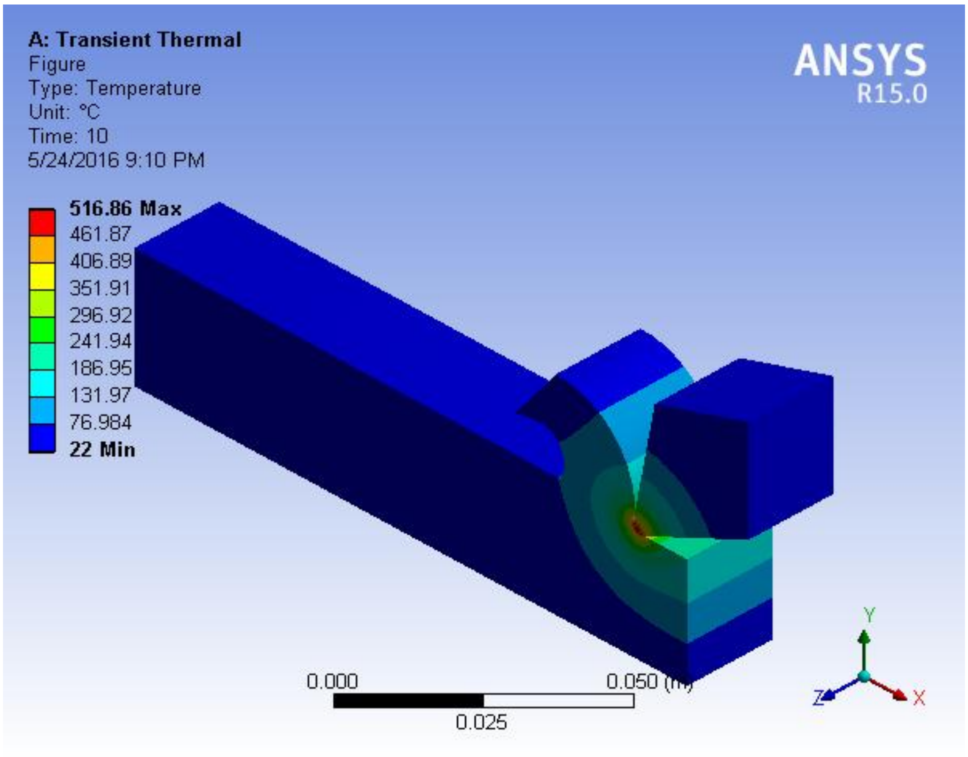

a)temperature

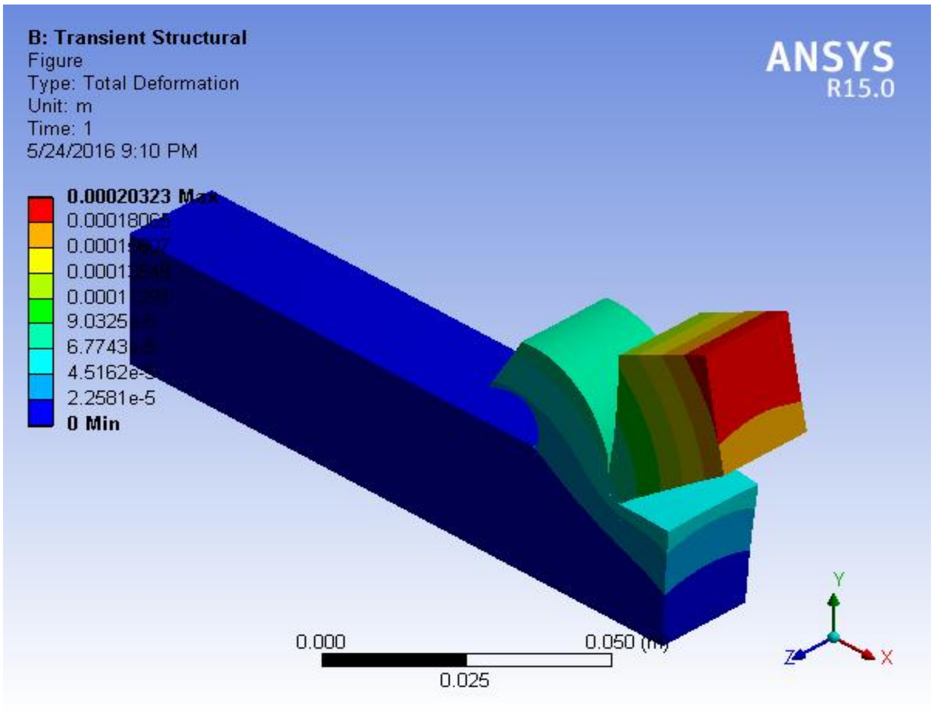

b)deformation

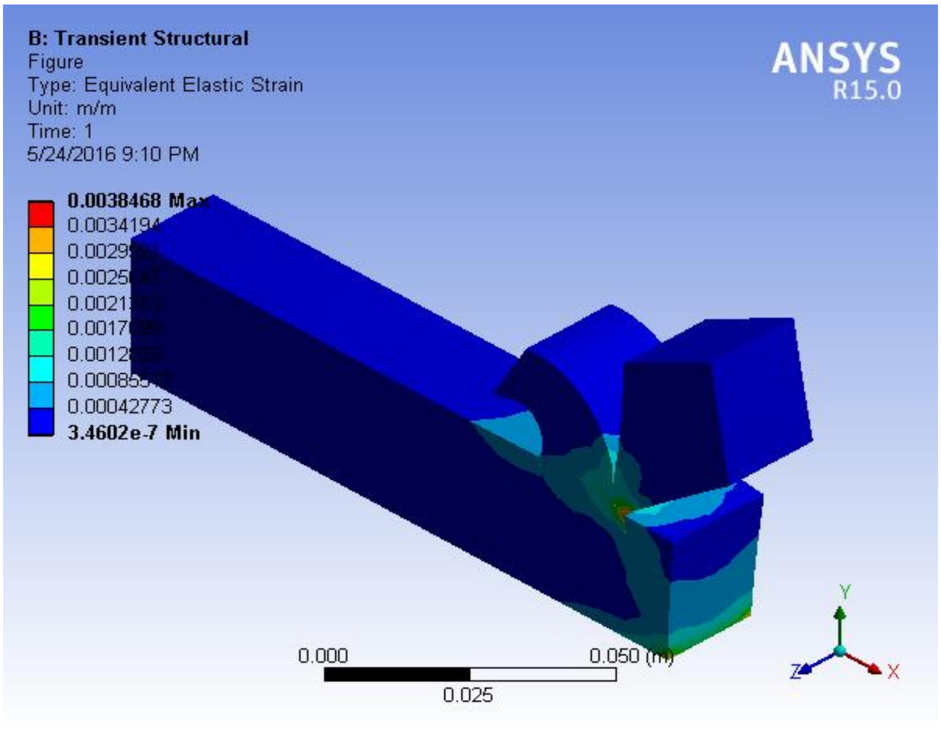

c)strain

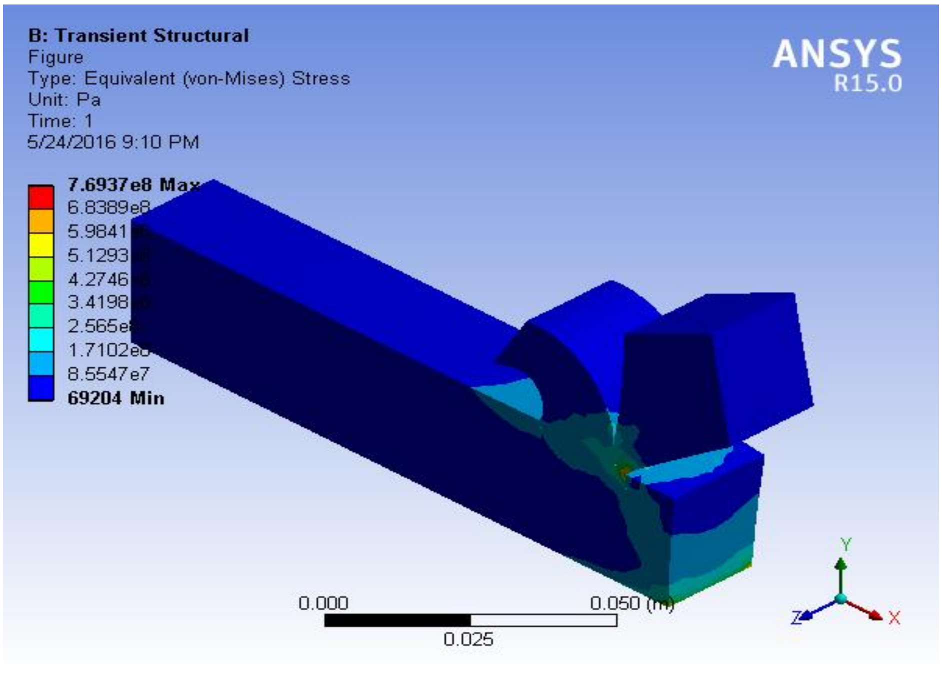

d)von-mises stress

Figure 5.12:a) temperature b)total deformation c)strain d) von-mises stress at v=1m/s and d=2mm

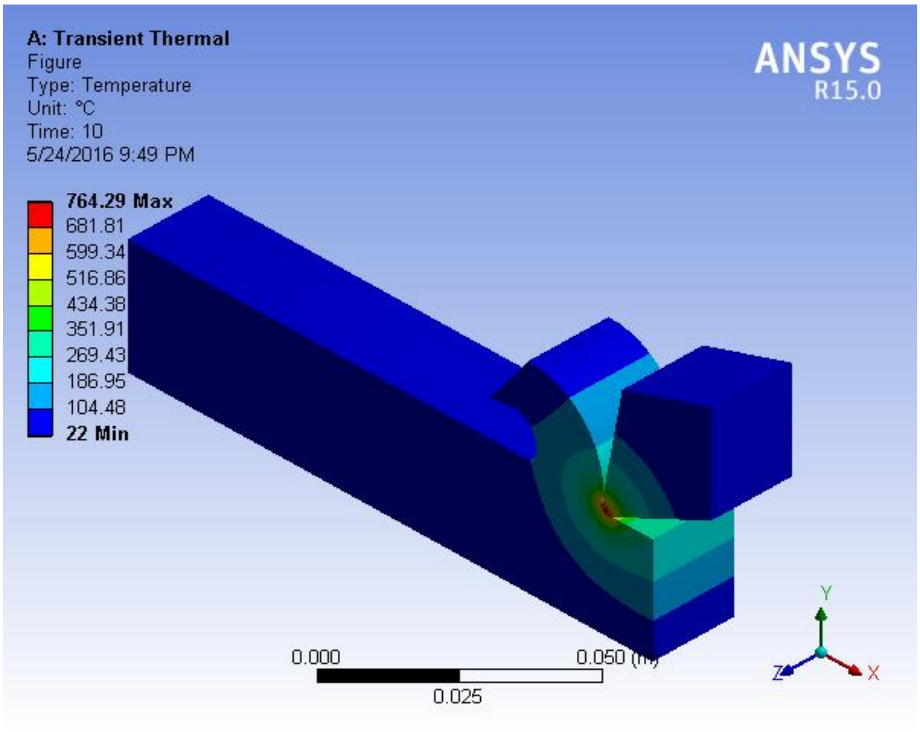

a)temperature

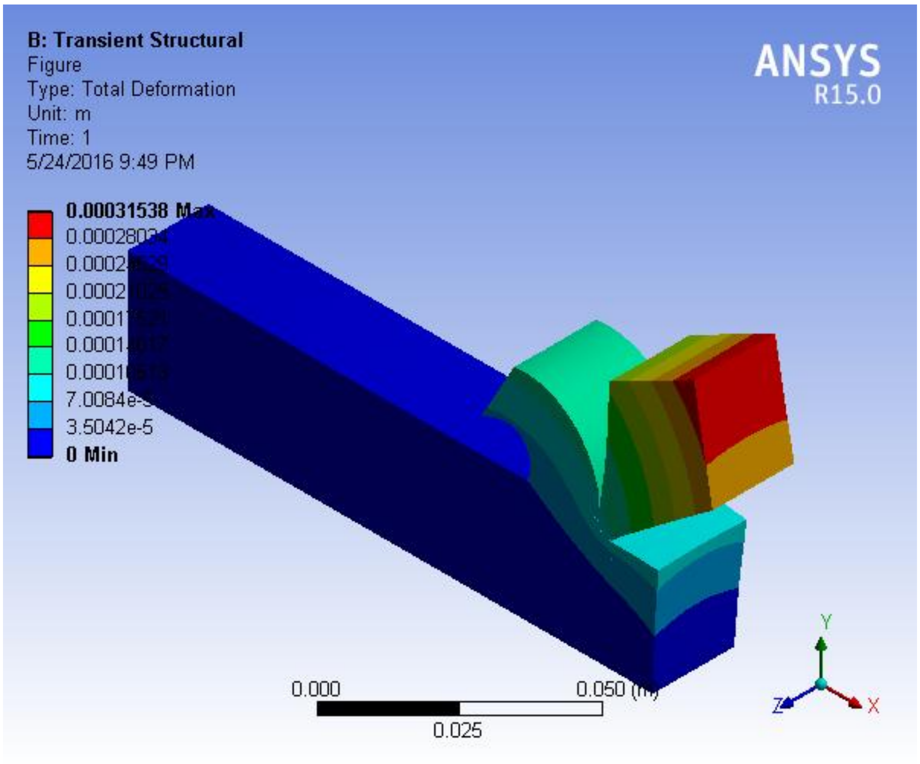

b)deformation

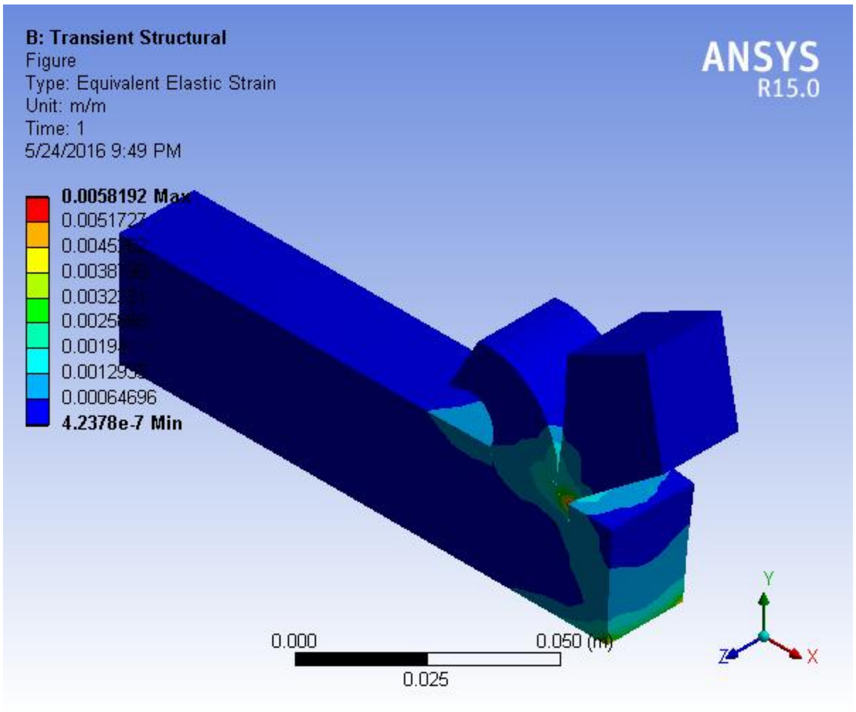

c)strain

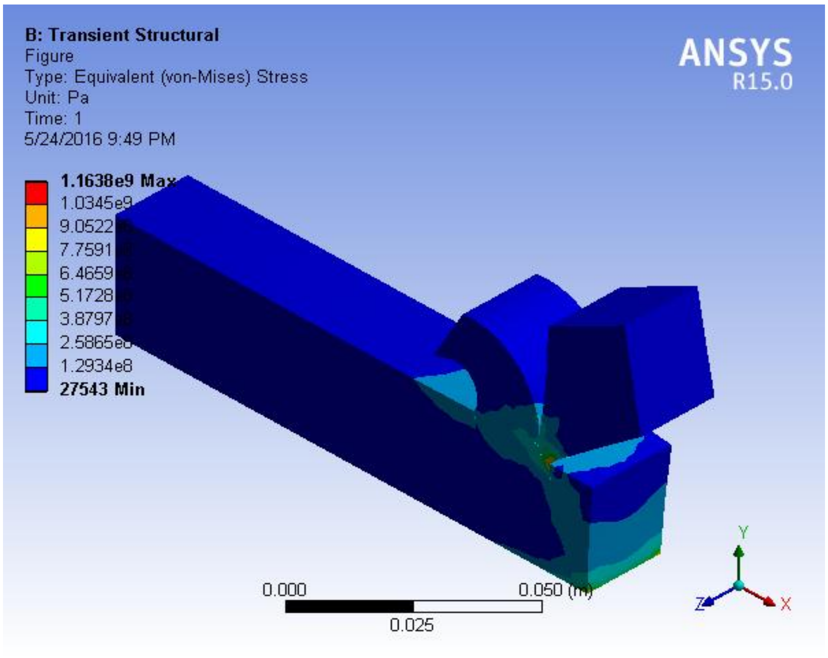

d)von-mises stress

Figure 5.13:a) temperature b)total deformation c)strain d) von-mises stress at v=1.5m/s and d=2mm

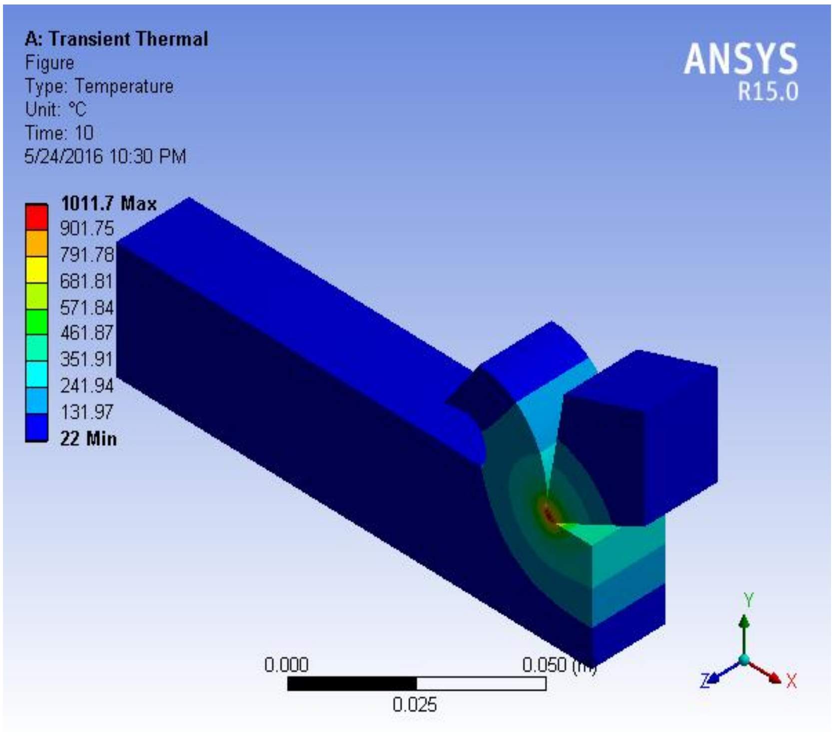

a)temperature

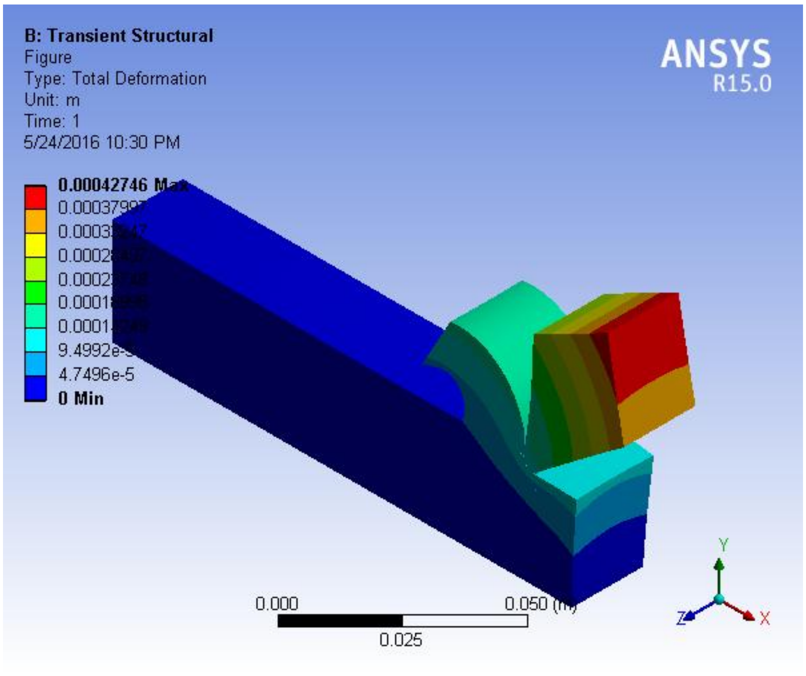

b)deformation

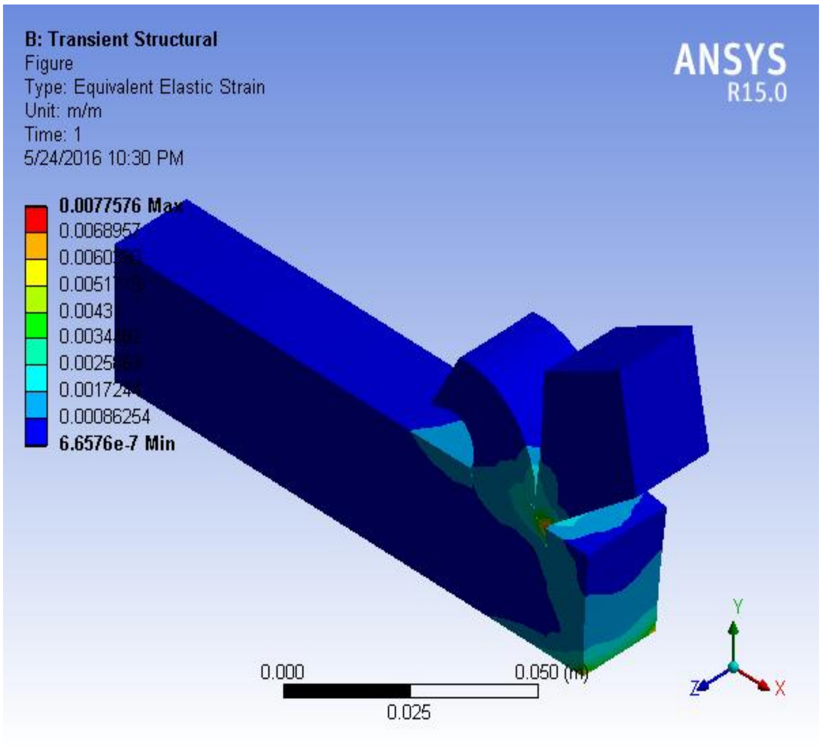

c)strain

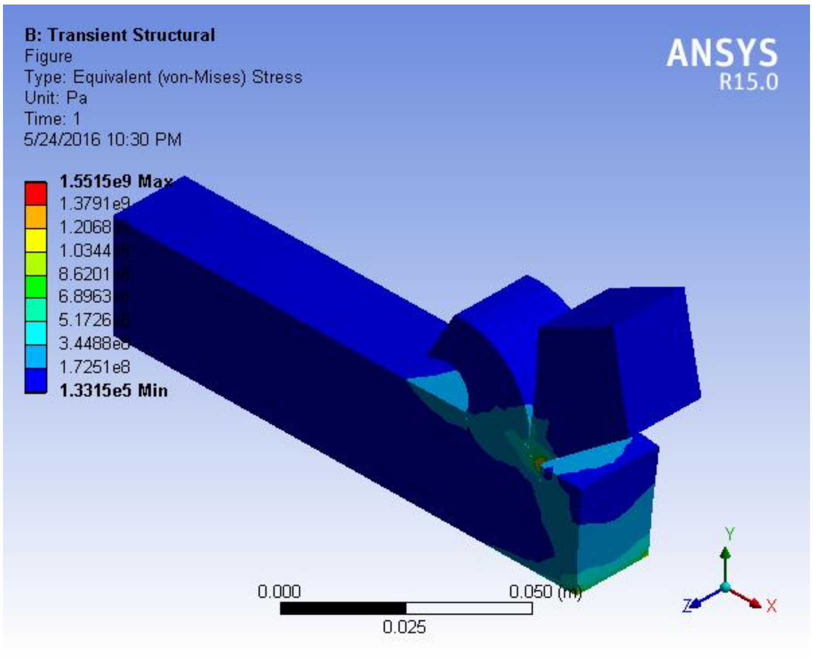

d)von-mises stress

Figure 5.14: a) temperature b) total deformation c)strain d) von-mises stress at v=2m/s and d=2mm

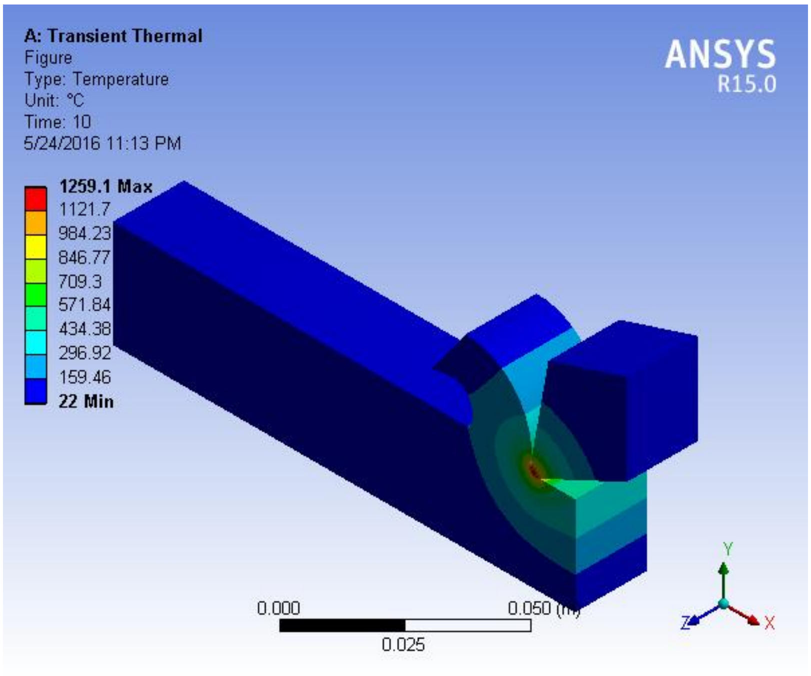

a)temperature

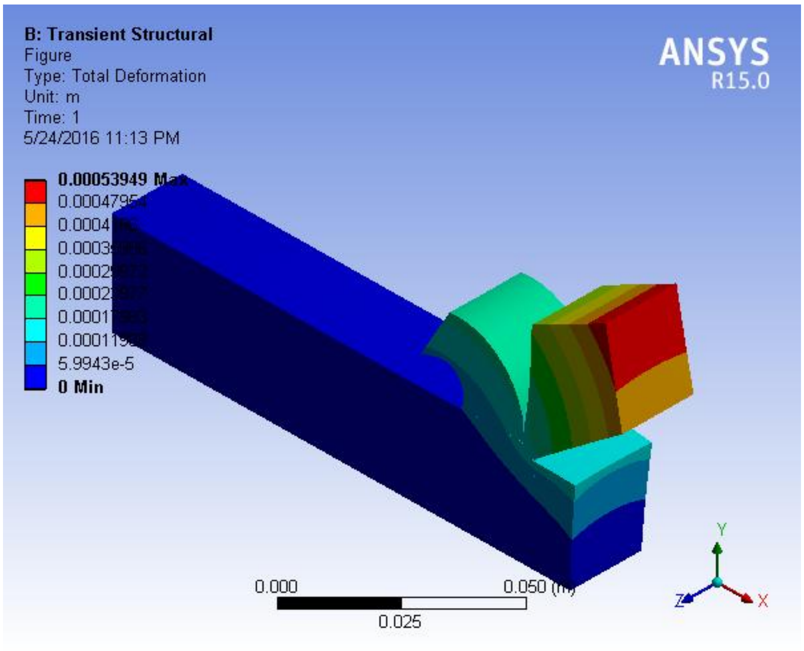

b)deformation

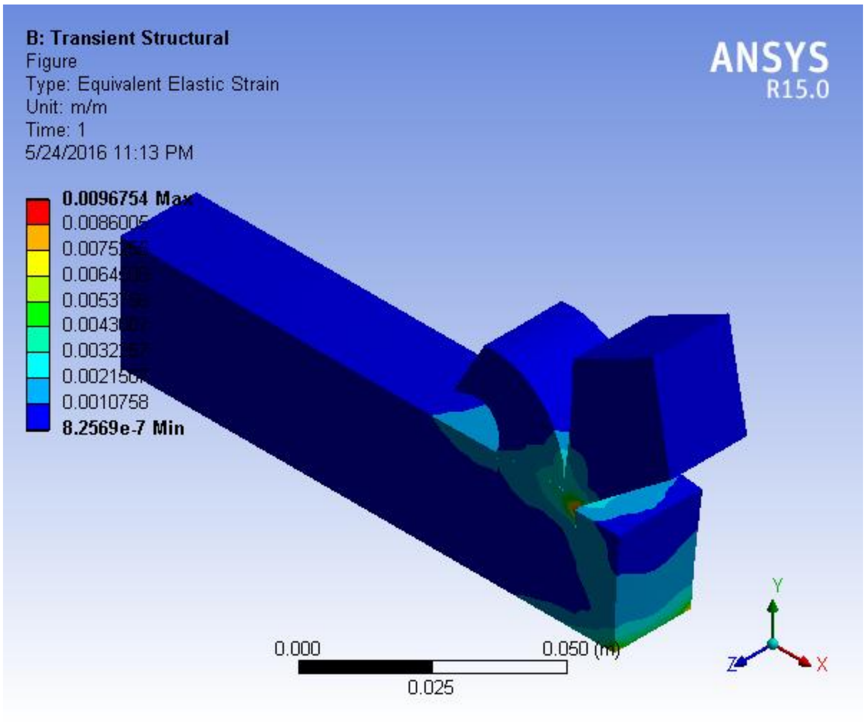

c)strain

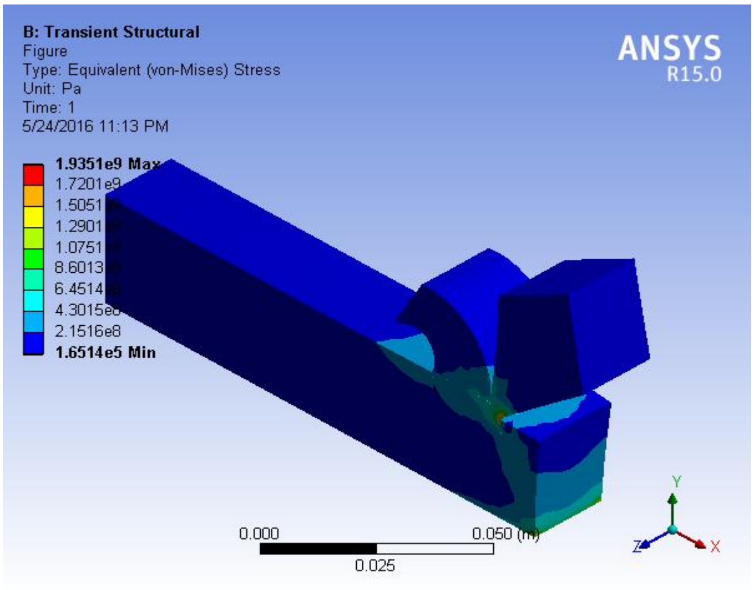

d)von-mises stress

Figure 5.15:a) temperature b)total deformation c)strain d) von-mises stress at v=2.5m/s and d=2mm

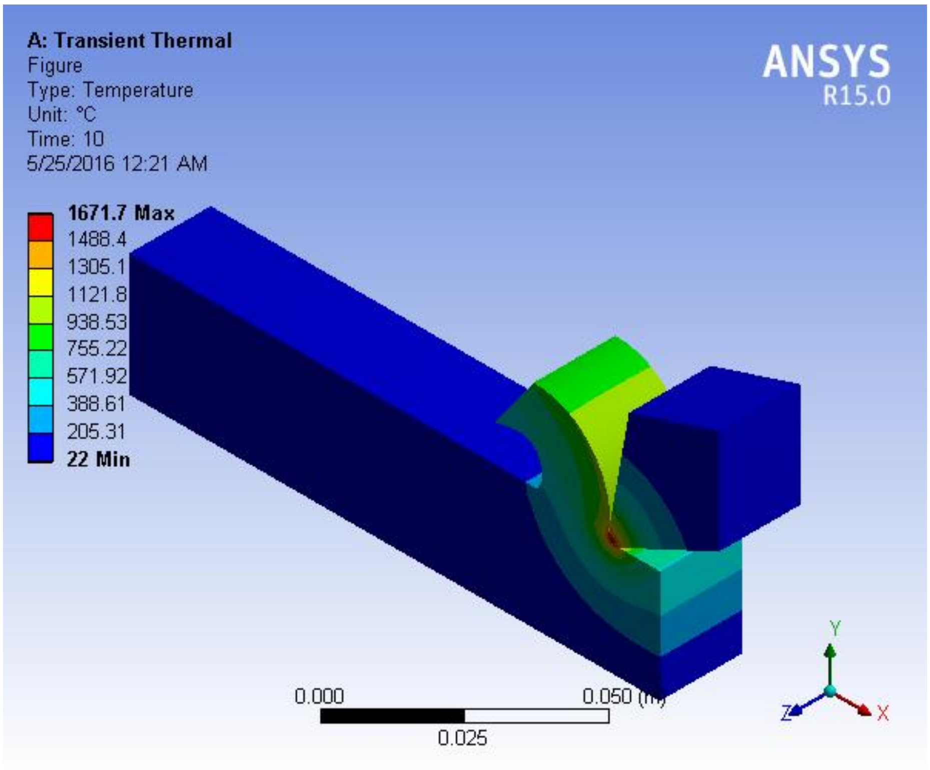

a)temperature

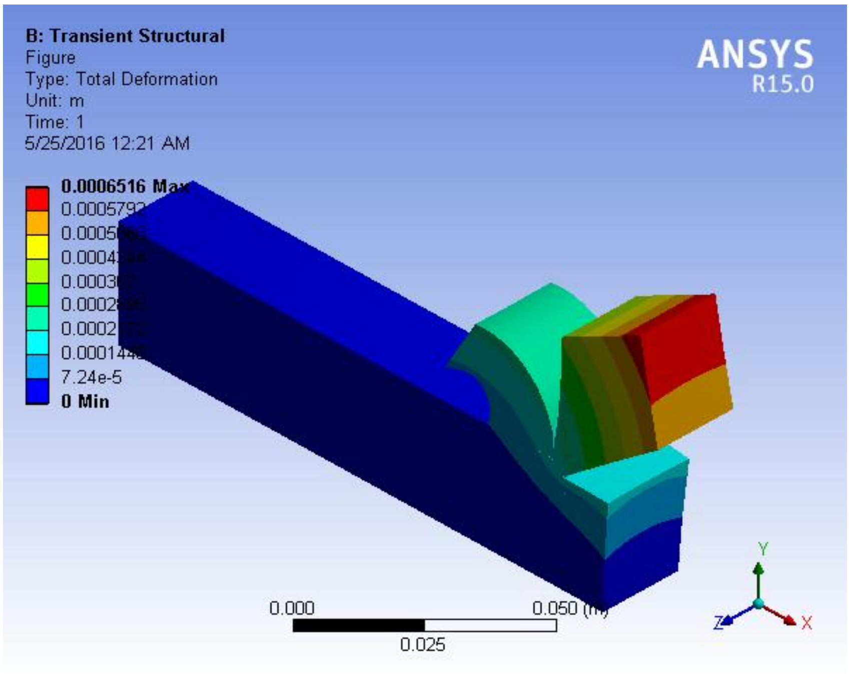

b)deformation

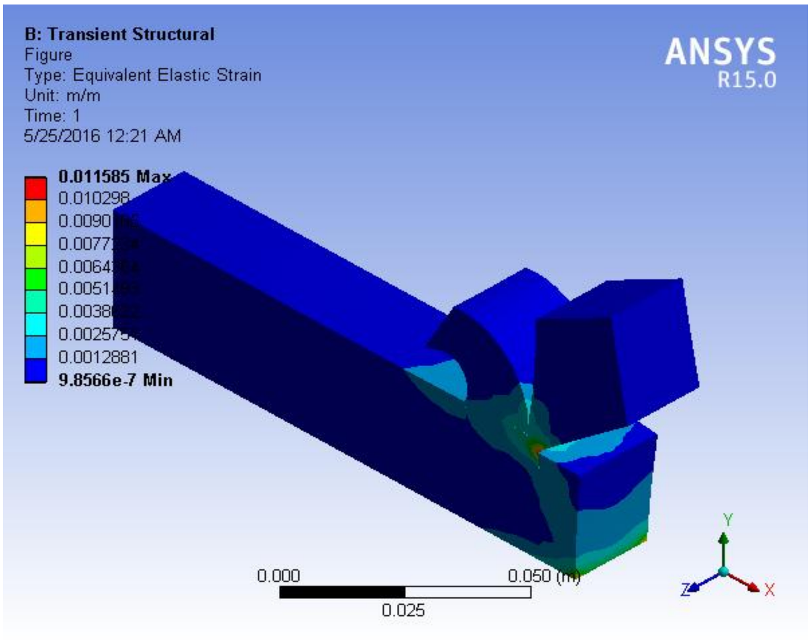

c)strain

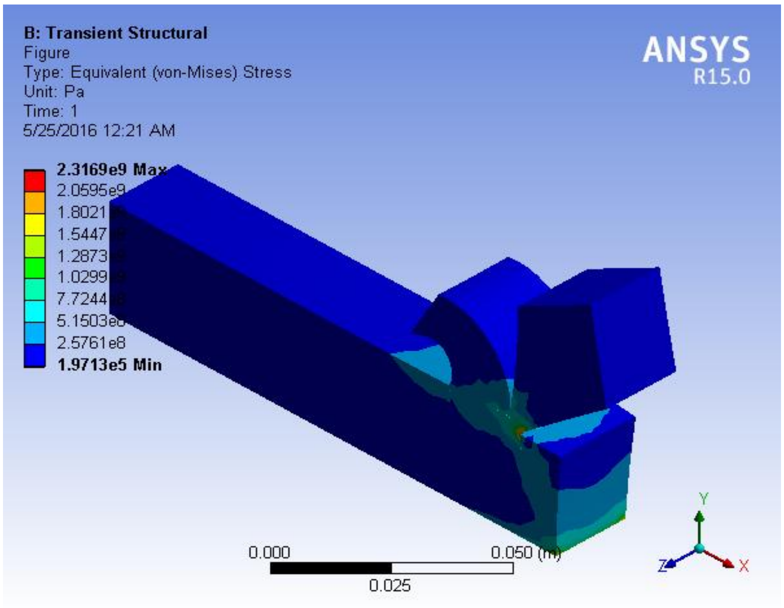

d)von-mises stress

Figure 5.16:a) temperature b)total deformation c)strain d) von-mises stress at v=3m/s and d=2mm

REFERENCES

[1] *Finite Element Simulation of Cutting Processes ,Simulation Techniques in Manufacturing Technology Lecture 8,Laboratory for Machine Tools and Production Engineering Chair of Manufacturing Technology Prof. Dr.-Ing c. F. Klocke.*

[2]Finite Element Modeling and Analysis CE 595: Course Part 2 Amit H. Varma

[3] Analytical Model for Estimating the Amount of Heat Generated During Friction Stir Welding:Application on Plates Made of Aluminium Alloy 2024 T351 Miroslav Mijajlović and Dragan Milčić.

[4] simulation of orthogonal metal cutting by finite element analysis a thesis submitted to the graduate school of natural and applied sciences of the middle east technical university by halil bil.

[5] Metal MachiningTheory and Applications Thomas Childs University of Leeds, UK Katsuhiro MaekawaA member of the Hodder Headline Group LONDON Copublished in North, Central and South America by John Wiley & Sons Inc. New York-Toronto First published in Great Britain in 2000 by Arnold, a member of the Hodder Headline Group, 338 Euston Road, London NW1 3BH.

[6]*Finite Element Analysis Prof. Dr. B. N. Rao Department of Civil Engineering Indian Institute of Technology, Madras Lecture No. # 36.*

[7] FEM analysis for WEDM process A Thesis Submitted in Partial Fulfillment For the Requirement for the Degree of Master of Technology In Production Engineering By BUDHRAM BOIPAI Department of Mechanical Engineering National Institute of Technology Rourkela –769008 2014.

[8] a methodology for practical cutting force evaluation based on the energy spent in the cutting system viktor p. astakhov and xinran xiao general motors business unit michigan state university, department of mechanical engineering, east lansing,michigan, USA.

[9] *Temperature evolution in a WC-6%Co cutting tool during turning machining: experiment and finite element simulations*

T. KAGNAYA M. LAZARD L. LAMBERT, C. BOHER ,T. CUTARD Toulouse University, Institut Clément Ader, Ecole Mines Albi, F-81013 Albi cedex,FRANCE

[10] Numerical simulation of orthogonal machining process using multilayer and single-layer coated tools İrfan Ucun & Kubilay Aslantas Received: 21 September 2010 / Accepted: November 2010 / Published online: 16 November 2010.

[11]Simulation of Laser Structuring by Three Dimensional Heat Transfer Model Bassim Bachy, Joerg Franke International Journal of Mechanical, Aerospace, Industrial and Mechatronics Engineering Vol:8, No:10, 2014.

[12] *Theoretical study of temperature distribution and heat flux variation in turning process Sana J. Yaseen Mechanical Engineering Department - College of Engineering - Basra University Al-Qadisiya Journal For Engineering Sciences, Vol. 5, No. 3, 299-313, Year 2012.*

[13] Coupled *Structural/Thermal Analysis University of Alberta ANSYS Tutorials - www.mece.ualberta.ca/tutorials/ansys/AT/Coupled/Coupled.html.*

[14] *Cutting is a process of extensive stresses and plastic deformations. Valery Marinov, Manufacturing Technology.*

[15] On ’solid-shell’ elements with linear and quadratic shape functions for small and large deformations m. harnau, k. schwe ize rhof, and r. hauptmann _institut f¨ur mechanik, universit¨at karlsruhe, 76128 karlsruhe, germany.

[16]An Investigation into the Effect of Three-flow Stress Models on the Finite Element Simulation of Orthogonal Cutting of AISI 1045 Steel K S Vijay Sekar, *Non-member* M Pradeep Kumar, *GradIE.*

[17] Investigation of cutting temperatures distribution in machining heat treated medium carbon steel on a lathe A. G. F. Alabi1, T. K. Ajiboye and H.D. Olusegun Department of Mechanical Engineering, Faculty of Engineering, University of Ilorin, Kwara State, Nigeria. Accepted 21 December, 2011.

[18]Analytical Modeling of Temperature Distribution in Metal Cutting: Finite ElementApproach. Onyechi, Pius C1, Oluwadare, Benjamin S, Obuka, Nnaemeka S.P1.(Corresponding Author), *Department of Mechanical Engineering, Ekiti State University, Ado Ekiti, Nigeria.*

[19] *an analytical-thermal modeling approach for predicting forces, stresses and temperatures in machining with worn tools yiğit karpat and tuğrul özel department of industrial and system engineering rutgers university piscataway, new jersey 08854, USA*

[20] *modelling and simulation of metal cutting by finite element method a thesis submitted to the graduate school of engineering and sciences of izmir institute of technology in partial fulfilment of the requirements for the degree of*
master of science in mechanical engineering by cenk kiliçaslan december 2009.

[21] A Review of Effects of Temperature Distribution on Tool Life in Turning Process by using Finite Element Analysis **Sushil D. Ghodam** M. Tech. Student, Production Engineering, Government College of Engineering, Amravati, (M.S) India.

[22] Takeyama, H. and Usui, E., A Photoelastic Analysis of Machining Stresses,
Journal Engineering for Industry, 1960.

[23] Zorev, N. N., Interrelationship Between Shear Process Occuring Along Tool Face and Shear Plane in Metal Cutting, American Society of Mechanical Engineers, 1963.